The regulation of cortical development by Neurogenin2

Randal A Hand

A dissertation submitted to the faculty of the University of North Carolina at Chapel Hill in partial fulfillment of the requirements for the degree of Doctor of Philosophy in the School of Medicine in the department of Pharmacology.

Chapel Hill
2009

Approved by:

Associate Professor Franck Polleux, PhD
Professor David Siderovski, PhD
Professor Gary Johnson, PhD
Associate Professor Larysa Pevny, PhD
Associate Professor Eva Anton, PhD

Abstract

Randal A Hand: The regulation of cortical development by Neurogenin2

(Under the direction of Franck Polleux, PhD)

The mammalian nervous system consists of complex neuronal networks formed by extremely diverse sub-groups of neurons located throughout the body. Neurons of the cerebral cortex form neural circuits with the brain and spinal cord allowing for mammals to sense and interact with their environment. The majority of neurons within the cerebral cortex are classified into two groups: inhibitory GABAergic interneurons and excitatory glutamatergic pyramidal neurons. Pyramidal neurons are the largest population of neurons accounting for approximately eighty percent of all neurons within the cerebral cortex. Pyramidal neurons have several defining features including the use of glutamate as an excitatory neurotransmitter, the mode in which they migrate along radial glia to reach their final location, a unipolar dendritic morphology, and a long projecting axon. Within the cerebral cortex, the basic helix loop helix transcription factor, Neurogenin2 regulates the acquisition of many of the cardinal features of

pyramidal neurons. Initially, Neurogenin2 was identified based on its ability to promote neuronal differentiation (proneural function) within the peripheral and central nervous systems. Elegant genetic studies demonstrated that Neurogenin2 also specifies the expression of glutamate as the neurotransmitter for pyramidal neurons. My research identified novel roles for Neurogenin2 including the regulation of radial glia guided migration, their pyramidal dendritic morphology and the axon projection of pyramidal neurons. In addition, I found that a C-terminal tyrosine phosphorylation site in Neurogenin2 was necessary to promote migration and the acquisition of the appropriate dendritic morphology. Loss of function assays revealed that Neurogenin2 regulates the guidance of callosal axons and formation of the corpus callosum. Here, I propose that Neurogenin2 is a master regulator of glutamatergic pyramidal neurons phenotype. Neurogenin2 regulates many aspects required for proper circuit formation including the physical location of neurons, the ability of a neuron to receive afferent signals through proper dendritic morphogenesis, and the ability of a neuron to innervate the proper tissue through the guidance of its long projecting axon. Since Neurogenin2 regulates these aspects of neural circuit formation, it is of no surprise that Neurogenin2 and many of the genes regulated by Neurogenin2 are implicated in mental retardation, epilepsy, and autism spectrum disorders.

Acknowledgements

This dissertation was completed with the constant support and guidance of my mentor, Franck Polleux. I would like to thank all members of my thesis committee for their time, effort, and consideration. I am grateful for all of the members of the Polleux Lab past and present for their helpful comments and suggestions. This work was supported by a Predoctoral Fellowship from the National Institutes of Mental Heath (5F31MH078665). Finally, I would like to thank my loving wife, Rebecca and our son Camden for without them this dissertation would not have been possible.

Table of Contents

List of Figures

List of Abbreviations

bHLH – basic helix-loop-helix

BDA – biotinylated dextrose amine

CP – Cortical plate

E – Embryonic day (days past conception)

EGFP – Enhanced green fluorescent protein

GABA – Gamma-aminobutyric acid

IZ – Intermediate Zone

LGE – Lateral ganglionic eminence

MGE – Medial ganglionic eminence

MZ – Marginal zone

Ngn2 – Neurogenin2

P – Postnatal days (days past birth)

PMI – Pyramidal morphology index

shRNA – short hairpin ribonucleic acid

SVZ – Subventricular zone

VZ – Ventricular zone

Chapter 1

General Introduction

Cortical development and neuronal migration

During mammalian embryogenesis the brain will form many unique and distinctive structures, including the cerebral cortex. The cerebral cortex is a region of the brain that allows for the interpretation and interaction with the environment. The cerebral cortex forms a highly structured tissue consisting of many different layers and will form connections with vast array of different structures throughout the nervous system.

The genesis of the cerebral cortex begins around embryonic day 10 (E10) in mice (Angevine, 1970). At this time the region that will give rise to the cerebral cortex, the neocortex consist of neural progenitor cells (NPCs), also known as radial glia. These neural progenitor cells have processes that span both the apical surface (ventricular surface) and the basal surface (pial surface) with their cell bodies residing in the ventricular zone (VZ) (Schmechel and Rakic, 1979). Radial glia undergo many divisions to expand the developing cortex and to generate glutamatergic pyramidal neurons. To generate glutamatergic pyramidal neurons, the radial glia will divide asymmetrically, to give rise to a immature

neuron and another radial glia (Noctor et al., 2001), while symmetric divisions serve to expand the progenitor pool and ultimately increase the size of the neocortex. The newly generated immature neuron will migrate to the pial surface by undergoing a somal translocation, in which the cell body will migrate towards the pial surface, forming the preplate (Allendoerfer and Shatz, 1994). This form of differentiation and migration occurs between embryonic days 10 and 12 and sets the stage for the massive expansion of neuronal differentiation that is to follow.

In addition to the generation of glutamatergic pyramidal neurons within the cortex, there are additional types of neurons formed outside of the cortex that migrate into the cortex and are instrumental to the formation of the six layered mammalian cortex. One important group of neurons are the Cajal-Retzius cells. The Cajal-Retzius cells are born between embyonic days 10 and 12 in several different regions including the cortical hem(Takiguchi-Hayashi et al., 2004), septum, and pallial-subpallial boundary (Bielle et al., 2005), and it is postulated that Cajal-Retzius cells could be generated in additional areas. The Cajal-Retzius cell migrate from these various locations and populate the dorsal surface of the dorsal telencephalon **(Figure 1.1)**. These Cajal-Retzius cells are critical for the next stage of migration in the neocortex and form the most dorsal layer of the cortex, Layer I.

Once the preplate has formed and the Cajal-Retzius cells have entered the neocortex, around embryonic day E12, the newly differentiated neurons within the neocortex begin to migrate in a unique fashion. As before, new

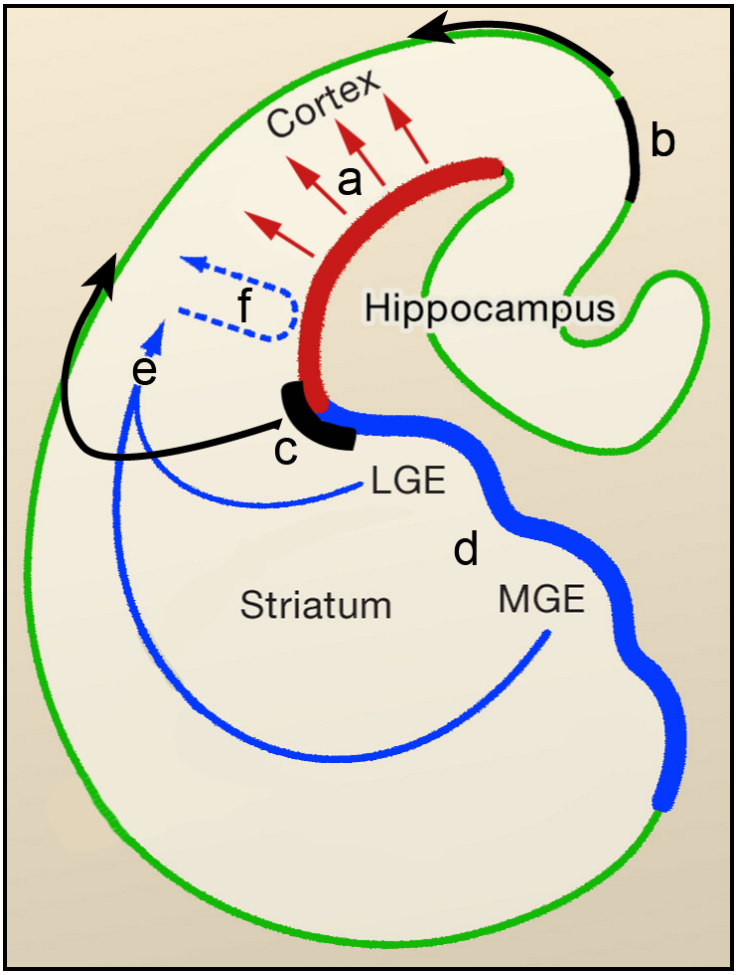

Figure 1.1 Cell origins and migration of cortical neurons

The neurons of the developing cortex are generated in several different areas within the brain. This representative image is a coronal section of one hemisphere of a mouse brain at embryonic day 14. The glutamatergic pyramidal neurons (red) differentiate locally from radial glia within the cortex, and migrate along the radial glia to reach their final position within the cortex (a). Cajal-Reztius cells (black) originate from several areas including the cortical hem (b) and pallial-subpallial boundary (c), and migrate along the dorsal surface of the developing cortex. The GABAergic interneurons (blue) are generated in the LGE and MGE (d) and migrate tangentially into the cortex (e). Upon reaching their destination in the cortex, GABAergic interneurons will often migrate along radial glia (f). This image was adapted from Ayala et al 2007.

glutamatergic pyramidal neurons are generated through asymmetric cell division from radial glia, but these newly differentiated neurons migrate to a region just above the VZ and begin to form the subventricular zone (SVZ) (Noctor et al., 2004). These newly differentiated neurons are known as intermediate progenitor cells (IPCs) and often undergo symmetric divisions in which two IPCs are generated (Noctor et al., 2004). The IPCs of the SVZ have a unique dynamic morphology consisting of many short rapidly protruding and retracting neurites. In response to a yet to be determined cue, the IPCs will polarize forming a unipolar leading process and a thin trailing process. These polarized neurons will attach to the radial glia cells, and begin a guided migration towards the pial surface. This migration is described as a locomotive migration in which the leading process will extend and adhere to the radial glia and the cell body will subsequently contract, allowing the cell to crawl along the radial glia (Marin and Rubenstein, 2003). This process will repeat many times as the cells move towards the pial surface. At this point the intermediate zone (IZ) is beginning to form. The IZ is a cell sparse zone in which newly formed axons fasciculate and project towards their distant targets. This region lies between the dividing progenitors and the differentiated neurons. As the neurons migrate through the IZ along radial glia and reach the preplate, the radially migrating cells will detach and populate the dorsal region of the neocortex. The detachment of the neurons from the radial glia cells is dependent on the large glycoprotein reelin . Reelin is secreted from the Cajal-Retzius cells in Layer I and is absolutely necessary form

the proper formation of the cerebral cortex(Ogawa et al., 1995). As the first wave of radially migrating cells reach the dorsal surface and form the cortical plate, they split the preplate to form the subplate (ventrally) and the marginal zone (dorsally) **(Figure 1.2)** (Gupta et al., 2002). This first wave of radial migration will form Layer VI of the cortex. After the first wave of neurogenesis and radial migration, several additional waves will follow. With each additional wave of neurogenesis the migrating neurons bypass their predecessors and form new layers. This pattern of migration is known as inside-first outside-last, where the youngest neurons form layers that are superficial to the layers formed by older neurons. Neuronal differentiation within the developing cortex occurs until embryonic day 18 (Angevine, 1970; Polleux et al., 1997; Takahashi et al., 1995), and by the first postnatal days (embryonic mice are born between embryonic day 19 and 21) all of the pyramidal neurons have reached there final laminar position. This method of neurogenesis and migration leads to the formation of six distinct layers, and each of these six layers will have common and distinctive features.

In addition to the Cajal-Retzius cell that form Layer I, another important type of cortical neuron is formed outside of the neocortex, the GABAergic interneuron. The inhibitory GABAergic interneurons compose approximately thirty percent of all cortical neurons and are important in modulating the activity of excitatory glutamatergic pyramidal neurons. GABAergic interneurons are generated from neural progenitors in the ventral telencephalon **(Figure1.1)** (Anderson et al., 1997). Upon differentiation, GABAergic interneurons migrate

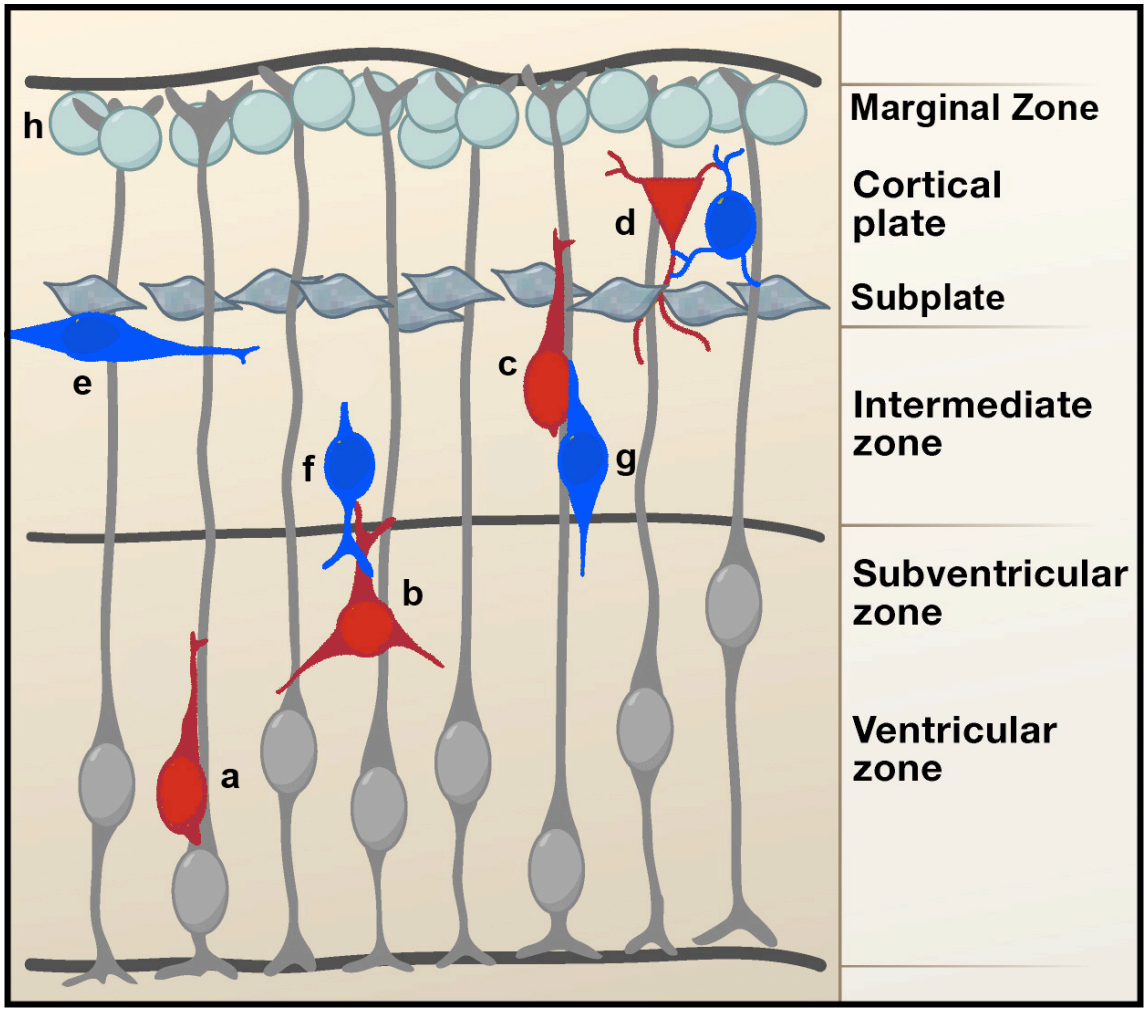

Figure 1.2 Migrating pyramidal and interneurons.

In the cortex, pyramidal neurons are generated through asymmetric divisions of radial glial cells (grey cells). Newly differentiated neurons, termed intermediate progenitor cells (IPCs) (a) migrate towards the subventricular zone and display a multipolar morphology consisting of rapidly protracting and retracting neurites (b). The IPCs will polarize forming a leading process and begin radial glia guided locomotive migration (c) until reaching the cortical plate (d). GABAergic interneurons (e) migrate into the cortex in either the marginal zone or intermediate zone. Upon migrating to their destination within the cortex, GABAergic interneurons will dive towards the

ventricular surface (f) and then migrate along radial glia (g) until reaching the cortical plate (d). Interestingly, GABAergic interneurons and pyramidal neurons that differentiate at the same time will occupy the same laminar position within the cortex (d).Cajal-Retzius cells located within the marginal zone (h). This image was adapted from Ayala et al 2007.

tangentially to reach the cerebral cortex (Anderson et al., 1997). The first GABAergic interneurons reach the cortex around embryonic day 13. Interesting, the bulk of the interneurons enter the neocortex by migrating through either the MZ or IZ. Once the interneuron has arrived in the neocortex, the interneuron will leave the MZ or the IZ and integrate into the neocortex, often migrating along radial glia **(Figure 1.2)** (Polleux et al., 2002). The interneurons will disperse amongst all layers of the cerebral cortex that were formed by the radially migrating pyramidal neurons. The tangentially migrating interneuron has a distinctive mode of migration that is substantially different from the directed streamline migration of pyramidal neurons. Interneurons migrate in an amoeboid manner, in which a leading process dynamically emerges as the interneurons often change direction (Polleux et al., 2002). This difference in migration properties between glutamatergic pyramidal neurons and GABAergic interneurons comprises only one of the major distinctions between the two groups of neurons. Beyond the difference in migration properties and neurotransmitter expression, pyramidal neurons and interneurons have unique and distinctive morphological differences.

Neuronal morphology of cortical neurons

All neurons have a basic polarized morphology that consists of dendrite(s) which receive afferent synaptic contacts and a unique axon that propagate efferent information through action potentials. The precise morphology of the

axons and dendrites will dictate how a neuron may receive and send signals. Within the mature cerebral cortex, the vast majority of cortical neurons fall within two groups GABAergic interneurons and glutamatergic pyramidal neurons. Each group has common characteristics and unique morphologies that may be subdivided into several subtypes.

All glutamatergic pyramidal neurons begin with the same basic morphology upon arriving in their final location within the cortex (Ramón y Cajal, 1995). All glutamatergic neurons of the neocortex have a unipolar leading process that will ultimately become the dendrite and a long trailing process that will become the axon **(Figure 1.3)**. Over time the pyramidal neurons from each layer will develop a subtly unique morphology. The basic morphology of a glutamatergic pyramidal neuron contains a large unipolar apical dendrite that is oriented towards the pial surface and a long projecting axon that innervates distant targets (Ramón y Cajal, 1995). The apical dendrite has a long sparsely branched shaft but with many branches emerging from the tip forming the apical tufts **(Figure 1.3)**. The apical tufts are rich with spines and are a major site of synaptogenesis. In addition to the branching at the tip of apical dendrites, many small spine rich basal dendrites arise from the soma of the pyramidal neuron **(Figure 1.3)** and the soma and basal dendrites are another major site of synaptogenesis. While this basic morphology is shared with all pyramidal neurons, there are subtle important differences. These differences include the location within the neocortex and the region in which the axon projects.

The precise location in the cortex will affect the neural circuits formed as different layers within the cortex are innervated by different regions within the brain. Layer VI pyramidal neurons are unique in that their cell bodies reside within Layer VI and their apical dendrites extend into Layer IV but do not reach the dorsal surface of the cerebral cortex **(Figure 1.4)**. The remaining pyramidal neurons are classified as either large pyramidal neurons or small pyramidal neurons. The large pyramidal neurons have cell bodies located in Layer V with apical dendrites that stretch all the way to the pial surface of the neocortex **(Figure 1.4)**. Similarly, the small pyramidal neurons have apical dendrites that reach the pial surface but their somas reside in Layers II and III **(Figure 1.4)**. While neurons located in Layers II, III, V, and VI all have the basic pyramidal morphology, there is one major morphological exception of glutamatergic neurons within the neocortex, the glutamatergic spiny stellate cells of Layer IV. While Layer IV neurons are not classified as pyramidal cells, but they are of common origin as the pyramidal neurons. Initially, the spiny stellate cells differentiate and migrate just as the glutamatergic pyramidal neurons, and upon arrival within the cortical plate they are indistinguishable from the pyramidal neurons. Postnatally, the spiny stellate cells undergo a massive morphological transformation, and obtain a multipolar dendritic morphology and a short locally projecting axon **(Figure 1.5)**. These spiny stellate cells are also unique since they are the only excitatory interneurons of the cerebral cortex. While there are subtle differences in physical location and dendritic morphology amongst glutamatergic

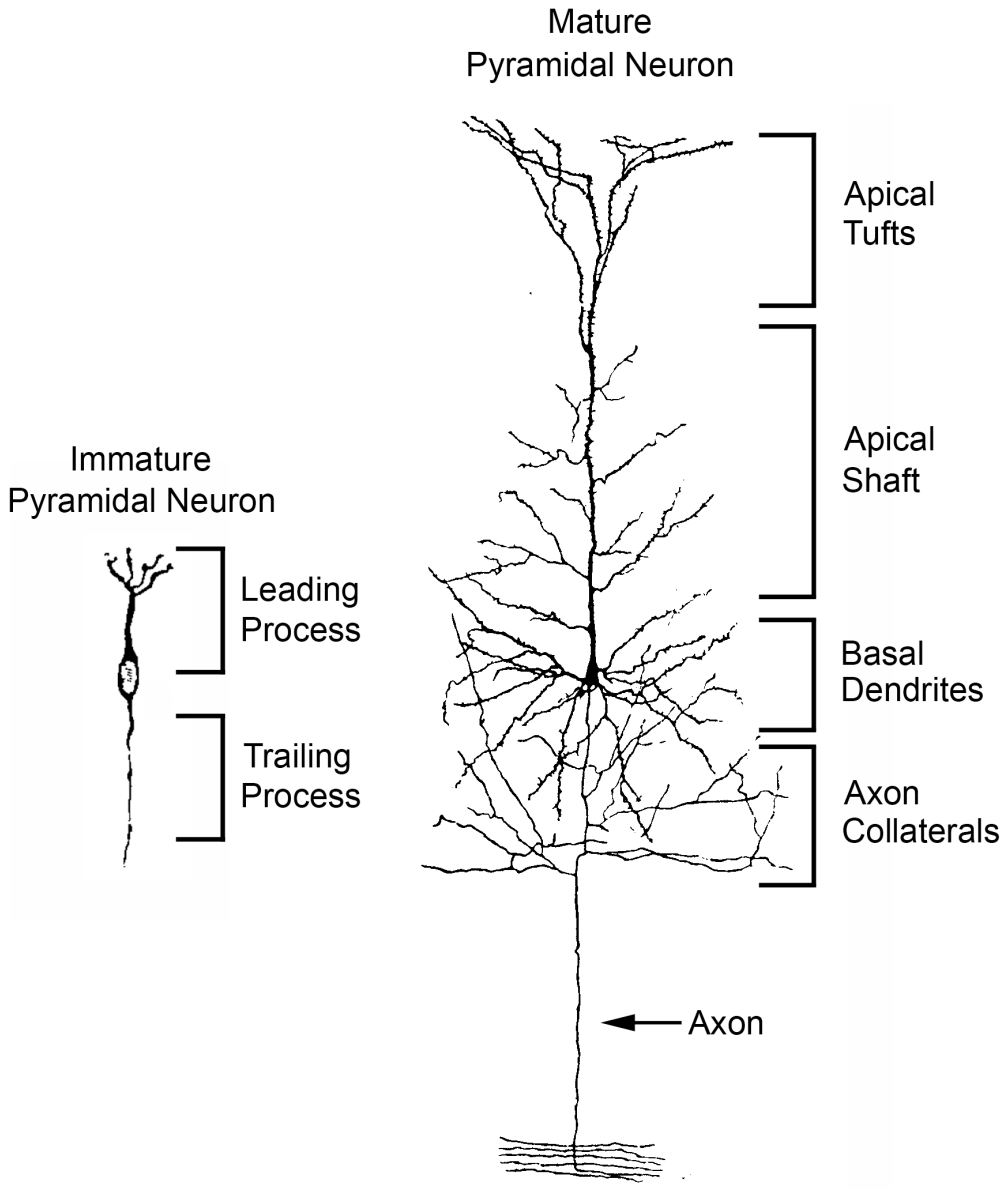

Figure 1.3 Morphology of a pyramidal neuron.

The immature pyramidal neuron (left) has the basic polarized morphology consisting of a leading process that will form the apical dendrite and a trailing process that will serve as the axon. The mature pyramidal neuron (right) has a complex dendritic and axonal morphology. Images were adapted from Ramon Y Cajal 1995

pyramidal, there major differences in the regions innervated by their long projecting axons.

Glutamatergic pyramidal axons innervate many different areas within the central nervous system. Each layer within the cerebral cortex tends to predominately innervate a specific tissue (Nieuwenhuys, 1994). Layer V and VI pyramidal neurons mainly innervate subcortical structures (Leone et al., 2008; Molyneaux et al., 2007). To innervate subcortical structures, the axons must initially project laterally to exit the cortex. The axons of Layer VI leave the cortex and innervate the thalamus, while Layer V pyramidal neurons innervate multiple areas, including the spinal cord, the striatum, and the cerebral cortex. Just as Layer VI pyramidal neurons, the axons of Layer V pyramidal neurons that target subcortical regions must initially project laterally. Layers II and III form intercortical circuits between the two hemispheres of the cerebral cortex. To reach the contralateral cortex, axons often cross the midline at the corpus callosum (Leone et al., 2008; Molyneaux et al., 2007). To cross the midline at the corpus callosum, axons must initially project medially towards the midline to reach the corpus callosum and target the contralateral cortex. This highlights one of the major differences between deep layer neurons that must initially project axons laterally, and superficial layer neurons that must initially project axons medially. Again, the glutamatergic spiny stellate cells of Layer IV are a major exception. These interneurons have short locally projecting axons that innervate the surrounding tissue mainly in Layers II and III (Nieuwenhuys, 1994). While all

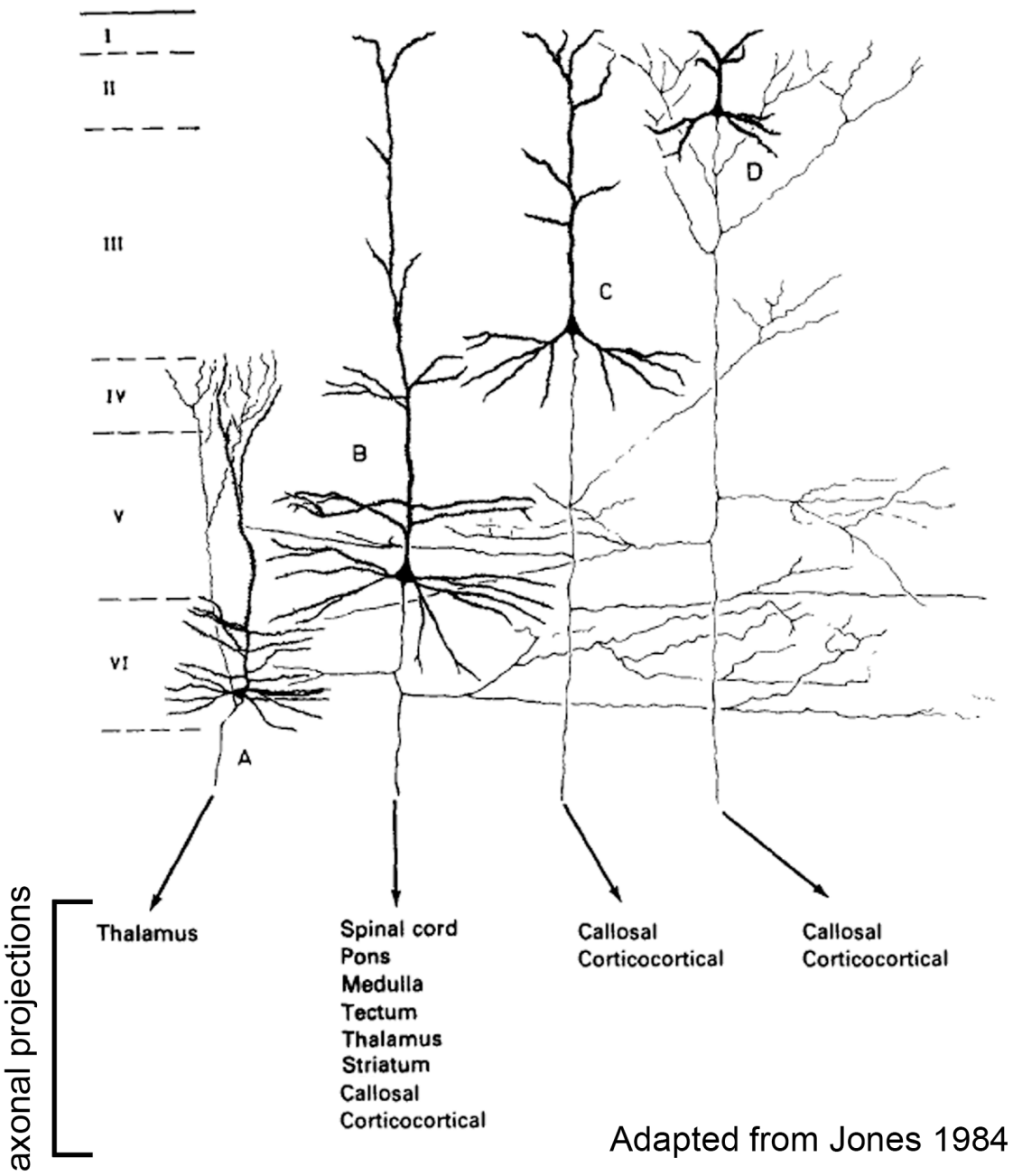

Figure 1.4 Differences in pyramidal neuron morphology and axonal projection.

All pyramidal neurons have the same basic morphology, but differences exist in their precise location within the cerebral cortex and the areas in which their axons project. These differences are important in proper formation of cortical circuits. (Peters and Jones, 1984)

pyramidal neurons have a long projecting axon they are contrasted by their initial axonal projection along the medial-lateral axis and with the final region of innervation.

The molecular mechanisms regulating this differential axonal projection has recently become an area of great interest. Currently, the axon guidance cues that control the initial axonal projection along the medial-lateral axis have not been identified. While the axon guidance cues are unknown, progress has been made identifying the transcriptional regulators of laminar fate and the corresponding axonal projections. Two zinc finger transcription factors Fezf2 and CTIP2 both regulate the deep layer, Layer V identity of cortical neurons and a genetic loss of either transcription factor leads to a decrease in deep layers and aberrantly projecting subcortical axonal projections (Chen et al., 2005a; Chen et al., 2005b; Molyneaux et al., 2005). In addition to these zinc finger transcription factors, other transcription factors have been identified as playing important roles in specifying the laminar fate and axonal projections of the deep layers V and VI, including Sox5 (Layer V) (Lai et al., 2008) and Tbr1 (Layer VI) (Hevner et al., 2001). While many transcription factors have been identified as regulators of deep layer identity, relatively little is known about factors regulating superficial layer identity and axonal projections. Interestingly, the chromatin remodeling protein SATB2 is required for proper axonal projections and laminar identity of superficial neurons by repressing CTIP2 expression (Alcamo et al., 2008; Britanova et al., 2008). With the genetic loss of SATB2, fewer axons from layer II-

III project contralaterally and instead project subcortically. This impressive change in projection pattern is caused by an up regulation of CTIP2 expression in the superficial layers. While it is clear that many transcription factors are required for the proper laminar identity of pyramidal neurons, which in turn regulates the axonal projections of cortical neurons, to date, no protein has been identified that directly regulates the initial axon projection of pyramidal neurons along the medial-lateral axis.

GABAergic interneurons are contrasted by glutamatergic pyramidal neurons by having complex multipolar dendritic morphologies and a relatively short axon that locally innervates within the cerebral cortex. Interneurons may be classified into many different subtypes based on their morphology and electrophysiological properties. These subtypes include basket cells (~50% of all neocortical interneurons), chandelier cells, martinotti cells, bipolar cells, double bouquet cells, bitufted cells, and neurogliaform cells **(Figure 1.5)** (Markram et al., 2004). Interestingly, different types of interneurons innervate different sites on pyramidal neurons and other interneurons within the cortex. The precise location of synaptogenesis on a neuron has a profound effect how a interneuron modulates the electrophysiological properties of its post-synaptic target neuron (Markram et al., 2004). While interneurons like pyramidal neurons share common characteristics, they also have unique differences in morphology, location, and synaptic targets.

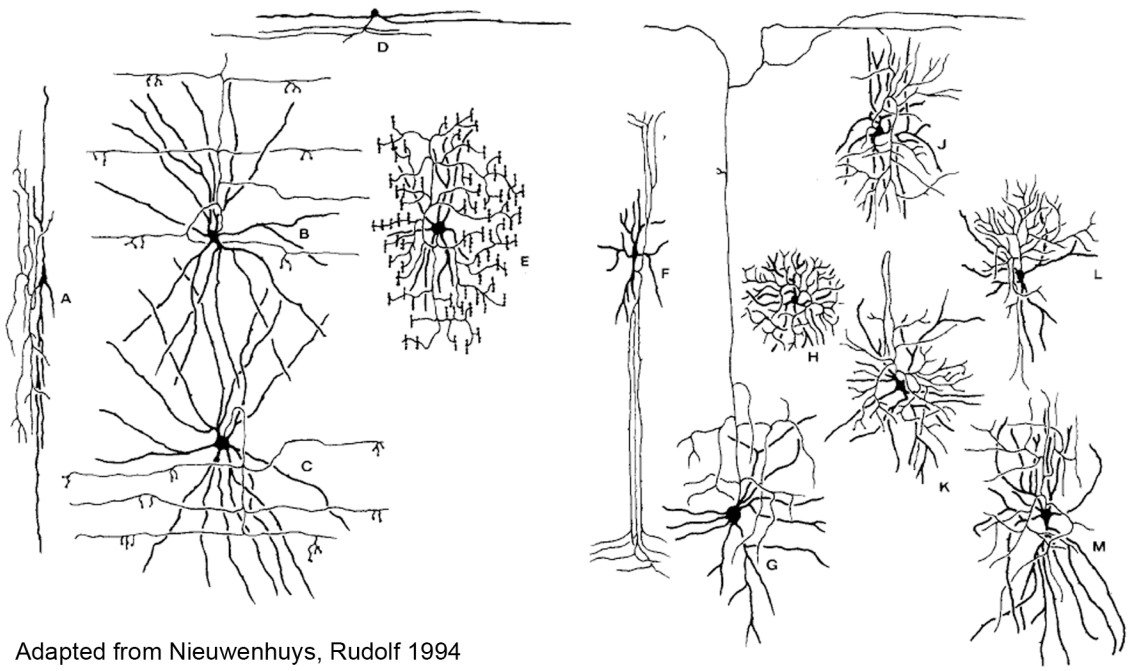

Adapted from Nieuwenhuys, Rudolf 1994

Figure 1.5 Interneuron morphology in the cerebral cortex.

There is a great diversity of interneurons within the cortex. There are characterized by a complex dendritic morphology and a short locally projecting axon. There are two main types of interneurons, inhibitory GABAergic (A-K) and excitatory glutamatergic (L&M). There is a great diversity of GABAergic interneurons each with a unique morphology and physiological properties. These include bipolar cells (A), large basket cells (B,C), horizontal cells (D), chandelier cells (E), double bouquet cell (F), Martinotti cells (G), neurogliaform cells (H), and small basket cells (K&J). The spiny stellate cells (L&M) are the excitatory glutamatergic interneurons that reside in Layer IV. These neurons differentiate within the neocortex and they are initially indistinguishable from immature pyramidal neurons **(Figure 1.3 left)**. This image was adapted from Nieuwenhuys 1994.

All neurons share basic properties including a polarized morphology, but significant differences occur between population of neurons. These differences are exemplified within the cortex. The generation of the highly structured cortex relies on different populations of neurons successfully migrating to the proper position within the cortex, developing the proper dendritic and axonal morphology, and establishing the appropriate connection with other neurons.

Neurogenin2

Many of the advances in understanding cortical development has come from studying transcription factors. Many transcription factors are expressed regionally within the telencephalon. Within the developing cortex, the Neurogenins (Neurogenin1 and Neurogenin2) are expressed in the germinal zones of the cortex (Sommer et al., 1996), and have been identified for their importance in forming the cerebral cortex.

Neurogenin2 is a basic-helix-loop-helix (bHLH) transcription factor. The bHLH domain serves two main functions, binding DNA and dimerizing with other bHLH transcription factors **(Figure 1.6)** (Bertrand et al., 2002). The basic domain is primarily responsible for binding target regions within the DNA. Neurogenin2 binds the E-box consensus sequence CANNTG where N represents any nucleotide. The helix-loop-helix domain is involved in dimerizing with other transcription factors and repressors containing HLH domains. In addition to interacting with other transcription factors, Neurogenin2 is known to bind to

several transcriptional co-activators including the paralogs p300 and CBP (Sun et al., 2001). These paralogs are histone acetyl transferases (HATs), that promote transcription by acetylating histones (Marmorstein and Roth, 2001), which frees DNA from histones and this is conducive to transcription. While Neurogenin2 has a defined bHLH domain comprising approximately one-third of the protein, Neurogenin2 also has two relatively large regions with unknown function. These regions are amino terminal and carboxy terminal to the bHLH domain and comprise the remaining two-thirds of the protein. Neurogenin2 has a relative simple structure consisting of a single domain, but little is known about the function of regions outside of the bHLH domain.

Neurogenins (1-3) were first studied due to their homology to transcription factors from invertebrates (Ma et al., 1996). In *Drosophila melanogaster,* the bHLH transcription factor Atonal was identified as regulating the differentiation of the external sense organs (neurons) (Jarman et al., 1993). Interestingly, the genetic loss of Atonal reduced the number of sensory hair cells and increased the number of glia, and gain of function studies demonstrated ectopic expression of Atonal induced ectopic formation of external sense organs (Jarman et al., 1993). Based on these results demonstrating the proneural effects of Atonal, researchers began looking for the mammalian orthologs. Several different bHLH transcription factors were identified as proneural transcription factors in mice. Included in these are the NeuroD and Neurogenin transcription factors (Ma et al., 1996; Sommer et al., 1996), that were named after their myogenic equivalents

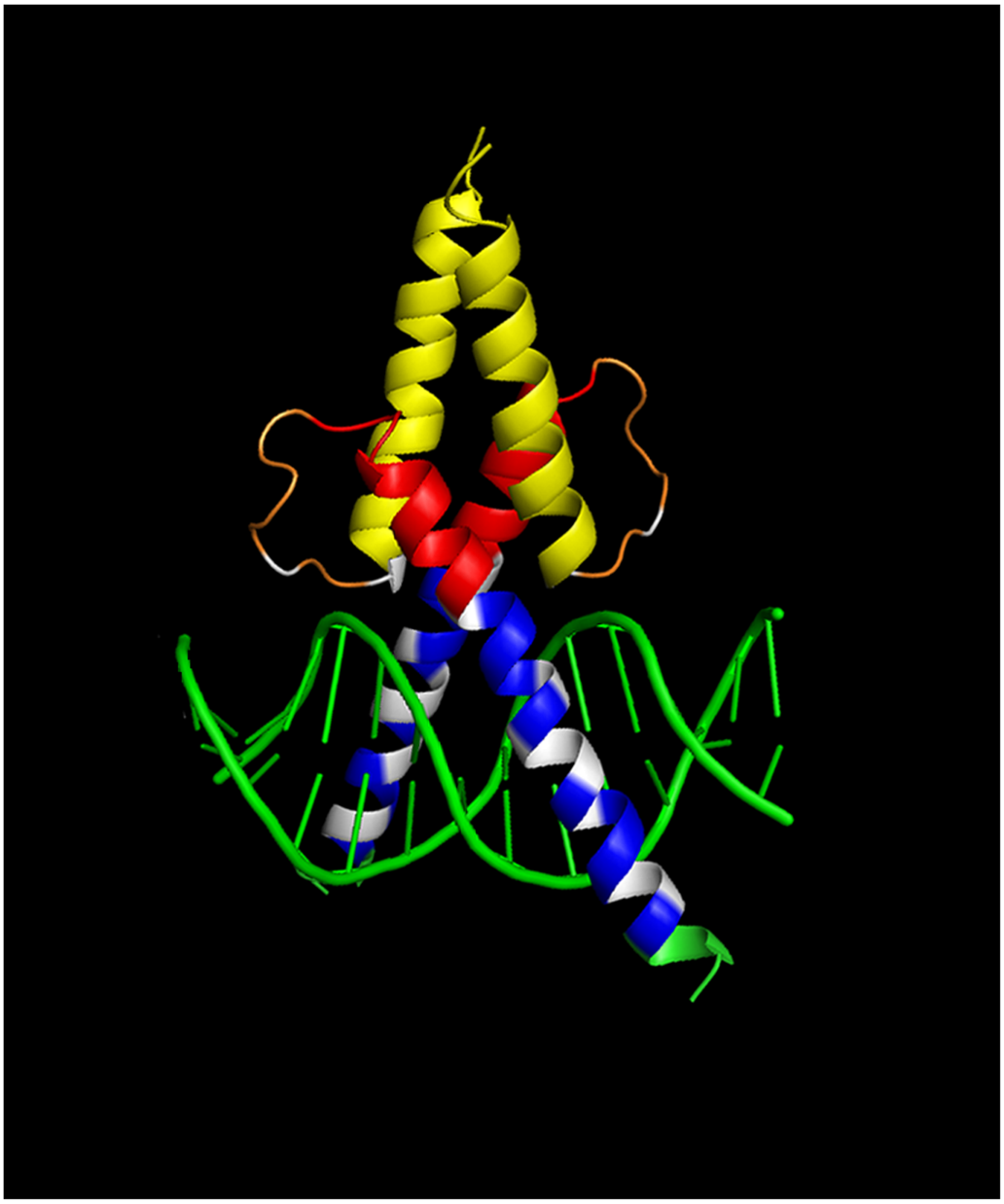

Figure 1.6 The structure of a dimerized bHLH bound to DNA

A visual representation derived from the MyoD-DNA crystal structure (Ma et al., 1994). The blue region represents the basic domain, the red region represents Helix1, the orange region represents the Loop, and the yellow region represents Helix2. DNA contacting residues are depicted in white.

MyoD and myogenin respectively. The first studies identified Neurogenin2 as a proneural transcription factor regulating neuronal differentiation in sensory neurons (Fode et al., 1998; Ma et al., 1999). Soon after, Neurogenin2 was found to regulate neuronal differentiation of interneurons and motor neurons within the spinal cord (Lee et al., 2005; Scardigli et al., 2001), and several regions within the brain, including cerebral cortex (Nieto et al., 2001). As in invertebrates, Neurogenin2 regulates neuronal differentiation through Notch signaling (Bertrand et al., 2002). Notch is a transmembrane signaling protein that negatively regulates neuronal differentiation by inhibiting Neurogenin2. Notch achieves this inhibition by inducing the transcription of the bHLH and HLH repressor proteins Hes and Id, respectively (Kageyama et al., 2005). In progenitor cells where Notch signaling is sufficiently low, Neurogenins will induce the transcription of proteins necessary for neuronal differentiation, and in cells where Notch signaling is sufficiently high, cells will inhibit Neurogenins and maintain their progenitor status (Kageyama et al., 2005). While the proneural effects of Neurogenin2 seem to be universal throughout the nervous system, Neurogenin2 is capable of regulating unique attributes of different neurons within the nervous system.

In the developing cortex, the Neurogenins (1 and 2) are expressed in the germinal zones of the developing cortex (VZ and SVZ) in accordance with their well defined role in neuronal differentiation. Elegant genetic studies revealed novel functions for the Neurogenins in specifying the neurotransmitter fate (Parras et al., 2002). With the genetic loss of Neurogenin2, a general decrease

was found in glutamatergic markers and a general increase in GABAergic markers. This effect was dramatically increased with the additional loss of Neurogenin1. Similarly, the decrease in neuronal differentiation within the cortex is mild with the loss of either Neurogenin1 or Neurogenin2 (Schuurmans et al., 2004), suggesting that these closely related transcription factors are capable for compensating for one other. This regulation of neurotransmitter fate within the cortex was the first suggestion that Neurogenin2 may regulate other aspects of cortical development other than neuronal differentiation. Yet this result left many questions unanswered including what additional aspects of cortical development Neurogenin2 may regulate and how developing neurons may regulate Neurogenin2 function.

Summary

The aim of my dissertation is to study in depth of how Neurogenin2 regulates cortical development and to discover novel aspects of cortical development regulated by Neurogenin2. The two articles presented in this dissertation identify the regulation of Neurogenin2 and novel functions of Neurogenin2 including the regulation of pyramidal neuron migration, dendritic morphology, and axonal projections. The final location of a pyramidal neuron within the cortex, its neuronal morphology, and its neurotransmitter dictates the neural circuits formed by a pyramidal neuron and ultimately underlies the function of the cerebral cortex itself. The proper formation of cortical circuits is critical as the cerebral cortex is the region of the brain allowing for the interpretation and

interaction with the environment. Understanding how the cerebral cortex is formed at the molecular level is of great importances as cortical malformations result in many neurological pathologies including mental retardation, epilepsy, and it is believed to underlie autism spectrum disorders.

Chapter 2

Title: Phosphorylation of *Neurogenin2* specifies the migration properties and the dendritic morphology of pyramidal neurons in the neocortex

Randal Hand [1*], Dante Bortone [1*], Pierre Mattar [2], Laurent Nguyen [3], Julian Ik-Tsen Heng [3], Sabrice Guerrier [1], Elizabeth Boutt [1], Eldon Peters [1], Anthony P Barnes [1], Carlos Parras [3], Carol Schuurmans [2], François Guillemot [3] and Franck Polleux [1#]

[1] Univ. North Carolina- Neuroscience Center- Department of Phamacology- Chapel Hill, NC 27599-7250-USA

[2] University of Calgary, Calgary, Alberta, Canada T2N 4N1

[3] Div. Mol. Neurobiol., NIMR- MRC, Mill Hill-UK

***** These two authors contributed equally to this work.

(Published in Neuron 2005)

Summary

The developmental mechanisms specifying the dendritic morphology of different neuronal subtypes are poorly understood at the molecular level. Here we demonstrate that the bHLH transcription factor Neurogenin2 (Ngn2) is both necessary and sufficient to specify the dendritic morphology of pyramidal neurons in vivo by specifying the polarity of its leading process outgrowth during the initiation of radial migration. The ability of Ngn2 to promote a polarized leading process outgrowth during the initiation of migration requires the phosphorylation of a tyrosine residue at position 241, an event that is neither involved in Ngn2 proneural function nor its direct transactivation properties. Interestingly, the migration defect observed in the Ngn2 knockout and in progenitors expressing $Ngn2^{Y241F}$ can be significantly rescued by inhibiting the activity of the small-GTPase RhoA in cortical progenitors. Our results demonstrate that Ngn2 coordinates the acquisition of the radial migration properties and the unipolar dendritic morphology characterizing pyramidal neurons through molecular mechanisms distinct from those mediating its proneural activity.

Introduction

The astonishing diversity of dendritic morphologies characterizing distinct neuronal subtypes underlies their sophisticated signal processing and computational properties (Hausser et al., 2000). Although an extensive amount of work performed over the past decade has identified the extracellular cues, the receptors and some of the corresponding signaling pathways controlling axon growth and guidance (Huber et al., 2003; Tessier-Lavigne and Goodman, 1996; Yu and Bargmann, 2001), the cellular and molecular mechanisms specifying the dendritic shape of distinct sub-classes of neurons is still poorly understood in vertebrates (Jan and Jan, 2003; Scott and Luo, 2001; Whitford et al., 2002). In particular, although substantial progress has been made in characterizing the late, activity-dependent phase of dendritic branching and adaptation of the size of the dendritic arbor relative to presynaptic inputs (Gaudilliere et al., 2004; Van Aelst and Cline, 2004; Wong et al., 2001), the early developmental mechanisms specifying the overall dendritic morphology of a given neuronal subclass has not been explored. One of the key unresolved questions is the relative importance of intrinsic versus extrinsic control in establishing the dendritic arborization characteristic of a given neuronal subtype (Scott and Luo, 2001).

The development of dendritic morphology conceptually involves at least four steps (Scott and Luo, 2001): (1) dendritic initiation, (2) dendritic outgrowth and guidance, (3) dendritic branching including spine or synapse formation and (4) limitation of dendritic outgrowth. The first step dictates whether dendritic

outgrowth will be polarized or not and thereby determining whether the dendritic field of a neuron will sample the 'presynaptic space' uniformly or in a biased manner. In the neocortex and hippocampus, *pyramidal* neurons are initially characterized by a polarized outgrowth of one major dendrite i.e. the apical dendrite (Miller, 1981; Peters and Kara, 1985a), whereas the vast majority of cortical interneurons undergo an unpolarized dendritic outgrowth leading to a multipolar dendritic morphology that is by definition *non-pyramidal* (Miller, 1986) (Peters and Kara, 1985b). Interestingly, it has been recently shown that pyramidal and non-pyramidal neurons represent two developmentally distinct neuronal lineages generated by specialized and distinct sets of progenitors. Pyramidal neurons (1) originate from progenitors located in the *dorsal telencephalon* and express region-specific transcription factors that include *Emx1*, *Neurogenin* (*Ngn*) 1 and *Ngn2*, *Pax6* and *Tlx1/2* (2) migrate *radially* along a radial glial scaffold to reach their appropriate laminar position in an inside-first outside-last manner, (3) have an initially unipolar, unbranched pyramidal dendritic morphology characterized by an apical dendrite extending towards the pial surface, (4) generate axons that project over long distances to sub-cortical or to other cortical areas, and (5) use glutamate as an excitatory neurotransmitter. On the other hand, cortical interneurons (1) originate from progenitors located in the *ventral telencephalon* [medial and caudal ganglionic eminence (MGE and CGE respectively)] and express a different set of transcription factors such as *Mash1*, *Nkx2.1*, *Lhx6* and *Dlx1/2*, (2) migrate *tangentially* to reach the cortex, (3) display

a variety of multipolar, non-pyramidal dendritic morphologies, (4) have locally-projecting axons and (5) use GABA as an inhibitory neurotransmitter (reviewed in (Marin and Rubenstein, 2003; Schuurmans and Guillemot, 2002)).

In *Drosophila*, proneural basic-helix-loop-helix (bHLH) transcription factors such as *atonal* or *achaete-scute* have been isolated based on their ability to promote neural fates in external sense organs models ((Jarman et al., 1993); reviewed in (Bertrand et al., 2002)). Interestingly, in the fly central nervous system, *atonal* does not have proneural activity but is instead specifically required to control the pattern of axonal branching during larval and pupal development, an activity it carries out through interactions with Notch (Hassan et al., 2000). Furthermore, although the proneural activity of bHLH transcription factors has been demonstrated to reside in the DNA-binding basic region (Quan et al., 2004), there is evidence that neuronal subtype specification is controlled by residues outside the DNA-binding domain in both vertebrates and invertebrates (Huang et al., 2000; Nakada et al., 2004). In mammals, recent evidence has also supported the notion that the bHLH protein *Ngn2* plays a critical role not only in the acquisition of pan-neuronal properties (Lee and Pfaff, 2003; Nieto et al., 2001; Scardigli et al., 2001; Sun et al., 2001) but also in the specification of neuronal subtypes (Fode et al., 1998; Fode et al., 2000; Lee and Pfaff, 2003; Ma et al., 1999; Mizuguchi et al., 2001; Parras et al., 2002; Ross et al., 2003; Scardigli et al., 2001; Schuurmans et al., 2004; Seibt et al., 2003). Specifically, a recent study demonstrated that *Ngn1* and *Ngn2* specify the

expression of glutamate as the excitatory neurotransmitter in pyramidal cortical neurons (Schuurmans et al., 2004). These results raised the question of whether *Ngn2* function in cortical progenitors was limited to the specification of neurotransmitter expression or whether *Ngn2* also participates to the specification of other phenotypic traits of cortical glutamatergic neurons, such as their radial migration properties and their pyramidal dendritic morphology?

Interestingly, recent time-lapse confocal analysis of the early initiation of radial migration of cortical progenitors has revealed that upon cell-cycle exit, immature neurons display a striking transition from a multipolar to a unipolar morphology at the level of the subventricular zone (Noctor et al., 2004). These results strongly suggest that molecular mechanisms operating during the initiation of radial migration are specifying the polarity of the leading process extension ultimately determining the unipolar dendritic morphology of pyramidal neurons in the cortex (Kriegstein and Noctor, 2004).

In the present study, we provide genetic evidence that the coordinated specification of the radial migration properties and the pyramidal dendritic morphology is controlled by the transcription factor *Ngn2* at least in part by functionally repressing the activity of the small GTPase RhoA. We combined *in vivo* and *in vitro* gain- and loss-of-function approaches to demonstrate that *Ngn2* specifies the dendritic morphology of pyramidal neurons by controlling their early polarization during the initiation of radial migration. Importantly, this activity is mediated by phosphorylation of a tyrosine residue at position 241 in the C-

terminal domain of Ngn2, a residue that is not directly involved in mediating its transactivation properties or its proneural properties. Finally, we used time-lapse confocal microscopy of individual migrating neurons in slices and found that neurons expressing Ngn2^{Y241F} display a strikingly leading process polarity defect and a failure to undergo proper nucleokinesis.

Results

Neurogenin2 is expressed by cortical progenitors and transiently by post-mitotic neurons during the initiation of radial migration

It is well established that *Ngn2* mRNA is specifically expressed by cortical progenitors in both the ventricular zone (VZ) and sub-ventricular zone (SVZ) of the dorsal telencephalon throughout neurogenesis (Fode et al., 2000; Miyata et al., 2004; Schuurmans et al., 2004), while it is not expressed by progenitors located ventrally in the ganglionic eminence (GE). Moreover, it has been recently shown that Ngn2 protein expression is regulated in a cell-cycle specific manner in the cortical VZ (Miyata et al., 2004). In particular, Ngn2 is expressed by cortical progenitors during the window of time when they commit to the neuronal lineage both in the 'surface', proliferative divisions in the VZ and the 'non-surface' neurogenic divisions in the SVZ (Miyata et al., 2004; Murciano et al., 2002).

We wanted to explore more carefully the spatial pattern of Ngn2 expression in the cortical germinal zones at E16 (when both the VZ and SVZ are prominent) by performing immunofluorescent staining directed against Ngn2

(**Fig. 2.1**). We confirmed that cortical progenitors located in the VZ express Ngn2 (**Fig. 2.1A** and **2.1J**). Interestingly, Ngn2 was also expressed by a subset of cells in the SVZ and in the intermediate zone (IZ), where early post-mitotic neurons exit the cell cycle and initiate radial migration (**Fig. 2.1A-C**). In order to test directly if these cells were indeed post-mitotic neurons, we performed double staining for Ngn2 and three distinct early post-mitotic neuronal markers: NeuN (**Fig. 2.1 D-E'''**), Microtubule Associated Protein-2 or MAP2 (**Fig. 2.1F-G'''**) and β-III tubulin or TuJ1 (**Fig. 2.1H-I'''**). This analysis showed unequivocally that Ngn2 is expressed by a sub-population of post-mitotic cells in the SVZ and IZ (**Fig. 2.1E-E'''**, **G-G'''** and **I-I'''**). The quantification shown in **Figure 2.1J** shows that although the majority of cells expressing Ngn2 (green bars) were located in the VZ, the bulk of Ngn2-NeuN double-labeled neurons (orange bars in **Fig. 2.1J**) were located primarily in the SVZ. The percentage of Ngn2+ cells expressing NeuN increased almost linearly as a function of the distance from the ventricle (**Fig. 2.1H**) reaching approximately 50% in the SVZ and 80% in the IZ. Interestingly, Ngn2 is very rapidly down-regulated at the protein level once neurons are reaching the top of the IZ and the CP. This analysis shows that Ngn2 is expressed transiently by post-mitotic neurons located in the SVZ and the IZ, coinciding with the time when these neurons engage in radial migration and display a morphological transformation from multipolar to unipolar (Noctor et al., 2004).

***Neurogenin2* is necessary for the specification of the radial migration properties of cortical neurons**

Recent BrdU birthdating studies suggested that *Ngn2* knockout embryos were characterized by a pronounced migration defect in the cortex as suggested by the ectopic deep location of cells born between E12.5 and E14.5 in the germinal and intermediate zones of neonatal *Ngn2*-/- cortices (Schuurmans et al., 2004). We wanted to further explore the role of *Ngn2* in specifying the radial migration properties of cortical neurons. To do this we developed a new allele of *Ngn2* by replacing the entire *Ngn2* coding sequence with EGFP ([*Ngn2*^{KIFGP}; see Methods; (Seibt et al., 2003)). Throughout neurogenesis, EGFP faithfully reports the regional expression of *Ngn2* in the dorsal telencephalon of heterozygous *Ngn2*$^{KIGFP/+}$ embryos with the difference that EGFP is maintained much longer in neurons and acts as a lineage tracer (**Fig. 2.2A-B** at E14.5 and data not shown). Interestingly, homozygous *Ngn2*$^{KIGFP/KIGFP}$ embryos express approximately two-fold more EGFP compared to *Ngn2*$^{KIFGP/+}$ embryos (Compare **Fig. 2.2 A** and **C**). Similar to two previously described *Ngn2* null alleles, the majority of *Ngn2*$^{KIGFP/KIGFP}$ mice die shortly after birth (Fode et al., 1998; Fode et al., 2000). We will refer to mice homozygous for this EGFP allele as Ngn2-/- or Ngn2 knockout in the remainder of the study.

Comparison of hematoxylin/eosin-stained sagittal sections from *Ngn2*+/+ and *Ngn2*-/- neonatal cortices (**Fig. 2.2**) revealed the presence of large heterotopic cell clusters in the *Ngn2* mutants that are suggestive of a neuronal

migration defect (arrows in **Fig. 2.2D-F**) but not in *Ngn2*+/+ controls (**Fig. 2.2C-E**). We also noticed a pronounced decrease in the cell density of the cortical plate of *Ngn2-/-* (**Fig. 2.2F**) compared to *Ngn2*+/+ neonates (**Fig. 2.2E**) suggestive of a decreased level of migration in the Ngn2 knockout cortex. This is reinforced by the presence of streams of cells that seemed unable to exit the SVZ in the Ngn2-/- cortex (arrow in Fig. 2F). Other heterotopias are observed at the corticostriatal boundary and the hippocampus of the Ngn2-/- mice (arrows in **Fig. 2.2H** and **2.2J** respectively) but not in the control mice (**Fig. 2.2G** and **2.2I** respectively).

In order to test directly if radial migration was defective in *Ngn2-/-* embryos, we implemented a new technique that combines electroporation-mediated gene transfer and *in vitro* organotypic slice culture (see **Suppl. Fig. 2.1** for details). This *ex vivo* cortical electroporation technique allows the transfection of radial glial neural progenitors at reproducible efficiencies (up to 30% transfection efficiency among nestin+ VZ progenitors- Hand and Polleux-data not shown). After two days *in vitro* (2div), a cohort of post-mitotic neurons generated by the electroporated radial glial progenitors have engaged radial migration and are found in the IZ (**Suppl. Fig 2.1H**). By 4 div this single cohort of radially migrating neurons have reached their final position at the top of the cortical plate (**Suppl. Fig 2.1I**) recapitulating the same timing displayed *in vivo* as demonstrated by birthdating studies (Berry and Rogers, 1965) as well as using *in utero* electroporation technique (Hand, Bortone and Polleux, *manuscript in*

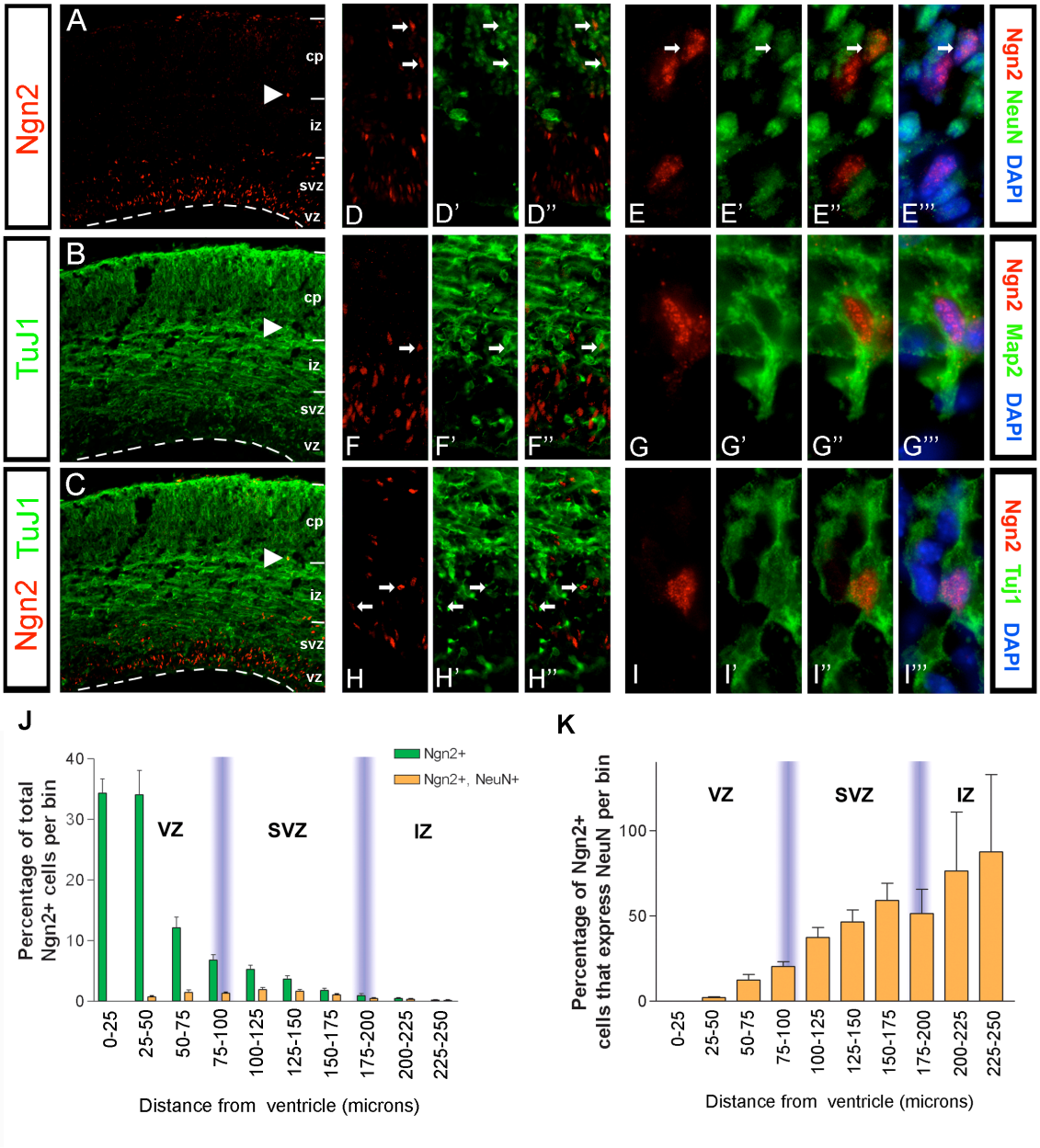

Figure 1 -Hand et al.

<u>Figure 2.1</u> Neurogenin2 is expressed both in neuronal progenitors and early post-mitotic neurons in the developing cortex

(A-C) Double immunofluorescent staining performed at embryonic day (E) 16 on cryostat sections from mouse cortex against Ngn2 protein (A) and the early nuclear neuronal marker βIII-

tubulin (TuJ1). (B). Ngn2 is expressed primarily by cortical dividing progenitors in both the VZ and SVZ and also transiently by early post-mitotic neurons located in the SVZ and IZ (arrowheads in A-C).

(D-D'') High magnification images of Ngn2 (D) and NeuN (D') double immunofluorescent staining in the VZ-SVZ layers showing the presence of several double immunopositive cells in the SVZ (arrows).

(E-E''') Higher magnification of Ngn2 (E) NeuN (E') double positive cell (E'') showing that Ngn2 is mainly nuclear as shown by the co-localization with DAPI positive nucleus (arrow in E''').

(F-F'' and G-G''') Double immunofluorescent staining of Ngn2 (F and G) and MAP2 (F' and G') also reveals the presence of double labeled neurons in the SVZ (arrow in F'' and G''-G''').

(H-H'' and I-I''') Double immunofluorescent staining of Ngn2 (H and I) and a neuron specific isoform of β-tubulin III (Tuj1- H' and I') confirms the presence of Ngn2-positive neurons in the SVZ (arrow in F'' and G''-G''').

(J) Quantification of the distribution of Ngn2 positive cells (green bars) and Ngn2/NeuN double positive neurons (orange bars) expressed as a percentage of the total number of Ngn2 positive cells found in 25 micron-wide bins. At E16, the vast majority of Ngn2+ cells are located in the VZ (approx. 80%), whereas the majority of Ngn2-NeuN double positive cells are concentrated in the SVZ (orange bars).

(K) Quantification of the radial distribution of Ngn2-NeuN double positive neurons. This histogram represents the frequency of Ngn2-NeuN double positive neurons calculated as a percentage of the total number of cells expressing Ngn2+ in each bin. The percentage of double positive neurons clearly increases linearly away from the ventricular surface. This analysis shows that approximately 40-50% of Ngn2+ cells are expressing NeuN in the SVZ and 80-90% of Ngn2+ cells are expressing NeuN in the IZ at E16.

Abbreviations: VZ, ventricular zone; SVZ, subventricular zone; IZ, intermediate zone.

preparation; see also (Bai et al., 2003; Hasegawa et al., 2004; Hatanaka and Murakami, 2002; Kawauchi et al., 2003; Shu et al., 2004; Tabata and Nakajima, 2003). Therefore, this technique allows the modification of gene expression in a synchronous cohort of cortical neurons and the subsequent examination of their migration properties and their final dendritic morphology *in vitro*.

Cortical progenitors electroporated at E14.5 (during the production layer 5 (Polleux et al., 1997)) give rise to neurons migrating radially into the intermediate zone and accumulating in the cortical plate of control cortex after 4 div (**Fig. 2.2K**). On the other hand, cortical electroporation of E14.5 *Ngn2*-/- littermate embryos revealed a pronounced migration defect resulting in the accumulation of transfected cells in the SVZ and IZ (**Fig. 2.2J**). Few cells successfully migrated into the cortical plate in the *Ngn2*-/- slices after 4 div (star in **Fig. 2.2J**). We quantified neuronal migration by using an automatized cell profile counting method where the total number of cell profiles along the radial axis of the cortical wall is expressed as normalized percentage of the total distance between the ventricle and the pial surface (**Fig. 2.2K-L** see Methods for details). This normalized distribution analysis demonstrates that after 4 div, approximately 30% of electroporated cells successfully migrated to the CP-MZ layers in *Ngn2+/+* slices whereas less than 10% of electroporated cells do so in the *Ngn2-/-* slices (**Fig. 2.2M-N**). In contrast a significantly higher percentage of electroporated cells remain in the lower IZ and SVZ regions of the *Ngn2-/-* slices compared to control *Ngn2+/+* slices (**Fig. 2.2M-N**).

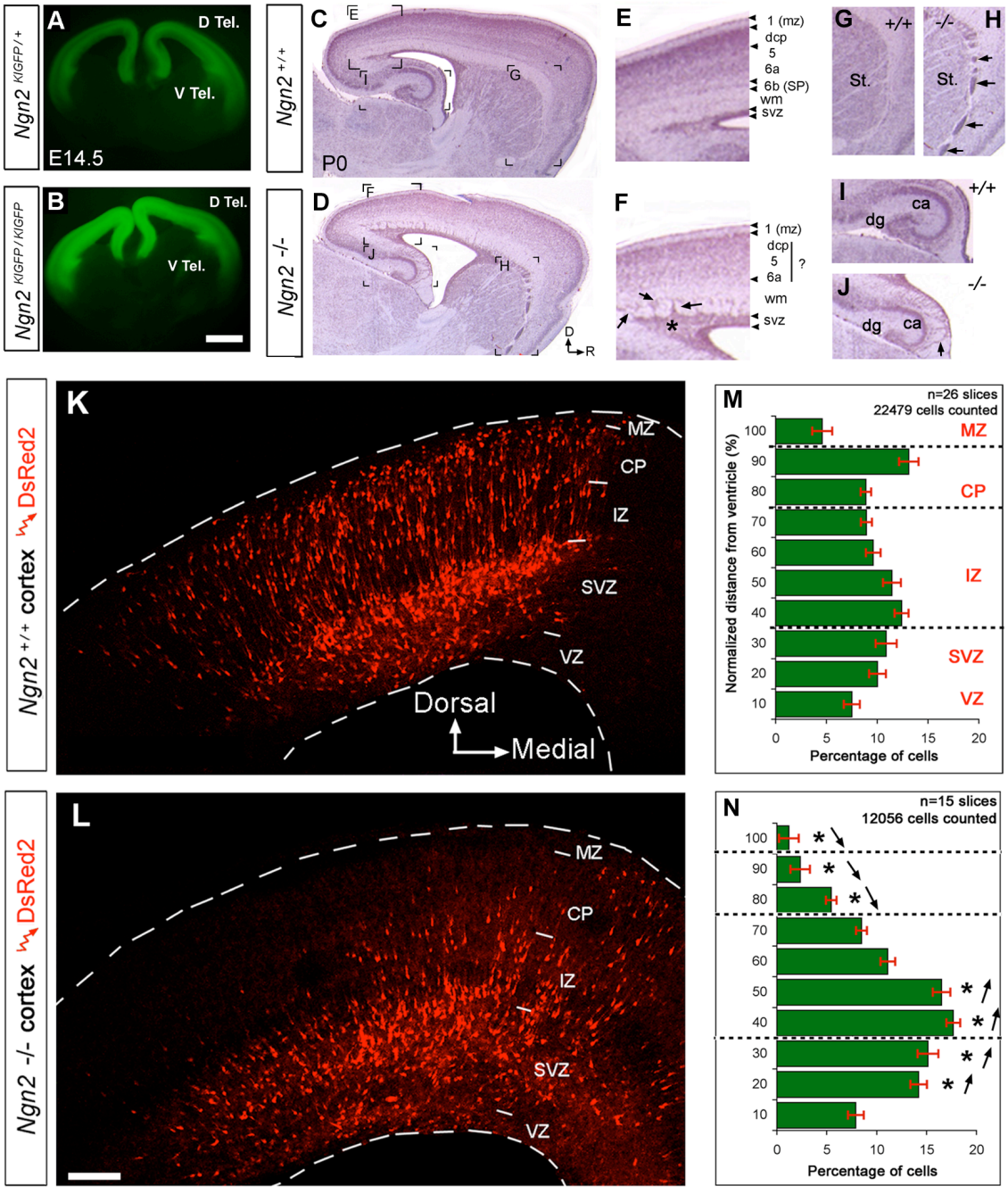

Figure 2.2 ***Neurogenin2*** **is required** ***in vivo*** **for the proper migration of cortical neurons.**

(A-B) GFP epifluorescence in live coronal organotypic slices isolated from E14.5 *Neurogenin2* GFP knockin heterozygous mouse embryos (*Ngn2*$^{KIGFP/+}$; A-B) reports expression of *Ngn2* in the

dorsal telencephalon (D Tel.). Note the sharp boundary of GFP expression at the border between the dorsal and ventral telencephalon (V Tel.), where Ngn2 is not expressed. Organotypic slices isolated from E14.5 homozygous *Ngn2*$^{KIGFP/KIGFP}$ embryos (C-D) display approximately two-fold higher GFP expression in the dorsal telencephalon, but the regionalized expression of *Ngn2* is unchanged compared to heterozygous mice.

(C-J) Sagittal cryostat sections from post-natal day 0 (P0) *Ngn2+/+* (C-E-G and I) and *Ngn2-/-* (D-F-H and J) mice counterstained with hematoxylin-eosin reveals the cytoarchitecture of the cortex at birth. At higher magnification streams of ectopic cells emerging from the SVZ (star in F) are detected in *Ngn2-/-* mice (arrows in F) but not in control *Ngn2+/+* mice (E). Heterotopic cell clusters are also found at the cortico-striatal boundary and underneath the developing CA regions of the hippocampus of the Ngn2-/- (arrows in H and J respectively) but not the Ngn2+/+ mice (G and I).

(K-L) *Ex vivo* electroporation of DsRed2 in cortical progenitors of *Ngn2+/+* E14.5 embryos followed by organotypic culture for 4 days *in vitro* (div) reveals the radial migration potential of post-mitotic neurons that already started to accumulate in the CP of Ngn2+/+ slices (K) but not in Ngn2-/- slices (L).

(M-N) Quantification of the distribution of DsRed2-expressing cells along the radial axis of E14.5 Ngn2+/+ (M) and Ngn2-/- slices (N) after 4 div. (* $p<0.001$ Chi-square test comparing the proportion of DsRed2-expressing cells in corresponding bins of Ngn2+/+ and Ngn2-/- slices).

Abbreviations: ca: Ammon's horn regions of the hippocampus; CP, cortical plate; dg: dentate gyrus; IZ, intermediate zone; VZ, ventricular zone; SVZ, subventricular zone; div, days in vitro.

This quantitative analysis suggests that *Ngn2* is required for the proper initiation of radial migration by cortical progenitors. However, a potential caveat of this analysis is due to the long-term consequences of the complete *Ngn2* loss-of-function on the fate of cortical progenitors. In fact, several studies have already demonstrated that *Ngn2* plays an essential role in the early specification of the molecular identity of dorsal telencephalic neurons (reviewed in (Schuurmans and Guillemot, 2002)). At E12.5 dorsal progenitors in *Ngn2* knockout upregulate *Mash1*, a bHLH transcription factor normally expressed predominantly by ventral progenitors of the GE which plays an important role in the specification of the phenotype of GABAergic neurons of the striatum and cortex (Fode et al., 2000; Parras et al., 2002; Schuurmans et al., 2004). Therefore, there are long-term fate changes of knocking out *Ngn2* expression in dorsal telencephalic progenitors that could indirectly affect the migratory properties of their daughter neurons.

Acute conditional deletion of *Neurogenin2* in cortical progenitors alters the initiation of radial migration

In order to circumvent some of these long-term effects, we performed an acute deletion of *Ngn2* expression in cortical progenitors, using Cre-mediated deletion of *Ngn2* specifically in dorsal telencephalic progenitors. This was achieved by using *ex vivo* electroporation of a plasmid expressing Cre recombinase-IRES-EGFP in E14.5 cortical progenitors harboring a conditional allele of Ngn2 (*Ngn2*^{KIFloxNgn2Flox}; see Methods for detail). As shown in Figure 3A-

B, our electroporation technique leads to a high co-expression of high levels of Cre-recombinase and EGFP in E14.5 cortical progenitors within the VZ in less than 24 hours *in vitro*. In order to demonstrate that this electroporation-mediated Cre-recombinase expression is efficiently knocking out Neurogenin2 protein expression, we performed anti-Ngn2 immunofluorescent staining of the slices electroporated with pCIG2:Cre-IRES-EGFP. As shown in **Figure 2.3C-D** Ngn2 immunoreactivity is markedly decreased in cells expressing Cre recombinase-IRES-EGFP. After 4 div, control (EGFP only) electroporation of *Ngn2*^{KIFloxNgn2Flox} E14.5 cortical slices results in a robust neuronal migration outside the VZ-SVZ into the IZ and up to the CP (**Fig. 2.3E** and **2.3G**). In contrast E14.5 *Ngn2*^{KIFloxNgn2Flox} cortical slices electroporated with Cre-recombinase present a pronounced neuronal migration defect with very few neurons reaching the CP (**Fig. 2.3F** and **2.3G**). These results reinforce our conclusion that *Ngn2* is necessary to specify the migration properties of cortical neurons.

One caveat of this interpretation is that this acute loss of Ngn2 function approach affects the percentage of electroporated EGFP-expressing cells expressing pan-neuronal markers such as HuC/D as an index of the proneural potential of cortical progenitors (**Fig. 2.3H**). This quantification reveals that after 4 div, only 15% of cells electroporated with Cre-expressing vector in *Ngn2*^{KIFloxNgn2Flox} slices expressed the neuronal marker HuC/D against approximately 60% in *Ngn2*^{KIFloxNgn2Flox} slices electroporated with control (EGFP only). This result suggests a strong proneural defect due to the acute inactivation

of Ngn2 expression in cortical progenitors which is compatible with the well-documented function of *Neurogenins* (reviewed in (Bertrand et al., 2002)). Therefore, the migration defect characterizing both the complete and the conditional loss of *Ngn2* function could be a secondary consequence of the inability of cortical progenitors to initiate neuronal differentiation and possibly exit the cell cycle. The dominant proneural function of this class of transcription factors represents one of the main limitations in the exploration of their other potential functions in neuronal subtype specification. To overcome this limitation, we decided to perform a structure-function analysis of Ngn2 in order to isolate potential residues that could uncouple the proneural activity of Neurogenin2 from its potential function in the phenotypic specification of neuronal subtypes.

Neurogenin2 is tyrosine phosphorylated *in vivo*

The alignment of chick (*Gallus gallus*), mouse (*Mus musculus*) and human (*Homo sapiens*) Ngn2 protein sequences revealed a complete conservation of the bHLH domains and a partial conservation of domains of unknown function in the amino- (N-) and carboxy- (C-) terminal domains (**Fig. 2.4A**). Interestingly, the N- and C-terminal domains of Ngn2 are also highly divergent from Ngn1 and Ngn3, two of its most closely related homologues in the mouse genome (**Fig. 2.4B**). In order to isolate potential residues of Ngn2 outside the DNA-binding domain that might mediate neuronal subtype specification, we first sought to determine if Ngn2 was post-translationally modified and specifically if it was

phosphorylated in cortical progenitors. Using electroporation of myc-tagged Ngn2 in E14.5 cortical progenitors followed by 24 hours of cortical wholemount culture *in vitro* in the presence of $^{\gamma 32}$P-labeled ATP (**Fig. 2.4C**) we found that Ngn2 is phosphorylated in cortical precursors (**Fig. 2.4D**).

To examine the putative phosphorylation sites in Ngn2, we used a sequence- and structure-based prediction program ((Blom et al., 1999); see Experimental Procedures) which predicted 15 potential serine residues, 4 threonine residues and 3 tyrosine residues displaying a significant ($p>0.90$) probability of phosphorylation (data not shown). Using electroporation of a GST-Ngn2 fusion protein in cortical precursors followed by GST-pulldown and thrombin cleavage of Ngn2 from GST, we found that Ngn2 is tyrosine phosphorylated *in vivo* using anti-phosphotyrosine immunoblotting (**Fig. 2.4E**). Using GST-pulldown in undifferentiated P19 cells in order to increase the protein yield we were able to confirm that Ngn2 is tyrosine phosphorylated (**Fig. 2.4F**). Furthermore we found that tyrosine 241 is the major site for tyrosine phosphorylation in Ngn2 since its mutation into a non-phosphorylatable phenylalanine residue (Ngn2^{Y241F}) drastically reduced the signal detected by phosphotyrosine immunoblotting.

Therefore we focused our effort on the effects of mutating tyrosine 241. In addition, mutations of the two other tyrosine residues presenting a high probability to get phosphorylated (Y226F and Y252F) did not produce any detectable effects on the acquisition of neuronal migration properties or dendritic

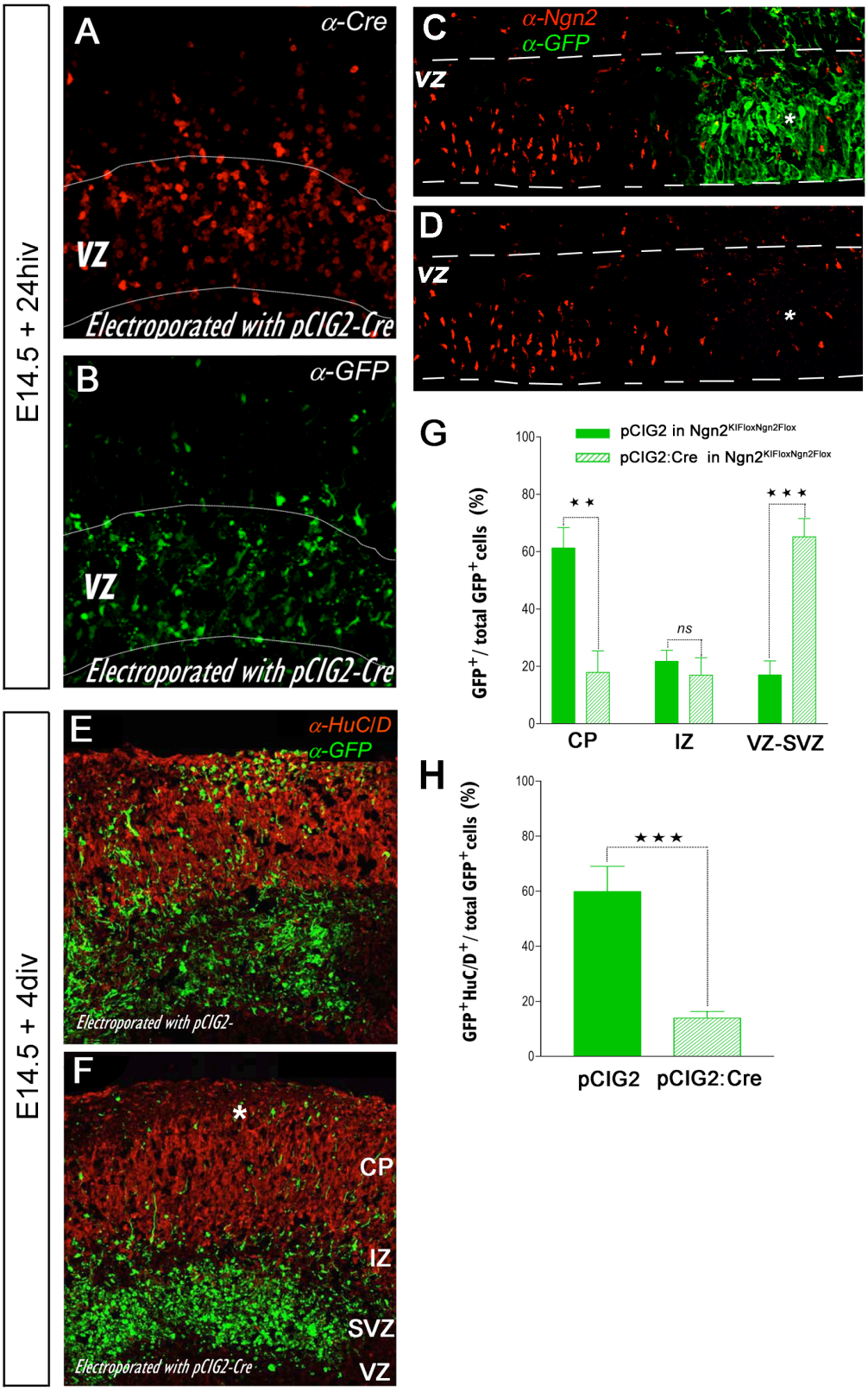
E14.5 + 24hiv
A
α-Cre
VZ
Electroporated with pCIG2-Cre
B
α-GFP
VZ
Electroporated with pCIG2-Cre
C
α-Ngn2
α-GFP
VZ
*
D
VZ
*
G
pCIG2 in Ngn2KIFloxNgn2Flox
pCIG2:Cre in Ngn2KIFloxNgn2Flox
GFP+ / total GFP+cells (%)
100
80
60
40
20
0
**
ns
***
CP
IZ
VZ-SVZ
E14.5 + 4div
E
α-HuC/D
α-GFP
Electroporated with pCIG2-
F
*
CP
IZ
SVZ
VZ
Electroporated with pCIG2-Cre
H
GFP+HuC/D+ / total GFP+cells (%)
100
80
60
40
20
0
***
pCIG2
pCIG2:Cre

Figure 2.3 Acute deletion of Ngn2 expression in E14.5 cortical progenitors impairs radial migration

(A-B) *Ex vivo* electroporation of E14.5 dorsal telencephalic progenitors using a pCIG2:Cre-IRES-EGFP recombinase-IRES-EGFP followed by *in vitro* organotypic slice culture for 24 hours *in vitro* results in high-level of co-expression of Cre-recombinase (A) and EGFP (B).

(C-D) Electroporation of Cre-recombinase in cortical progenitors from *Ngn2*^{KIFloxNgn2Flox} E14.5 embryos (C) results in a pronounced down-regulation of Ngn2 protein expression (star in C-D) in EGFP-electroporated VZ progenitors but not in adjacent non-electroporated regions.

(E-F) Acute deletion of Ngn2 expression in cortical progenitors results in a pronounced decrease in the number of neurons reaching the CP (star in F) compared to *Ngn2*^{KIFloxNgn2Flox} E14.5 progenitors electroporated with control empty pCIG2 (E). Immunofluorescence against the neuronal marker HuC/D (red in E and F) reveals the cytoarchitecture of the slices after 4 div where HuC/D positive post-mitotic neurons are mainly found in the CP.

(G) Quantification of the percentage of EGFP+ cells located in the VZ-SVZ, IZ or CP compartments. Cre-mediated recombination of *Ngn2*^{KIFloxNgn2Flox} allele in cortical progenitors results in a pronounced decrease in the proportion of cells in the CP and a corresponding increase in the percentage of cells found in VZ/SVZ region. For both G and H panels, n= 7 slices, unpaired t-test, ** $p<0.01$, *** $p<0.001$.

(H) Quantification of the percentage of GFP+ cells that express the neuronal marker HuC/D reveals a pronounced proneural defect in progenitors where Ngn2 was recombined (pCIG2::Cre) compared to control transfected progenitors (pCIG2).

morphologies (see **Suppl. Fig 2.5** and data not shown). Interestingly, tyrosine 241 (i) is part of a proline-rich motif (YWQPPPP, boxed in **Fig. 2.4A**) that constitutes a predicted binding site for SH3-containing proteins, (ii) is mammalian-specific (not conserved in chick but perfectly conserved in human) and (iii) is specific to Ngn2 (not present in mouse Ngn1 or mouse Ngn3; see box in **Fig. 2.4B**).

In order to test the requirement of the DNA-binding properties of Ngn2 in mediating some of its biological functions, we also produced a DNA-binding incompetent form of Ngn2 by substituting the last two basic/polar residues of the basic domain (position 123-124 respectively NR; arrows in **Fig. 2.4A**) into non-polar residues (AQ). This double substitution (e.g. $Ngn2^{NR->AQ}$) was previously shown to abolish Ngn1- and Ngn2-mediated DNA-binding and therefore the transactivation of its direct target promoter sequences in a dominant-negative manner (Lee and Pfaff, 2003; Sun et al., 2001) without interfering with its nuclear translocation (see **Suppl. Fig. 2.2**).

We first wanted to determine if tyrosine 241 was located within the transcription-activation (transactivation) domain (TAD) of Ngn2. To our knowledge, the TAD of Ngn2 has never been mapped before. Therefore we performed a standard TAD mapping using a modified Gal4-UAS system (**Fig. 2.4G**). The TAD of most proneural bHLH transcription factors lies in the proximal or the distal portion of the C-terminal domain of the protein (Sharma et al., 1999). Therefore, we designed three Gal4 fusion proteins containing respectively (1) the

entire C-terminal tail of Ngn2 (residues 181 to 263), (2) the proximal part of the C-terminal tail (residues 181 to 213; hatched in **Fig. 2.4G**) and (3) the distal domain of the C-terminal tail (residues 214-263; black in **Fig. 2.4G**). Using a normalized UAS-Luciferase reporter assay, we found that the first half of the C-terminal tail proximal to the second helix (181-213) displays transactivation properties comparable to the entire C-terminal tail (**Fig. 2.4G**). Interestingly, the distal portion encompassing residues 214 to 263 (including tyrosine 241) did not have any significant transactivation properties (**Fig. 2.4F**).

To assess more directly the transactivation properties of the mutant forms of Ngn2 used in this study, we used the 1.7 kB promoter region of *NeuroD* previously shown to be strongly transactivated by Ngn3 (Huang et al., 2000a). We subcloned this portion of the *NeuroD* promoter upstream of a luciferase reporter system and used constitutive Renilla expression to normalize for transfection efficiency in undifferentiated P19 cells. We found that Ngn2 strongly transactivates the *NeuroD* promoter (**Fig. 2.4H**; on average 20 fold $p<0.01$ Mann Whitney test n=3), whereas $Ngn2^{NR->AQ}$ and $Ngn2^{\Delta basic}$ (presenting a complete deletion of the basic domain) both failed to transactivate the *NeuroD* promoter (**Fig. 2.4H**). Interestingly, the mutation of tyrosine 241 did not interfere with Ngn2-mediated transactivation of the *NeuroD* promoter (**Fig. 2.4H**).

Taken together with the transactivation mapping, these results suggest that tyrosine 241 does not affect the ability of Ngn2 to heterodimerize with class-I bHLH transcription factors such as E12 or E47, a function primarily mediated by

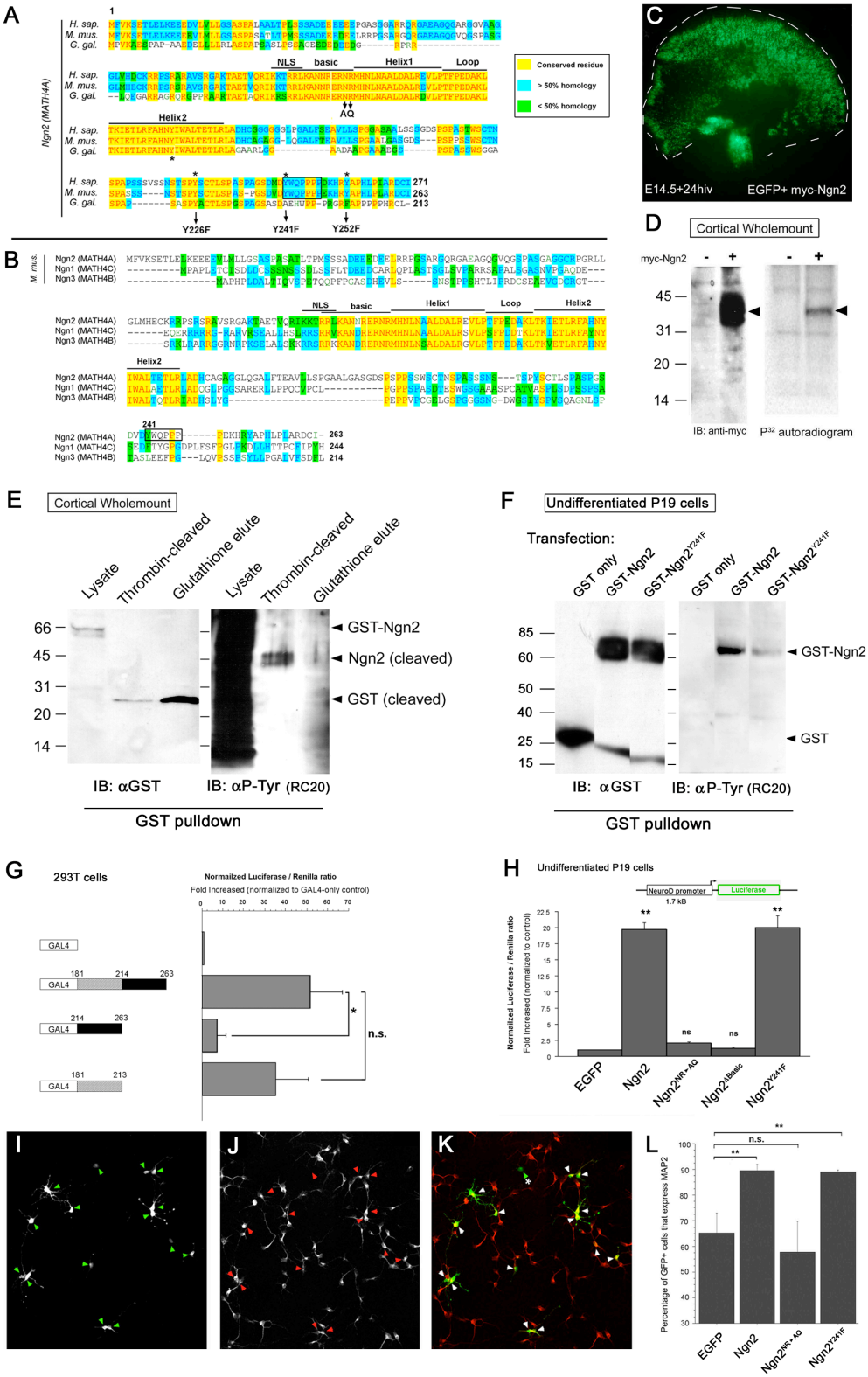
A
Ngn2 (MATH4A)
H. sap.
M. mus.
G. gal.
NLS
basic
Helix1
Loop
Helix2
AQ
Conserved residue
> 50% homology
< 50% homology
Y226F
Y241F
Y252F
B
M. mus.
Ngn2 (MATH4A)
Ngn1 (MATH4C)
Ngn3 (MATH4B)
NLS
basic
Helix1
Loop
Helix2
C
E14.5+24hiv
EGFP+ myc-Ngn2
D
Cortical Wholemount
myc-Ngn2
45
31
20
14
IB: anti-myc
P32 autoradiogram
E
Cortical Wholemount
Lysate
Thrombin-cleaved
Glutathione elute
GST-Ngn2
Ngn2 (cleaved)
GST (cleaved)
IB: αGST
IB: αP-Tyr (RC20)
GST pulldown
F
Undifferentiated P19 cells
Transfection:
GST only
GST-Ngn2
GST-Ngn2Y241F
GST
IB: αGST
IB: αP-Tyr (RC20)
GST pulldown
G
293T cells
Normalized Luciferase / Renilla ratio
Fold Increased (normalized to GAL4-only control)
GAL4
n.s.
H
Undifferentiated P19 cells
NeuroD promoter
Luciferase
1.7 kB
Normalized Luciferase / Renilla ratio
Fold Increased (normalized to control)
EGFP
Ngn2
Ngn2NR+AQ
Ngn2ΔBasic
Ngn2Y241F
I
J
K
L
Percentage of GFP+ cells that express MAP2
n.s.

Figure 2.4. Neurogenin2 is tyrosine-phosphorylated in cortical precursors

(A) Alignment of human (*Homo sapiens* NP_076924), mouse (*Mus musculus* NP_033848) and chick (*Gallus gallus* NP_990127) Ngn2 protein sequences reveals almost perfect conservation of the basic (DNA binding domain) Helix1, Loop and Helix2 domains and partially conserved stretches of residues in the N- and C-terminal domains. The nuclear localization sequence (NLS) is partially overlapping with the basic domain necessary for DNA-binding. The asterisks indicate the position of the four tyrosine residues conserved in mouse and human Ngn2 proteins. The arrowheads overlying specific residues indicate the position of the residues mutated in mouse Ngn2: NR residues in position 123-124 of the basic domain were mutated into AQ to abolish DNA-binding and tyrosine (Y) residue in position 241 was mutated into a phenylalanine (F) to prevent potential phosphorylation.

(B) Alignment of mouse Ngn2 (MATH4A; NP_033848), Ngn1 (MATH4C; NP_035026) and Ngn3 (MATH4B; NP_033849) protein sequences reveals a high level of conservation of their bHLH domains but a low level of conservation of the N- and C-terminal domains including the YWQPPPP motif in the C-terminal domain of Ngn2 (boxed in A and B) which is not found in Ngn3 and Ngn1.

(C) Photomicrograph showing the high transfection efficiency and high level of expression obtained by *ex vivo* electroporation of E14.5 dorsal telencephalic progenitors subsequently cultured as dorsal telencephalic wholemount for 24 hours *in vitro* (hiv).

(D) Electroporation was used to overexpress myc-tagged Ngn2 (myc-Ngn2-IRES-EGFP) in cortical progenitors followed by immunoprecipitation with myc-antibodies (arrowhead, 'plus' lane in left-hand side panel). No myc-tagged protein was immunoprecipitated in control (EGFP only) transfected cortical progenitors ('minus' lane in left-hand side panel). When the telencephalic wholemount cultures were performed in the presence of γ^{32}P-labeled ATP, a phosphorylated protein of the molecular weight corresponding to myc-Ngn2 (arrowhead at 36-40kDa; 'plus' lane in right-hand side panel) was immunoprecipitated but not in control cultures ('minus' lane in right-

hand side panel), suggesting that Ngn2 is phosphorylated *in vivo* in E14.5 cortical progenitors (repeated in 3 independent experiments).

(E) A GST-Ngn2 fusion protein was expressed using cortical electroporation at E14.5 followed by 24 hours *in vitro* as described in A. Lysate from cortical precursors were used to perform GST-pulldown using glutathione-beads (line 1) which leads to the detection of a double-band product at the appropriate molecular weight (65kDa) using anti-GST immunoblotting. Cleavage of the GST-Ngn2 fusion protein bound to the beads releases a small amount of GST (lane 2 at 25kDa) but also releases a product corresponding to Ngn2 detected using an anti-phosphotyrosine antibody (lane 5). Note that GST is efficiently released by glutathione elution (lane 3) but is not tyrosine phosphorylated (lane 6).

(F) Ngn2 is phosphorylated on tyrosine residue 241 in undifferentiated P19 cells. Transfection of undifferentiated P19 cell line with GST-, GST-Ngn2 fusion or GST-Ngn2^{Y241F} fusion followed by GST-pulldown using glutathione-beads, elution and immunoblotting with anti-GST antibody (left blot) or anti-phosphotyrosine antibody (RC20) demonstrates (i) that Ngn2 (but not GST) is tyrosine phosphorylated in P19 cells and (ii) importantly that Ngn2^{Y241F} mutant protein presents a significant decrease in tyrosine phosphorylation signal (normalized to GST signal) showing that tyrosine 241 is the major phosphorylated tyrosine residue in Ngn2.

(G) Mapping of the transcriptional activation domain of mouse Ngn2 using the Gal4-UAS-Luciferase system. Gal4-fusion proteins where made to specific fragment of Ngn2 including from top to bottom: the entire C-terminal region (following the second Helix aa 181 to 263), the distal half of the C-terminal tail (aa 214-263) and the proximal half of the C-terminal tail (aa 181-213). Gal4-Ngn2$^{[181-263]}$ is able to transactivate robustly a UAS-Luciferase reporter to a similar extent then Gal4-Ngn2$^{[181-213]}$ fusion protein suggesting that the minimal transactivation domain is located between residues 181 and 213 in Ngn2. The Gal4-Ngn2$^{[214-263]}$ fusion protein does not present significant transactivation properties. All fold activation values were expressed as a normalized ratio of the Luciferase/constitutive Renilla luminescence for controlling variation in transfection efficiencies. * $p<0.01$ Mann-Whitney non-parametric test (n=6); n.s. non-significant.

(H) Transcriptional activity of full-length Ngn2 and various mutant forms assayed using the Luciferase-Renilla system in undifferentiated P19 cells. Full-length Ngn2 induces a robust 20-fold

increase (compared to control, ** p<0.001 Mann-Whitney test) in transactivation of the *NeuroD* promoter. Both the NR to AQ substitution within the basic domain ($Ngn2^{NR->AQ}$) or the deletion of the complete basic domain ($Ngn2^{\Delta basic}$) forms of Ngn2 result in the complete loss of *NeuroD* promoter transactivation (ns: not significantly different from control). Interestingly, mutation of $tyrosine^{241}$ into phenylalanine does not interfere with the ability of Ngn2 to transactivate the *NeuroD* promoter.

(I-K) Immunofluorescence staining for EGFP and MAP2 allows the assessment of the proportion of E14.5 cortical progenitors differentiating into neurons in different experimental conditions after culturing dissociated E14.5 progenitors for 5div. EGFP+ cells (green arrows in E) are either MAP2 positive (red arrows in F) or MAP2 negative (blue arrow in F). In this field of view, out of the 15 total EGFP+ cells, 14 are also MAP2 + (white arrows in G) and one is MAP2- (asterisk in G).

(L) Histogram representing the percentage of neurons (MAP2 –expressing cells) calculated from the total number of EGFP+ cells. Electroporation of Ngn2 in cortical progenitors significantly increases the percentage of cortical neurons differentiating from dissociated cultures from E14.5. This analysis reveals that Ngn2 overexpression induces a significant increase in the level of neuronal (vs glial) differentiation, while mutation of the DNA-binding properties ($Ngn2^{NR->AQ}$) of Ngn2 abolishes its proneural activity, and mutating $tyrosine^{241}$ into a phenylalanine residue ($Ngn2^{Y241F}$) does not have any effect on Ngn2's ability to promote neuronal differentiation. (** p<0.01; n.s.: non significant –Chi^2 analysis).

the HLH domains, or to bind DNA, a function primarily mediated by the basic domain (Bertrand et al., 2002; Puri and Sartorelli, 2000).

Tyrosine 241 of Neurogenin2 is not involved in mediating its proneural activity

Next we wanted to assess the functional effect of mutating tyrosine 241 on the proneural function of N*gn2*. To do this, E14.5 cortical progenitors were electroporated, dissociated and cultured for 5 days *in vitro* at medium cell density (**Fig. 2.4I-K**). The proneural activity of Ngn2 was assessed quantitatively by scoring the percentage of Ngn2-transfected progenitors that express MAP2 after 5 div. This analysis revealed that under our serum-free culture conditions, over-expression of Ngn2 significantly increased the bias of progenitors to differentiate into MAP2+ neurons (approximately 90%; n=481 cells from 3 independent experiments; **Fig. 2.4L**) compared to control EGFP-only transfected progenitors (63%; n=357 from 3 independent experiments; **Fig. 2.4L**). Importantly, expression of $Ngn2^{NR->AQ}$ was unable to promote neuronal differentiation (n=509 cells; 4 independent experiments; **Fig. 2.4L**) whereas expression of $Ngn2^{Y241F}$ had a proneural activity that was undistinguishable from wild-type Ngn2 (n=377 cells; 4 independent experiments; **Fig. 2.4L**). These results demonstrate that the proneural activity of Ngn2 is (1) at least partially dependent on its DNA-binding properties as previously shown (Lee and Pfaff, 2003; Sun et al., 2001), and (2)

importantly the proneural activity of Ngn2 does not require the integrity of tyrosine 241.

Ngn2 specifies the radial migration properties of cortical progenitors in a DNA-binding independent manner

We used the *ex vivo* cortical electroporation technique to study the radial migration properties of neurons generated by cortical progenitors forced to express various mutant forms of Ngn2. As shown above, control electroporations performed at E14.5 resulted in the radial migration of a synchronous cohort of neurons, with approximately one third of the total number of cells electroporated accumulating at the top of the cortical plate after 4 div (**Fig. 2.5A** and **2.5E**). Overexpression of wild-type Ngn2 in E14.5 cortical progenitors, increases significantly the proportion of cells recruited to the SVZ and the proportion of neurons initiating radial migration and accumulating in the CP (**Fig. 2.5B** and **F**).

Surprisingly, the radial distribution of cells expressing $Ngn2^{NR->AQ}$ did not differ significantly from the distribution observed after expression of full length Ngn2 and certainly did not impair the radial migration properties of E14.5 cortical neurons (**Fig. 2.5C** and **2.5G**). Importantly, expression of $Ngn2^{Y241F}$ in E14.5 cortical progenitors almost completely abolished the radial migration of cortical neurons into the cortical plate, with the majority of neurons accumulating in the IZ and being unable to penetrate into the CP (**Fig. 2.5D** and **2.5H**). None of the differences in migration exhibited following forced expression of $Ngn2^{Y241F}$ could

be attributed to defects in neuronal differentiation as the same proportion of EGFP+ expressed the post-mitotic markers TuJ1 and MAP2 in the IZ of electroporated slices (RH, DB and FP data not shown; see also **Fig. 2.4H-K**). It is worth emphasizing that the forced expression of $Ngn2^{Y241F}$, but not expression of $Ngn2^{NR->AQ}$, phenocopies the complete and the conditional loss of *Ngn2* function (see **Fig. 2.2** and **Fig. 2.3**). The radial migration arrest in the IZ due to expression of $Ngn2^{Y241F}$ by cortical progenitors is unlikely to be due to an indirect effect on the structure of the radial scaffold since both at short-term (36 hiv) and long-term (4 div) time points, radial glial processes are unaffected by expression of $Ngn2^{Y241F}$ (**Suppl. Fig 2.3**).

These results strongly suggest that the inhibition of radial migration resulting from the expression $Ngn2^{Y241F}$ in cortical progenitor is dominant over endogenously expressed Ngn2 in cortical progenitors (see **Fig. 2.1**). In order to test directly if $Ngn2^{Y241F}$ acts as a dominant-negative over Ngn2, we performed a set of co-electroporations aimed at expressing different ratios of full length Ngn2 and $Ngn2^{Y241F}$ (**Suppl. Fig. 2.4**). When expressed at a 1:1 or even a 10:1 ratio over full length Ngn2, $Ngn2^{Y241F}$ (**Suppl. Fig. 2.4B** and **2.4C** respectively) is still inhibiting significantly radial migration compared to control electroporation of wild-type Ngn2 alone (**Suppl. Fig. 2.4A**). Therefore, we conclude that $Ngn2^{Y241F}$ acts as a dominant-negative over Ngn2, probably by binding competitively to rate-limiting effectors and therefore preventing wild-type Ngn2 to interact with these effectors that could be necessary to transactivate specific target promoters of

genes involved in regulating radial migration and/or neuronal polarity (see below and **Fig. 2.9**).

Expression of Ngn2^{Y241F} impairs the polarity and nucleokinesis of radially migrating neurons

In order to gain insights into the cellular mechanisms underlying the function of the Y241 residue in Ngn2, we coupled *ex vivo* cortical electroporation with slice culture and time-lapse confocal microscopy to document the dynamics of radial migration of neurons expressing endogenous wild-type Ngn2 (**Fig. 2.6A** as well as **Suppl. Movies 1**) or Ngn2^{Y241F} (**Fig. 2.6B** plus **Suppl. Movies 2**). This analysis reveals that progenitors expressing Ngn2^{Y241F} are able to transit from the SVZ into the IZ but when they should engage radial migration these cells display a striking loss of the polarity of their leading process outgrowth (red arrow in **Fig. 2.6B**) as well as failure to undergo nucleokinesis (three cells pointed in **Fig. 2.6B**). Our quantification demonstrate that cells expressing Ngn2^{Y241F} display a significant decrease of the rate of cell body translocation (**Suppl. Fig. 2.5A**) and a significant increase of the rate of leading process branching (**Suppl. Fig. 2.5B**) compared to progenitors expressing endogenous wild-type Ngn2.

Rescue of the migration defect due to *Neurogenin2* loss-of-function by inhibition of RhoA function

In order to improve our understanding of the molecular mechanisms underlying the role of *Ngn2* in specifying the radial migration properties of pyramidal neurons, we took advantage of a recent substractive hybridization screen (Mattar et al., 2004) that led to the identification of several Ngn2-target genes in the developing cortex. Interestingly, several of these putative Ngn2-target genes have been previously shown to be critical for radial migration such as *Doublecortin* (*Dcx*; (Bai et al., 2003; des Portes et al., 1998; Gleeson et al., 1998)). However, several other target genes have no known function in regulating neuronal migration. Among those, two genes encode two distinct Rho-family of GTPase Activating Proteins (Rho-GAPs) called *RhoGAP5* (also called *ARHGAP5* or *p190 Rho-GAPb*) and *Formin Binding Protein 2* (*FNBP2*; (Katoh, 2004); also called *srGAP2* (Coyle et al., 2004; Wong et al., 2001)). Interestingly, *FNBP2* is specifically down-regulated in cortical progenitors of E13.5 Ngn2 knockout mice compared to wild-type littermates (Mattar et al., 2004). Rho-GAPs act as negative regulators of small-GTPase activity by increasing GTPase catalytic activity therefore promoting the GTP to GDP exchange (Ridley et al., 2003). Interestingly, the small-GTPase RhoA itself is specifically expressed at high levels by cortical progenitors but is sharply down-regulated during the initiation of radial migration in the IZ (Olenik et al., 1999). Given the known function of activated-RhoA in inhibiting non-neuronal cell migration (Arthur and

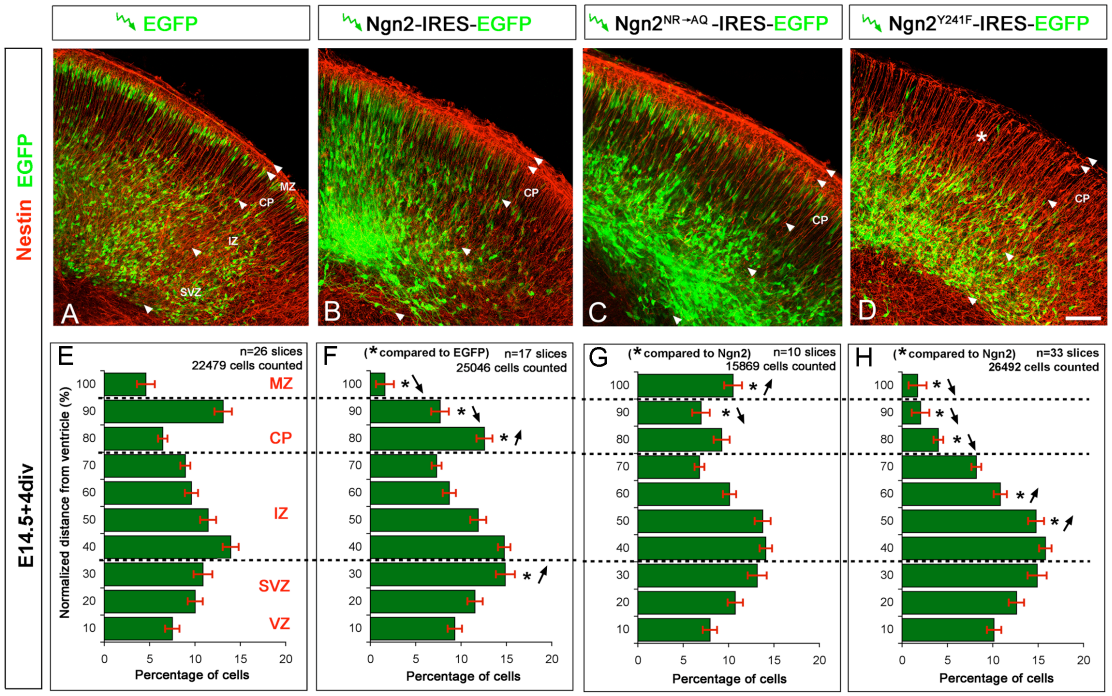

<u>Figure 2.5</u> *Neurogenin2* specifies the radial migration properties of cortical progenitors in a DNA-binding independent manner.

(A) *Ex vivo* electroporation of E14.5 cortical progenitors followed by *in vitro* organotypic slice culture for four days *in vitro* (4 div; see Supplementary Fig. 1) allows the visualization of the radial translocation of a single cohort of neurons to the top of the CP. In panels A-D, the red counterstaining is anti-Nestin (Rat-401) immunofluorescence which reveals the intact structure of the radial glial scaffold in all four conditions.

(B) Electroporation of full-length Ngn2 increases significantly the number of cortical progenitors engaging in radial migration in the intermediate zone (IZ) and reaching the CP.

(C) Electroporation of the DNA-binding deficient form of Ngn2, Ngn2$^{NR->AQ}$, increases the number of cortical progenitors initiating radial migration (increased cell density in IZ) and does not affect the ability of cortical progenitors to initiate radial migration and reach upper layers of the CP.

(D) Electroporation of Ngn2^{Y241F} abolishes the effect of Ngn2 on radial migration and results in a premature arrest of migration in the intermediate zone (star) beneath the CP.

(E-H) Histograms of the frequency distribution of EGFP+ cells along the radial extent of the cortical wall (normalized as a percentage). Error bars represent standard error to the mean. Stars indicate significant ($p<0.01$- Chi square) differences of the proportion of neurons find in similar bins (for example comparing the 50% normalized distance bins between EGFP and Ngn2 conditions). The Chi-square comparisons where made between EGFP and Ngn2 (F) or between Ngn2 mutations (NR->AQ and Y241F) and Ngn2 (G and H).

(I) Histogram comparing the absolute density of EGFP-expressing cells in the four electroporation conditions measured using an unbiased stereological counting method (optical dissector adapted from (Williams and Rakic, 1988); see Method for details) in three radial compartments indicated in the inset.

* $p<0.05$ and ** $p<0.001$ Mann-Whitney non-parametric test.

Scale bar in D: VZ, ventricular zone; SVZ, subventricular zone; IZ, intermediate zone; CP, cortical plate.

Burridge, 2001) and the down-regulation of two Rho-GAPs in Ngn2 knockout cortical progenitors, we hypothesized that (1) inhibition of RhoA activity is normally a pre-requisite to initiate radial migration outside the VZ/SVZ into the IZ and therefore that (2) a failure to up-regulate the expression of RhoGAPs such as *RhoGAP5/ARHGAP5* or *FNBP2/srGAP2* could lead to reduced inhibition of RhoA activity in Ngn2-/- cortical progenitors impairing their ability to initiate radial migration upon cell-cycle exit.

In order to test directly if cortical progenitors failed to initiate migration in Ngn2-/- cortex at least partially because of an inability to inhibit RhoA activity, we used the electroporation technique in order to rescue the migration phenotype characterizing the Ngn2-/- cortical progenitors by expressing a dominant-negative form of RhoA ($RhoA^{N19}$, (Olson et al., 1995)). Expression of $RhoA^{N19}$ in E14.5 cortical progenitors of *Ngn2* knockout embryos is sufficient to rescue partially the migration defect and induces a significant proportion of neurons to leave the VZ/SVZ and migrate into the IZ (**Fig. 2.7A-D**). However, this rescue was only partial as most migrating neurons stopped sharply at the boundary between the IZ and the CP after 4 div (**Fig. 2.7B** and **2.7D**).

Because the expression of many different genes might be altered in *Ngn2*-/- cortical progenitors that might directly or indirectly affect their migration properties, we wanted to determine if we could rescue more specifically the migration phenotype due to the expression of $Ngn2^{Y241F}$ in cortical progenitors by inhibiting RhoA activity. As shown in **Suppl. Fig. 2.7**, co-electroporation of two

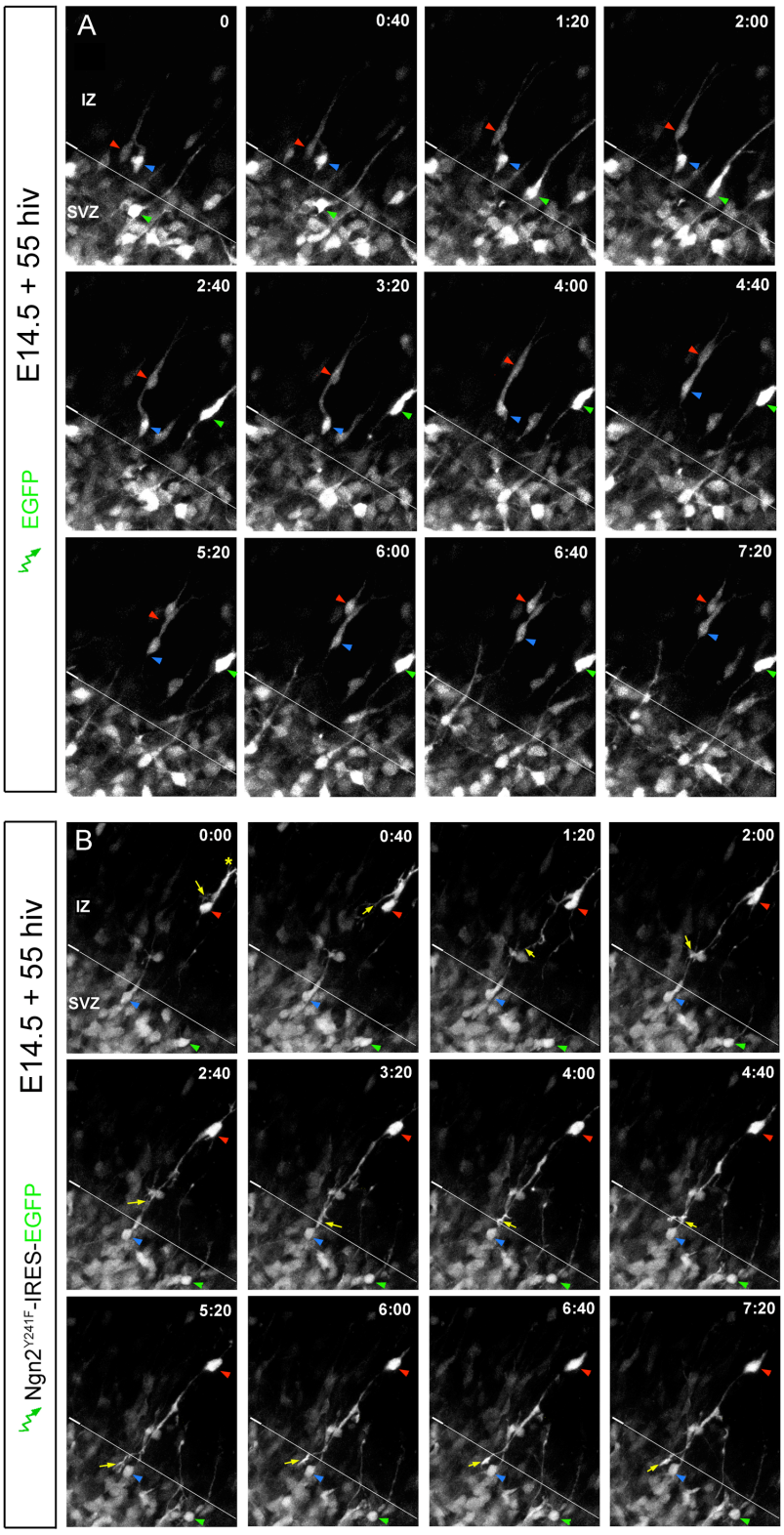
A
0
0:40
1:20
2:00
IZ
SVZ
2:40
3:20
4:00
4:40
5:20
6:00
6:40
7:20
EGFP
E14.5 + 55 hiv
B
0:00
0:40
1:20
2:00
IZ
SVZ
2:40
3:20
4:00
4:40
5:20
6:00
6:40
7:20
Ngn2Y241F-IRES-EGFP
E14.5 + 55 hiv

Figure 2.6. Expression of Ngn2^{Y241F} impairs the polarity of neurons initiating during radial migration

(A) Time-lapse confocal microscopy was used to follow the dynamics of neurons engaging radial migration when they transition from the SVZ to the IZ (see also **Suppl. Movie 1**). Colored arrows point to individual control cells electroporated with EGFP which display the characteristic unipolar morphology of migrating neurons with a single leading process directed towards the pial surface (top of the pictures).

(B) In contrast, neurons expressing Ngn2^{Y241F} display a striking polarity defect where some cells (red arrow) lose their pre-existing leading process (pointed by asterisk in B) and extend a major process towards the ventricle instead (yellow arrows). In addition, all three cells pointed by colored arrows fail to translocate their nucleus towards the leading process and as a result fail to move during the entire movie (see also **Suppl. Movie 2**).

constructs expressing RhoA^{N19}-IRES-DsRed2 and Ngn2^{Y241F}-IRES-EGFP leads to the very high rate of co-expression of both construct. Importantly, expression of RhoA^{N19} is sufficient to rescue very significantly the inhibition of migration due to expression of Ngn2^{Y241F} in cortical progenitors (**Fig. 2.7F-H**) to a level comparable to control electroporation of EGFP only (see **Fig. 2.5A** and **2.5E**) or wild-type Ngn2 (see **Fig. 2.5B** and **2.5F**).

These results demonstrate that tyrosine 241 in Ngn2 is required for the specification of the radial migration properties of cortical progenitors at least partially by inhibiting RhoA activity.

Neurogenin2 is sufficient to specify cell-autonomously the unipolar dendritic morphology of pyramidal neurons

In slices expressing EGFP only (**Fig. 2.8A**) or full length *Ngn2* (**Fig. 2.8B**), the vast majority of neurons accumulate at the top of the cortical plate after completion of their radial migration where they displayed a unipolar morphology with their leading process/apical dendrite directed towards the marginal zone (**Fig. 2.8E-F** respectively). Interestingly, expression of *Ngn2*$^{NR->AQ}$ resulted in a significant disorganization of the CP (**Fig. 2.8C**), even though the total number of neurons that successfully reached the upper cortical plate was comparable to full length *Ngn2*-electroporated slices (**Fig. 2.8B**). Moreover, *Ngn2*$^{NR->AQ}$ expressing neurons seem to ignore the upper limit of the CP and abnormally invade the MZ (**Fig. 2.5G** and see also **Fig. 2.8C**).

Importantly, expression of both *Ngn2*$^{NR->AQ}$ and *Ngn2*^{Y241F} led to more severe disruption of the dendritic morphology of neurons in the CP (**Fig. 2.8G-H**). Expression of either mutations of Ngn2 affected the unipolar the dendritic morphology of immature pyramidal neurons reaching the CP in fact, a significant number of cells expressing Ngn2$^{NR->AQ}$ or Ngn2^{Y241F} displayed a non-pyramidal morphology defined by the outgrowth of multiple primary dendrites from the cell body (red arrows in **Fig. 2.8G-H**). We specifically quantified the effect of expression of *Ngn2*^{Y241F} on the dendritic morphology of cortical neurons in slices using an computerized approach described below (see **Fig. 2.8N-P**) called the Pyramidal Morphology Index (**Suppl. Fig. 2.8**). These results suggested that the integrity of tyrosine 241 in Ngn2 is necessary to specify the polarity of leading process/apical dendrite outgrowth, one of the defining features of pyramidal neurons.

The interpretation of the effects we observed on the polarity of dendritic outgrowth in neurons expressing Ngn2^{Y241F} in slices is complicated by the fact that this defect could be a secondary consequence of migration defects as previously observed in the developing cortex of the *reeler* mutant mouse for example (Pinto Lord and Caviness, 1979; Pinto-Lord et al., 1982). In other words, the unipolar dendritic morphology of pyramidal neurons in the cortical plate may depend on the ability of these neurons to respond to appropriate extracellular cues, which may not be the case for neurons expressing Ngn2^{Y241F} given that their migration is abnormal or retarded.

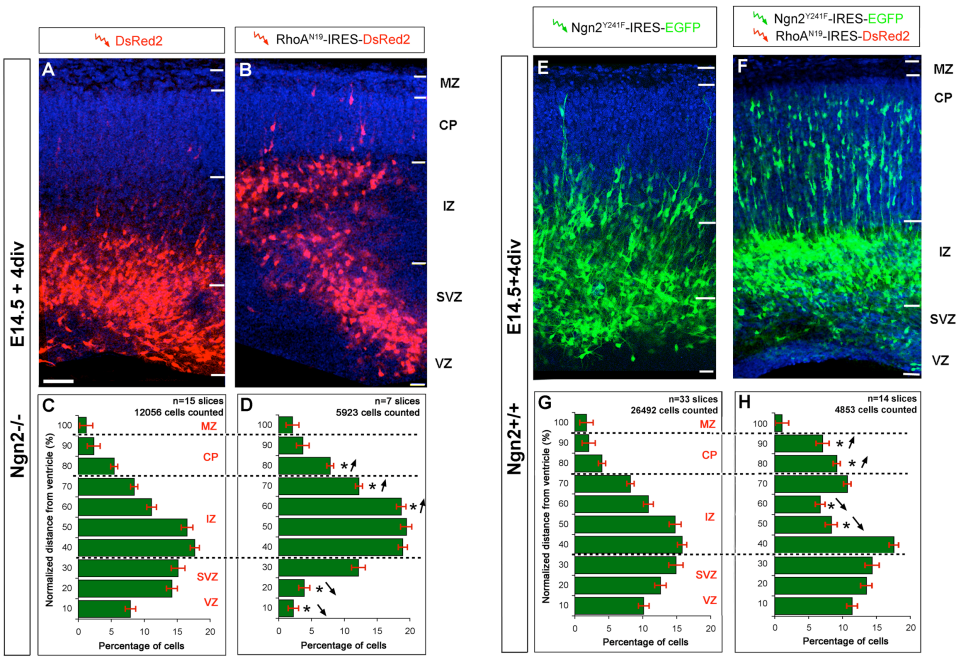

Figure 2.7. Inhibition of RhoA activity rescues the migration defect due to *Ngn2* loss-of-function

(A-D) *Ex vivo* electroporation of dominant negative RhoA ($RhoA^{N19}$; B) in E14.5 Ngn2-/- cortical progenitors increases the number of cells initiating migration into the IZ compared to control DsRed2 electroporation in Ngn2-/- progenitors (A). Note that this is a partial rescue since the cells expressing $RhoA^{N19}$ in the Ngn2-/- slices still fail to enter the cortical plate in their vast majority. The quantification of cell distribution demonstrates a significant decrease of the proportion of cells located in the VZ/SVZ compartment and a corresponding increase in the proportion of cells located in the IZ in Ngn2-/- slices electroporated $RhoA^{N19}$-IRES-DsRed2 (D) compared to Ngn2-/- slices electroporated with control DsRed2 only (C). * $p<0.01$ Chi square test. (E-H) Co-expression of dominant negative $RhoA^{N19}$ and $Ngn2^{Y241F}$ (F) rescues almost completely the migration defect caused by expression of $Ngn2^{Y241F}$ alone (E). Quantification of cell distribution along the radial axis reveals that a significantly higher proportion of cells migrated into the CP from the IZ when $RhoA^{N19}$ was co-expressed with $Ngn2^{Y241F}$ (H) than when $Ngn2^{Y241F}$ is expressed alone (G). * $p<0.01$ Chi square test.

Scale bar in A-B and E-F: 50 microns

In order to determine if *Ngn2* plays a direct role in the specification of the dendritic morphology of pyramidal neurons in the cortex, we took advantage of the fact that previous studies have shown that when cortical progenitors are dissociated and cultured from 5 to 7 days *in vitro* at low to medium cell density to minimize cell-cell contacts, these progenitors give rise to neurons that fail to display the unipolar morphology characterizing pyramidal neurons *in vivo* (Peters and Kara, 1985a; Peters et al., 1985) and instead display multipolar morphologies (Hayashi et al., 2002; Threadgill et al., 1997). Interestingly, *Ngn2* transcription is significantly down-regulated in dissociated cortical cultures (data not shown), raising the possibility that maintenance of proper level of *Ngn2* expression in cortical progenitors requires cell-cell contacts. As previously reported (Threadgill et al., 1997), cortical progenitors in dissociated cultures give rise to neurons displaying multipolar dendritic morphologies characterized by multiple dendrites emerging from the cell body (arrowheads in **Fig. 2.8I**), and therefore failed to establish a polarized dendritic outgrowth *in vitro*. Quantification using observer-based categorization (**Fig. 2.8M**) revealed that only 30% of the neurons in control cultures displayed a unipolar morphology characteristic of pyramidal neurons *in vivo* (i.e. one large apical dendrite emerging from the cell body), approximately 10% displayed a bipolar morphology (i.e. 2 equally wide dendrites emerging from the cell body) and approximately 60 % displayed multipolar, non-pyramidal morphologies (i.e. more than 2 dendrites emerging from the cell body). Strikingly, constitutive expression of *Ngn2* by electroporation

in cortical progenitors resulted in a dramatic switch in the polarity of dendritic outgrowth, causing 60% of all MAP2-positive neurons to display a unipolar dendritic morphology characterized by one large apical dendrite and a single axon emerging from the opposite side of the cell body (**Fig. 2.8J** and **2.8M**). Importantly, neither Ngn2$^{NR->AQ}$ (**Fig. 2.8K**) nor Ngn2^{Y241F} (**Fig. 2.8L**) exerted the same activity as wild-type Ngn2 as both failed to promote a unipolar morphology in cortical neurons (**Fig. 2.8M**), suggesting that both the DNA-binding properties and tyrosine 241 of Ngn2 are necessary to specify the polarized dendritic outgrowth characterizing cortical pyramidal neurons.

The categorization of the dendritic morphologies of neurons is subjective and therefore heavily observer-dependent (see Discussion in (Threadgill et al., 1997)). In order to circumvent this general problem of qualitative and therefore potentially biased categorization, we developed a quantitative, unbiased index called the Pyramidal Morphology Index (PMI). We defined the PMI as the ratio between the width of the largest process and the total number of processes emerging from the cell body (**Fig. 2.8O**). As shown in **Fig. 2.8N** on model cells, the PMI value obtained for a population of cells ranging from purely multipolar (cell a) to purely unipolar (cell g) increases with the polarity of dendritic outgrowth. The PMI index thus allows us to distinguish between two cells each of which has 3 dendrites emerging from the cell body (cells b and f), but one of which (cell f) has one apical-like dendrite process that makes it ‘more pyramidal’ than cell b. The measure of the width and number of processes was automatized

using an Image J-based macro that we developed. This program enables to draw a 'sampling' circle of fixed diameter (25 microns) centered on the cell body, allowing the extraction of the width of each dendritic process and the total number of dendrites crossing the sampling-circle (**Fig. 2.8O**). As shown in **Fig. 2.8P**, the PMI turns out to be a reliable measurement of the shift between multipolar morphologies observed in control (EGFP) cultures and unipolar morphologies observed in neurons constitutively expressing Ngn2 ($p=0.0014$; ANOVA-test). The increase in PMI values obtained in Ngn2-electroporated neurons compared to EGFP-control neurons actually corresponds to a doubling of the percentage of neurons displaying PMI values superior to 4 i.e. to most unipolar neurons.

Importantly, expression of both $Ngn2^{NR->AQ}$ and $Ngn2^{Y241F}$ failed to increase the average PMI values observed when over-expressing wild-type Ngn2 (**Fig. 2.8P**) demonstrating that both the DNA-binding properties and the tyrosine 241 residue of Ngn2 are necessary to specify the polarity of dendritic outgrowth characterizing immature pyramidal neurons.

Ngn1 promotes radial migration but does not promote unipolar dendritic morphology to the same extent than Ngn2

As mentioned previously the tyrosine 241 and its surrounding proline-rich motif (YWQPPPP) are not present in Ngn1 or Ngn3. We wanted to determine if Ngn2 function in the specification of the migration properties and the dendritic

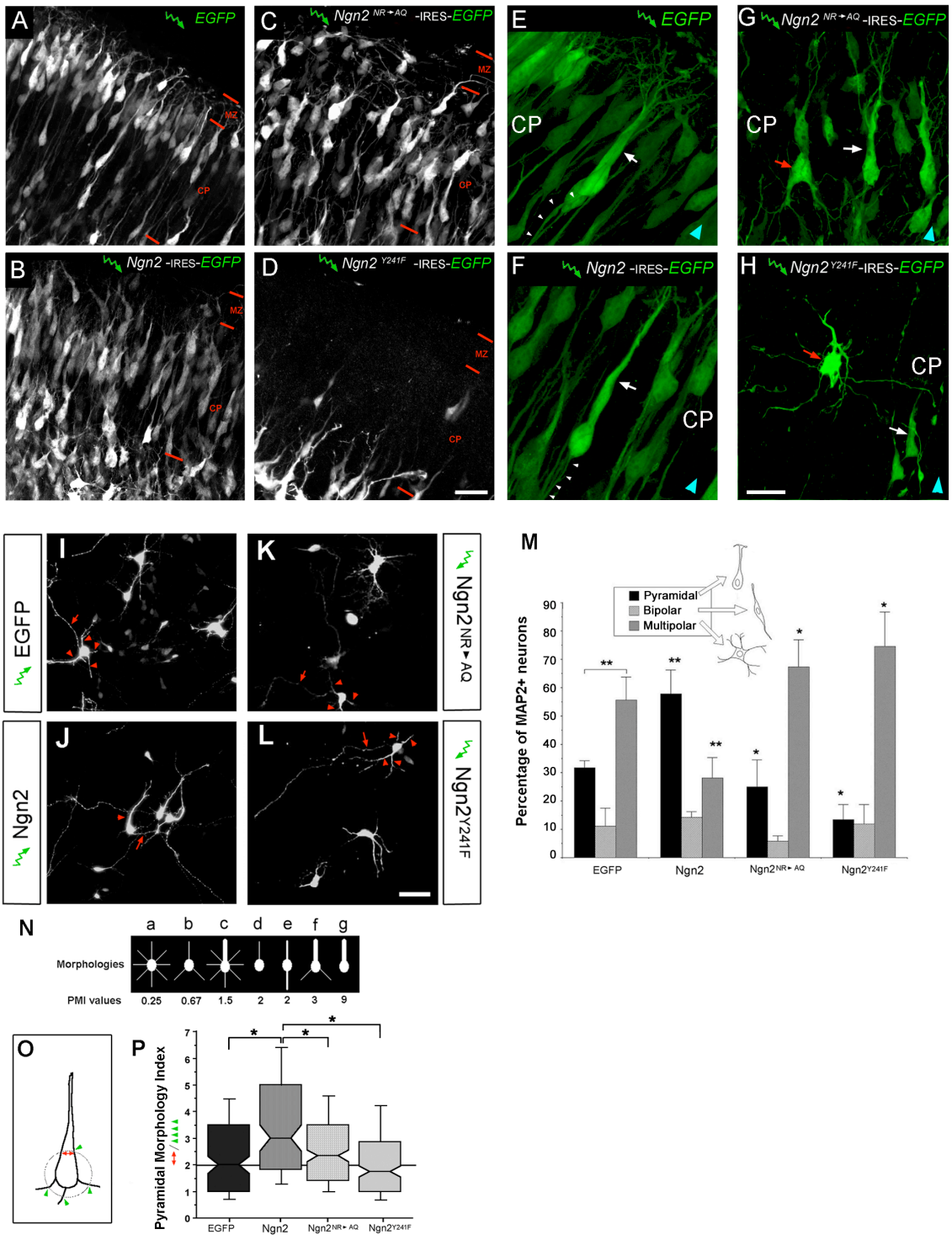

Figure 2.8. ***Ngn2*** **expression is sufficient to specify a pyramidal dendritic morphology**

(A-D) Confocal micrographs illustrating the normal cellular organization of the cortical plate in slices electroporated with EGFP (control; A) or wild-type Ngn2 (B). Electroporation of Ngn2$^{NR->AQ}$

results in a disorganized accumulation of neurons in the CP. Progenitors transfected with Ngn2^{Y241F} almost completely fail to invade the CP (D).

(E-H) At higher magnification, neurons expressing EGFP (E) or over-expressing full-length Ngn2 (F) display the characteristic unipolar morphology of immature pyramidal neurons with an apical dendrite (white arrow) directed towards the pial surface (direction indicated by the blue arrowhead) and a single axon directed towards the ventricle (small arrowheads). By contrast, cortical progenitors expressing Ngn2$^{NR->AQ}$ (G) or Ngn2^{Y241F} (H) give rise to neurons that do not display an apical dendrite and instead adopt a non-pyramidal multipolar morphology (red arrows in G and H respectively) characterized by multiple primary dendrites emerging from the cell body. The white arrows in G and H points to typical pyramidal neurons with an apical dendrite directed towards the pial surface.

(I-L) E14.5 cortical progenitors electroporated with a control plasmid (EGFP), dissociated and maintained for 5div on poly-lysine/laminin coated glass coverslips fail to establish a pyramidal morphology and instead display non-pyramidal morphologies with multiple, relatively thin dendritic processes (arrowheads; identified using MAP2, data not shown) and a unique, long and thin axonal process (arrow; MAP2 negative but neurofilament 165kD positive- data not shown). Expression of full-length Ngn2 (J) [but not Ngn2$^{NR->AQ}$ (K) or Ngn2^{Y241F} (L)] is sufficient to restore the unipolar pyramidal dendritic morphology characterized by a unique large apical process tapering away from the cell body (arrowhead in J) and a unique axon (arrow in J).

(M) Qualitative categorization of dendritic morphologies of cortical post-mitotic neurons emerging from E14.5 progenitors electroporated by the constructs indicated in panels I-L. Dendritic morphologies were classified into three categories schematized from top to bottom: unipolar/pyramidal (one main apical dendrite; black bars), bipolar (two main dendrites of equivalent diameter emerging from the cell body; hatched bars), mutlipolar (more than two primary dendrites emerging from the cell body; gray bars). Only 30% of cortical neurons display a pyramidal morphology in dissociated culture and forced expression of wild-type Ngn2 increases significantly the proportion of pyramidal-shaped neurons back to 60% approximately the percentage observed *in vivo*. Interestingly, the expression of the DNA-binding mutant form

Ngn2$^{NR->AQ}$ or the Ngn^{Y241F} mutant are not able to increase the percentage of pyramidal-shaped neurons compared to control EGFP-only expressing neurons. * $p<0.05$ and ** $p<0.01$ –Chi^2 analysis. A minimum of 150 neurons randomly sampled from 4 independent experiments were examined in each treatment.

(N-O) Definition of the Pyramidal Morphology Index (PMI) as a tool allowing unbiased categorization of dendritic morphology. The PMI is defined as the ratio between the width of the largest process and the total number of processes (as depicted in O) crossing a sampling circle of fixed diameter (25 microns; see Methods for details). In panel N, prototype neurons ranging from multipolar (left cell a) to unipolar/pyramidal morphologies (right cell g) with multiple intermediate combinations were computed using the macro we have developed. The measured PMI values indicated below each example are the actual values obtained using the software. This shows that the PMI is a quantitative and continuous index of multipolar (low values) or unipolar (high values) dendritic morphology.

(P) Box plots illustrating the distribution of Pyramidal Morphology Index values calculated for a minimum of 150 neurons per experimental set (from 4 independent experiments). The expression of *Ngn2* (but not Ngn2$^{NR->AQ}$ or Ngn2^{Y241F}) significantly increases the PMI values of neurons in dissociated cultures compared to control (EGFP only) electroporated progenitors, reflecting an increase in the proportion of neurons displaying unipolar/pyramidal dendritic morphologies. Horizontal bar represents the median of the control (EGFP only) condition. (* $p<0.01$ ANOVA one-way test).

Error bars in M indicate standard error to the mean. Box plot in P indicates the median (bottleneck), the 25th and 75th percentiles (main box) as well as the 90th and 10th percentiles (top and bottom bars respectively). Scale bars: 40 microns A-D; 20 microns E-H; 30 microns I-L.

morphology of pyramidal neurons was specific to Ngn2 of if this is a property shared by other Neurogenins. In order to test this we electroporated both mouse Ngn1-IRES-EGFP at E14.5 to assess the migration properties of cortical progenitors in organotypic slice culture. Our quantitative analysis demonstrate that Ngn1 (**Suppl. Fig. 2.9A** and **2.9C**) promotes the radial migration of cortical progenitors to the same overall extent than Ngn2 (**Suppl. Fig. 2.9B** and **2.9D**) despite minor differences in the actual distribution of post-mitotic neurons in the CP and MZ.

However, we found that Ngn1 does not specify the pyramidal neuronal morphology in dissociated culture of E14.5 cortical progenitors to the same extent than Ngn2 (**Suppl. Fig. 2.9E-F**). In fact the Pyramidal Morphology Index values obtained for progenitors overexpressing Ngn1 were not significantly different from control EGFP-electroporated cortical progenitors (**Suppl. Fig. 2.9F**) suggesting that Ngn2 is unique with regard to its ability to promote pyramidal dendritic morphology.

Discussion

In the present study, we identified *Ngn2* as a critical element in the specification of the radial migration properties and the polarized dendritic outgrowth characterizing immature pyramidal cortical neurons. In particular, we showed that specification of the radial migration properties of cortical neurons and specifically their ability to migrate through the intermediate zone into the

upper cortical plate, is controlled by Ngn2 largely through a DNA-binding-independent mechanism, but that these functions are instead critically dependent on the phosphorylation of tyrosine 241 in its C-terminal domain (**Fig. 2.4**). Interestingly, we found that tyrosine 241 is not required for Ngn2-mediated transactivation of the *NeuroD* promoter and therefore this residue is unlikely to be involved in Ngn2 DNA-binding properties, transcriptional activation (e.g. ability to recruit the general transcription machinery such as RNA polymerase II complex) or the ability to hetero-dimerize with E box proteins or Class I bHLH transcription factors (such as E12 or E47), all of which are required to transactivate Ngn2-target promoters (Bertrand et al., 2002; Puri and Sartorelli, 2000; Skowronska-Krawczyk et al., 2004). We also found that the inhibition of neuronal migration due to the expression of $Ngn2^{Y241F}$ can be largely rescued by inhibition of the small-GTPase RhoA. The third important finding in the present study is that Ngn2 specifies the polarized outgrowth of the apical dendrite, a characteristic feature of cortical pyramidal neurons. In contrast to Ngn2 function in migration, the ability of Ngn2 to specify a polarized dendritic outgrowth requires both the integrity of its DNA-binding properties and phosphorylation of tyrosine 241.

Coordinated specification of the radial migration properties and dendritic morphology of pyramidal neurons

Using time-lapse analysis of the morphology of single neuronal progenitors exiting the cell-cycle, several studies recently demonstrated that

newly-generated neurons transiently display a multipolar, exploratory morphology in the SVZ before achieving a polarized morphology at the point when neurons initiate radial translocation into the IZ (Noctor et al., 2004; Tabata and Nakajima, 2003). The molecular cues and signaling pathways triggering this striking transition are unknown at present. Our results show for the first time that the coordinated initiation of radial migration and the acquisition of a unipolar leading process/apical dendrite outgrowth is dynamically controlled by Ngn2. Interestingly, the constitutive (**Fig. 2.2**) or the acute (**Fig. 2.3**) loss-of-Ngn2 function in cortical progenitors leads to a defect in the initiation of radial migration. However, we demonstrate that part of this defect is likely due to the proneural function of Ngn2 resulting in a pronounced defect of neuronal differentiation or cell cycle exit which precluded the analysis of other functions of bHLH proneural transcription factors. The expression of $Ngn2^{Y241F}$ uncouples for the first time the neuronal-subtype specification functions of *Ngn2* from its generic proneural function. Interestingly, a recent study in chick spinal cord has also shown that the proneural and the subtype specification functions of bHLH transcription factors such as Mash1 and Math1 are actually dependent on residues located outside the basic DNA-binding region, in the second Helix region (Nakada et al., 2004). These results strongly suggest that (1) bHLH transcription factors such as Ngn2 are coordinating the acquisition of pan-neuronal properties through the control of the transcription of genes allowing cell cycle exit and initiation of generic (non-subtype specific) neuronal differentiation

program involving expression of pan-neuronal markers (MAP2, βIII-tubulin, etc…) but (2) at the same time these bHLH TFs regulate the transcription of region-specific genes specifying neuronal subtype identity including migration properties (radial vs tangential) or the dendritic morphology (unipolar vs multipolar). The main finding of this study is that these two distinct functions involve different molecular modules within Ngn2.

New classification of dendritic morphology: polarized versus unpolarized initiation of dendrite outgrowth

We propose a model in which the unipolar dendritic morphology of pyramidal neurons represents a cellular consequence of their radial migration properties. Our results from dissociated cultures of cortical progenitors demonstrate that when progenitors give rise to neurons *in vitro*, the absence of appropriate cell-cell contacts (and maybe decreased Notch receptor activation), such as those that occur normally between radial glial cells and early post-mitotic neurons, results in a failure to establish a polarized, pyramidal morphology, with neurons instead acquiring a multipolar, non-pyramidal morphology characterized by an unrestricted number of primary dendrites emerging from the cell body (see **Figure 2.9** in present study and (Threadgill et al., 1997)). Interestingly, dissociated cortical progenitors are able to differentiate into unipolar pyramidal neurons when plated onto cortical slices in the slice overlay assay (unpublished observations; (Polleux et al., 2000)). Taken together these results strongly

suggest that extracellular cues present in the environment of cortical progenitors during and after completion of radial migration are required for the establishment of a polarized dendritic outgrowth (Whitford et al., 2002). These results also strongly suggest that the molecular machinery specifying the migration properties of cortical neurons (radial vs tangential) also regulate their dendritic morphology (unipolar/pyramidal vs mutlipolar/non-pyramidal). Future experiments will be aimed at determining the molecular basis linking the migration properties to the dendritic morphology of pyramidal glutamatergic and non-pyramidal interneurons in the cortex.

Candidate genes underlying the role of *Neurogenin2* in the specification of pyramidal dendritic morphology

What are the signaling pathways underlying the ability of *Ngn2* to promote radial migration and a pyramidal dendritic morphology? As mentioned earlier, a hint comes from a recent subtractive hybridization screen performed in order to identify direct and indirect downstream targets of *Ngn2* in mouse cortical progenitors (Mattar et al., 2004). Several candidate genes that might explain the effects of Ngn2 on neuronal migration and dendritic morphology were found to be downregulated in *Ngn2* knockout cortical progenitors, including the microtubule-binding protein *Doublecortin* and known regulators of Rho-like small GTPase activity involved in cell polarity and cytoskeleton dynamics, such as *Forming-Binding Protein 2* (*FNBP2* also annotated as *srGAP2* (slit-Robo GAP2; (Coyle et

al., 2004; Katoh, 2004)) as well as *RhoGAP5* (also called *ARHGAP5* and *p190-RhoGAPb*) (Mattar et al., 2004). Our results provide strong evidence that at least one of the pathway downstream of Ngn2 that regulate radial migration involves inhibition of the activity of the small-GTPase RhoA. Therefore, down-regulation of FNBP2 and/or RhoGAP5 in cortical progenitors could actually be causal to the migration defect characterizing Ngn2 loss-of-function. Future experiments will test directly the involvement of these two genes in the control of neuronal migration and dendritic morphology.

Our results also provide novel insights into the molecular control of neuronal migration and dendritic polarity in the cortex because in both rescue experiments (Ngn2 knockout and Ngn2^{Y241F} electroporation), expression of dominant-negative RhoA is sufficient to recruit the migrating neurons into the IZ but a lot of migrating neurons are stalled beneath the CP and seem to be unable to enter their final environment by bypassing their predecessors. This suggests a two step model of radial migration with a first step when early post-mitotic neurons exit the VZ/SVZ neuroepithelium and migrate into the IZ which requires phosphorylation of Ngn2 at tyrosine 241 leading to transient inhibition of RhoA activity (and maybe expression of Doublecortin; (Mattar et al., 2004)) and a second step controlled by Rac1/Cdc42 activity (Kawauchi et al., 2003) where neurons migrate through from the IZ into the CP (reviewed in (Gupta et al., 2002)).

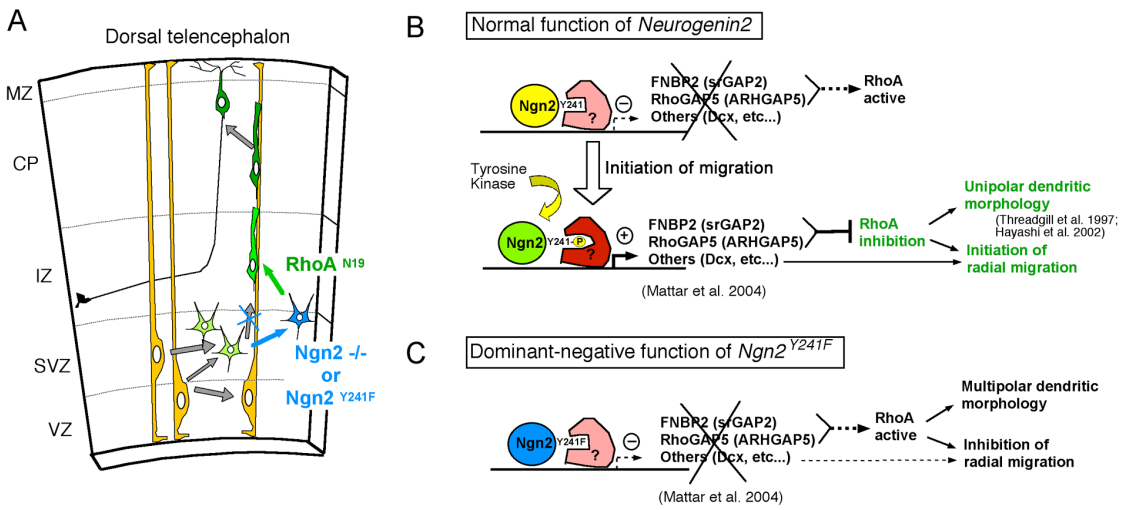

Figure 2.9. Potential mechanisms underlying the function of *Ngn2* in the specification of the migration properties and the dendritic morphology of pyramidal neurons

(A) Schema illustrating the cellular compartments of the developing neocortex and the proposed model of Ngn2 function: radial glial cells (yellow) are proliferating and producing neurons through both asymmetrical division in the VZ and symmetrical neurogenic divisions in the subventricular zone (SVZ) (Kriegstein and Noctor, 2004; Malatesta et al., 2000; Miyata et al., 2004; Noctor et al., 2001; Noctor et al., 2002; Noctor et al., 2004). In the present study we show that Ngn2 plays a critical role in the specification of the radial migration properties of cortical neurons through a mechanism that requires the integrity of its tyrosine residue 241 which is not required for the proneural activity of *Ngn2*. When progenitors express Ngn2^{Y241F} they generate post-mitotic neurons that fail to migrate past the intermediate zone and present unpolarized, multipolar dendritic morphologies. These defects are significantly (but not completely, see Discussion) rescued by inhibiting the activity of the small-GTPase RhoA. (B-C) Potential mechanisms underlying the function of *Ngn2* in the specification of the radial migration properties and the dendritic morphology of pyramidal neurons. We hypothesize that during the transition from a radial glial progenitor into a post-mitotic neuron initiating radial migration (B), Ngn2 is phosphorylated on tyrosine 241 which converts one of its putative interactor from a transcriptional repressor into a transcriptional activator (pink protein becoming red). This event might regulate the transcription of genes that are necessary to initiate radial migration and

unipolar dendritic morphology such as Rho-GAP proteins (FNBP2 or RhoGAP5) but also other genes known to regulate migration such as Doublecortin (Mattar et al., 2004) which are all distinct from proneural target genes. Interestingly, high levels of RhoA activity has been previously shown to inhibit non-neuronal cell migration (Arthur and Burridge, 2001; Ridley et al., 2003) and lead to multipolar dendritic morphology in cortical neurons (Hayashi et al., 2002; Threadgill et al., 1997). (C) We explain the dominant negative effect of the Ngn2^{Y241F} mutation by an inability to convert this hypothetical Ngn2 interactor into a transcriptional activator.

Potential signaling pathways involved in the DNA-binding independent function of Ngn2

Several studies have already illustrated the importance of protein-protein interactions and post-translational modifications in mediating some of the biological functions of bHLH transcription factors ((Lee and Pfaff, 2003; Moore et al., 2002; Olson et al., 1995; Sun et al., 2001; Talikka et al., 2002; Vojtek et al., 2003); reviewed in (Puri and Sartorelli, 2000)). Our results show that the DNA-binding independent function of Ngn2 in the specification of the neuronal migration properties and dendritic morphology of cortical neurons is mediated by phosphorylation of tyrosine 241. This tyrosine residue is part of a larger proline rich domain (YWQPPPP) motif that constitutes a putative SH2-binding site for non-receptor tyrosine kinase of the Tec family. This includes Interleukin-2 regulated Tyrosine Kinase (ITK; (Smith et al., 2001)) which is expressed by immature cortical neurons at E14.5 (Hand and Polleux, data not shown). Future experiments will be aimed at determining if ITK or other non-receptor tyrosine kinases phosphorylate tyrosine 241 of Ngn2 and how the potential phosphorylation of Y241 regulates Ngn2 function.

We hypothesize that the subtype specification activity mediated by phosphorylation of tyrosine 241 in Ngn2 involves protein-protein interaction, for example by converting a transcriptional repressor into an activator thereby inducing the transcription of downstream target genes regulating neuronal migration and dendritic polarity such as specific Rho-GAPs (**Fig. 2.9**). This is

actually the only model that would explain why Ngn2^{Y241F} is acting as a dominant-negative over Ngn2 since this dominant-negative activity must involve some interaction between Ngn2^{Y241F} that cannot be competed by the wild-type Ngn2. Current experiments are aimed at identifying phosphorylation-dependent interactors of the tyrosine 241 residue of Ngn2.

Is the phosphorylation of Y241 in Ngn2 a mammalian-specific feature?

The tyrosine residue in position 241 of Ngn2 that we characterized in the present study is conserved in mammals (human, rat and mouse) but not in non-mammalian vertebrates such as birds (chick). Interestingly, neurons in the dorsal telencephalon of birds (and reptiles also) accumulate according to a loose 'outside-first, inside-last' sequence (Tsai et al., 1981a, b), a pattern opposite to the inside-first, outside-last pattern characterizing all mammals (Sidman and Rakic, 1973), leading to a loosely laminated structure that lacks the six layers characteristic of the mammalian neocortex. Furthermore, studies examining the dendritic morphology of neurons in the avian telencephalic cortex revealed that very few if any neurons display a pyramidal morphology (Molla et al., 1986), contrasting to the mammalian neocortex where approximately 70 to 80% of all cortical neurons are pyramidal (Peters and Kara, 1985a; Peters et al., 1985). The ability of migrating pyramidal neurons to develop a unipolar morphology, invade the cortical plate and therefore bypass its predecessors by perforating the cell-dense cortical plate (leading to an inside-out accumulation pattern) is therefore a

mammalian-specific feature (Bar et al., 2000; Gupta et al., 2002). It is tempting to speculate that tyrosine 241 belongs to a molecular motif (YWQPPPP) representing a mammalian-specific protein-protein interaction module that might have enabled the coordinated appearance of a pyramidal unipolar morphology and the inside-out laminar accumulation of neurons during brain evolution.

Finally, this motif is specific to mammalian *Ngn2* as it is not found in the closely related mouse *Ngn1* or *Ngn3* (**Fig. 2.4B**). Interestingly, expression of mouse *Ngn1* promotes radial migration just as efficiently as Ngn2 but we found that Ngn1 does not promote pyramidal dendritic morphology of E14.5 cortical progenitors. Therefore, this implies that Ngn1 might be able to control the transactivation of RhoGAPs genes using a mechanism distinct from phosphorylation of Y241 which is not present in Ngn1. However, Ngn2 is unique in its ability to promote unipolar dendritic morphology and therefore, the phosphorylation of tyrosine 241 in cortical progenitors might represent a unique molecular mechanism among Neurogenins. Future experiments will determine the molecular basis underlying the potential differences between chick *Ngn2*, mouse *Ngn1*, mouse *Ngn3* and mouse *Ngn2* functions in the specification of cortical neurons phenotype.

Experimental Procedures

Animals

Mice were used according to a protocol approved by the Institutional Animal Care and Use Committee at the University of North Carolina, and in accordance with NIH guidelines. All experiments were performed on wild-type C57Bl6/J mouse strain (JAX) or on Ngn2 GFP-knockin allele backcross with C57Bl6/J mouse strain. Time-pregnant females were obtained by overnight breeding with males of the same strain and the morning following the breeding is considered as E0.5.

Immunofluorescence on cryostat sections

See supplementary Experimental Procedures.

Constructs

All Ngn2 cDNAs were subcloned into a pCIG2 vector that we modified from the pCIG vector (kind gift of Dr Andy Mc Mahon; Harvard University), which contains a (cDNA)-IRES-EGFP or a (cDNA)-IRES-DsRed2 cassette expressed under the control of a CMV-enhancer and a chicken β-actin promoter (Megason and McMahon, 2002). pCIG2 differs from pCIG in that the SV40 nuclear localization sequence 3' of the EGFP coding sequence was removed. The Cre recombinase coding sequence fused to SV40 nuclear localization sequence was obtained from pSK-Cre1 (a generous gift from Malcom Logan) and inserted into pCIG2.

Ex vivo electroporation and organotypic slice culture

A detailed protocol describing the combination of *ex vivo* electroporation of embryonic mouse cortex and organotypic slice culture will be published separately (Hand and Polleux, manuscript in preparation) and is available upon request. Briefly, electroporation of dorsal telencephalic progenitors was performed by injecting pCIG2 plasmid DNA into the lateral ventricles of isolated E14.5 embryonic mouse heads that were decapitated and placed in complete HBSS [see Supplementary Figure 1 and [(Polleux and Ghosh, 2002)]. Injections were performed using a Picospritzer III (General Valve) injector with 20 psi input pressure and one to four 4 msec long pulses as needed to fill the lateral ventricles. To visualize the DNA-containing solution we add 0.5% Fast Green (Sigma) at a 1:20 ratio with a high-titer plasmid DNA solution (3µg/µl endotoxin-free plasmid DNA; MEGA-Prep kit from Clontech). Electroporations were performed on the whole head with gold-coated electrodes (GenePads 5x7mm BTX; Supplementary Figure 1) using an ECM 830 electroporator (BTX) and the following parameters: two to four 100 ms-long pulses separated by 100ms-long intervals at 55V. In our transfected areas, we obtained transfection rates of close to 30% of all Nestin+ progenitors in the cortical ventricular zone of E14.5 mouse (Hand and Polleux, data not shown). Immediately after electroporation, the brain was extracted and 250 microns thick slices were cut using a LEICA VT1000S vibratome with special care towards the integrity of the pial surface. The resulting slices were maintained in organotypic slice cultures, fixed and stained for immunofluorescence as previously described (Polleux and Ghosh, 2002).

The primary antibodies used for immunofluorescence on slices were: mouse monoclonal anti-Nestin (Rat 401 Developmental Hybridoma Bank; 1:10); mouse monoclonal anti-MAP2 (Sigma); rabbit polyclonal anti-GFP and chicken polyclonal anti-GFP (Molecular Probes); rabbit polyclonal anti-Ngn2 that we developed [directed against amino-acid 35-49:C-SSADEEEDEELRRPG, BioGenes GmbH, Germany; used in **Suppl. Figure 2.2**] and another rabbit polyclonal anti-Ngn2 antibody (kind gift of Dr. M. Nakafuku; used in **Figure 2.1**), rabbit polyclonal anti-Cre recombinase (Covance Research Product, 1:3000), mouse anti-HuC/D (Molecular probes, 1:200).

Dissociated cortical cultures

Dissociated E14.5 cortical cultures were performed using a papain-based enzymatic dissociation method as previously described (Polleux and Ghosh, 2002; Polleux et al., 2000). Dissociated and electroporated cortical progenitors were cultured on glass-bottom dishes coated with Laminin and Poly-L-Lysine for 5 days in serum-free culture medium (NeuroBasal +B27+N2 supplements).

Confocal microscopy

Fluorescent immunostaining was observed using a LEICA TCS-SL laser scanning confocal microscope equipped with an Argon laser (488 nm), green Helium-Neon laser (546nm) and red Helium-Neon laser line (633nm) for

observation of Alexa488-, Alexa-546 conjugated secondary antibodies (Molecular Probes) and Draq5 nucleic acid staining (Alexis), respectively.

ACKNOWLEDGMENTS

We are grateful to K. Burridge, A. McMahon, M.J. Tsai and A. Ghosh for providing constructs and Dr Nakafuku for providing the polyclonal anti-Ngn2 antibody. We also thank P. Vanderhaeghen for his comments on an earlier version of the manuscript. The Nestin (Rat-401) monoclonal antibody developed by Dr Susan Hockfield was obtained through the Developmental Studies Hybridoma Bank developed under the auspices of the NICHD and maintained by The University of Iowa, Department of Biological Sciences, Iowa City, IA 52242. We thank all members of the Polleux lab for fruitful discussions and comments on the manuscript. This project was partially funded by the National Institute of Neurological Disorders and Stroke (NIH-NINDS NS047701-01) (FP), by the Confocal and Multiphoton Imaging Facility of the NINDS Institutional Center Core Grant to Support Neuroscience Research (P30 NS45892-01) and the March of Dimes Foundation for Birth Defects (FP). PM is a recipient of a CIHR Doctoral award, LN is supported by a EMBO long-term fellowship, JITH is supported by a Postdoctoral training fellowship from Australian NHMRC. FG's lab contribution was supported by MRC core funding and an European Commission RTD Program grant.

Supplemental Figures

Supplementary Movie 2.1. Dynamics of radial migration of cortical progenitors electroporated with EGFP. Movie may be downloaded at:

http://download.cell.com/neuron/mmcs/journals/0896-6273/PIIS0896627305007361.mmc2.mov

Supplementary Movie 2.2. Cortical progenitors electroporated with $Ngn2^{Y241F}$ display a loss of leading process polarity (red arrow cell) and failed nucleokinesis (red, green and blue arrow). Movie may be downloaded at:

http://download.cell.com/neuron/mmcs/journals/0896-6273/PIIS0896627305007361.mmc3.mov

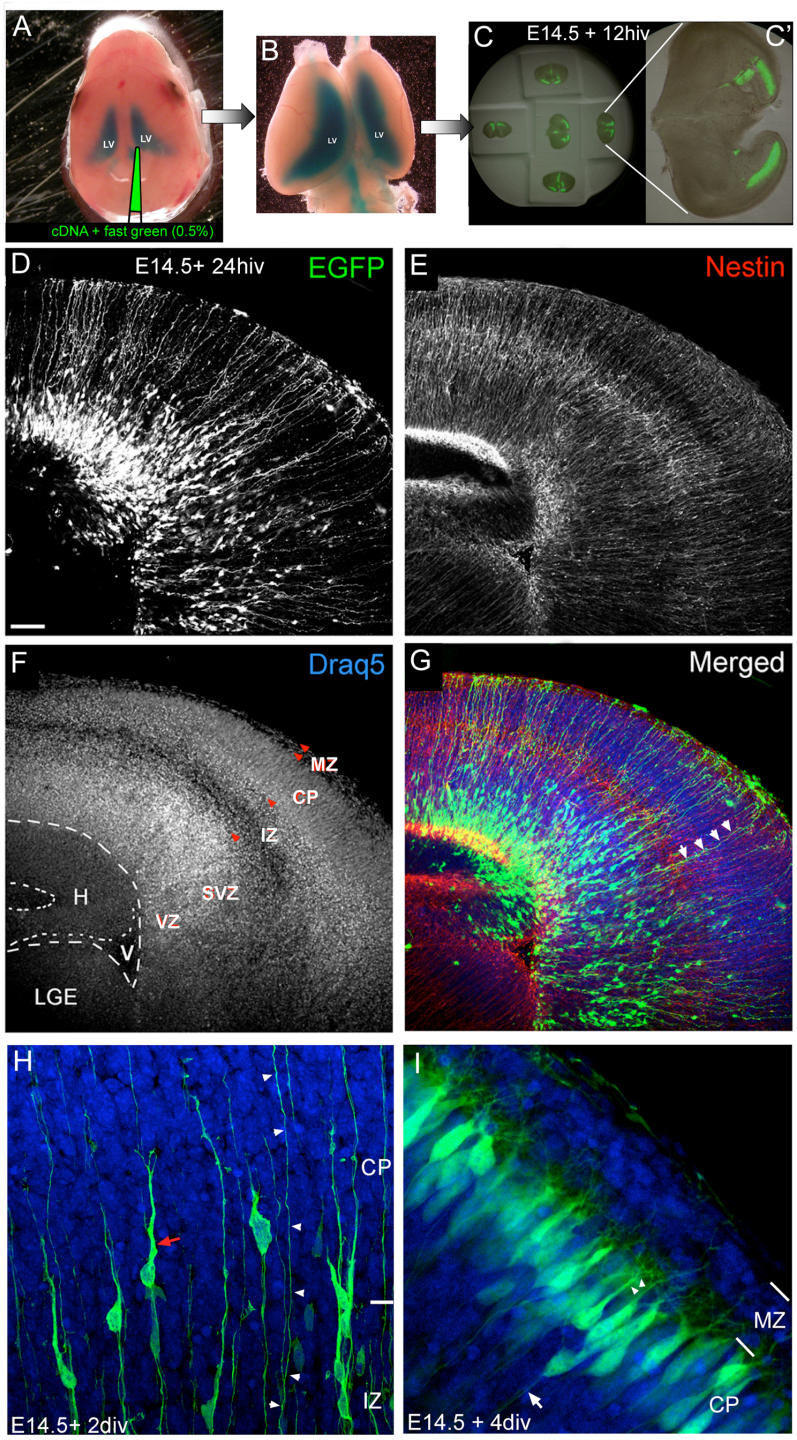

Suppl. Fig. 1 -Hand et al.

<u>Supplementary Figure 2.1.</u> ***Ex vivo*** **electroporation of cortical progenitors coupled to organotypic slice culture is a powerful technique to study the migration properties and dendritic morphology of cortical neurons**

(A-C') Intact head of E14.5 mouse embryos where a solution containing a pCIG2 plasmid mixed with 0.5% Fast Green has been injected into the lateral ventricles (labeled LV in A). After electroporation, the brain is isolated (B) and immediately sliced using a vibratome (see Method for details). 250 microns thick sections are then plated onto a semi-permeable organotypic membrane (C) as described previously (Polleux and Ghosh, 2002). After 12 hours *in vitro*, robust EGFP expression is specifically observed in cortical progenitors here shown on five slices (live picture in C-C'; see also **Suppl. Movie 2.1**). Note that the plasmid expression is precisely targeted dorsally and therefore does not transfect ventral progenitors in the ganglionic eminence.

(D-G) Confocal micrograph of a triple stained slice fixed 24 hours after electroporation showing that at this point, the vast majority of EGFP expressing cells (D) display radial glial morphologies with their cell bodies located in the VZ or SVZ and their radial glial process reaching the pial surface (arrowheads in G). The vast majority of EGFP expressing cells at 24 hiv express Nestin, a radial glial marker (E and data not shown). Nucleic acid dye Draq5 (blue) was systematically used to reveal the slices cytoarchitecture (F).

(H) After 2 days *in vitro*, EGFP+ neurons are found in the intermediate zone and start to invade the cortical plate displaying a typical unipolar morphology with a leading process directed towards the pial surface (red arrow). Arrowheads points to EGFP+ radial glial process still visible at this stage.

(I) After 4 days *in vitro*, EGFP+ neurons have reached the top of the cortical plate accumulating beneath the marginal zone (MZ). These pyramidal neurons already started differentiating with their apical dendrite branching in the MZ (arrowhead) and their axon growing ventrally towards the intermediate zone (arrow).

Abbreviations: CP: cortical plate; H: hippocampal anlage; LGE: lateral ganglionic eminence; MZ: marginal zone; IZ: intermediate zone; SVZ: subventricular zone; VZ: ventricular zone.

Scale bar values: D-G: 50 microns; H-I: 10 microns.

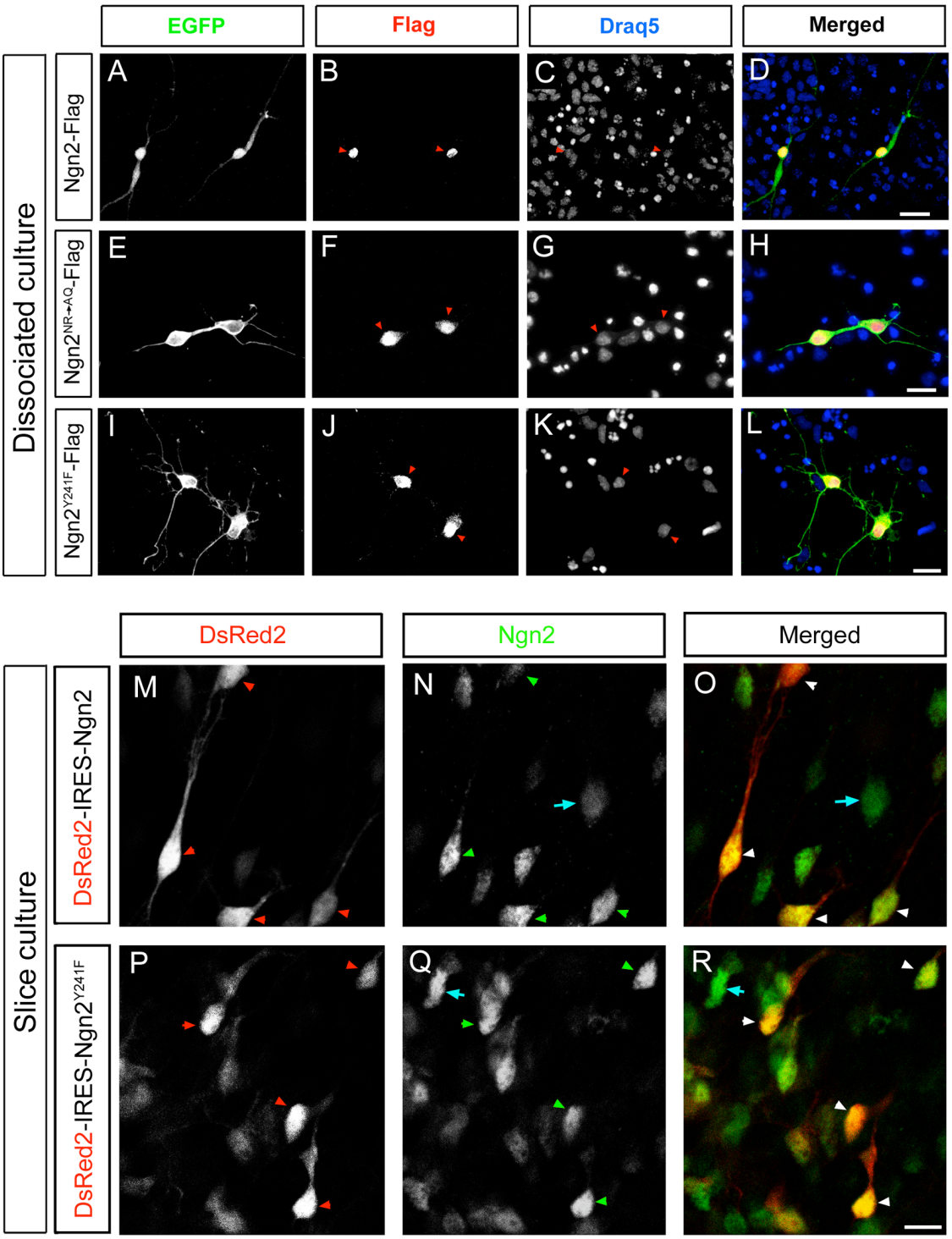

Supplementary Figure 2.2. Ngn2$^{NR->AQ}$ and Ngn2^{Y241F} are targeted normally to the nucleus

(A-D) Neurons derived from E14.5 progenitors successfully electroporated with a Flag epitope-tagged version of Ngn2 are identified by EGFP expression after 4 div (A). Immunofluorescence

directed against the Flag-epitope reveals a prominent nuclear localization of Ngn2-Flag (arrowheads in B) as confirmed by the identification of the nucleus using Draq5 (C).

(E-L) Expression of Flag-tagged $Ngn2^{NR->AQ}$ (E-H) or Flag-tagged $Ngn2^{Y241F}$ (I-L) also shows a prominent nuclear localization of Ngn2 (arrowheads in F and J respectively) demonstrating that these mutations do not interfere with nuclear targeting of Ngn2.

(M-R) Single confocal optical section (<1 microns z-section) showing that overexpression of wild-type Ngn2 or $Ngn2^{Y241F}$ by electroporation results in physiological levels of protein expression in cortical neurons in slice culture after 3 div. Immunofluorescence against Ngn2 using a polyclonal antibody allows comparison of the endogenous level of Ngn2 expression (blue arrows in N-O and Q-R) to the level of Ngn2 overexpression in electroporated cells identified by expression of DsRed2 (arrowheads in M-O for Ngn2 and P-R for $Ngn2^{Y241F}$). Note again the prominent nuclear localization of both endogenous Ngn2 and ectopically expressed Ngn2 or $Ngn2^{Y241F}$. These cells are migrating through the IZ after 3div and were imaged using single optical section (<1 microns z-section) by confocal microscopy.

Scale bar values: A-D: 30 microns; E-H: 15 microns; I-L: 20 microns; M-R: 10 microns.

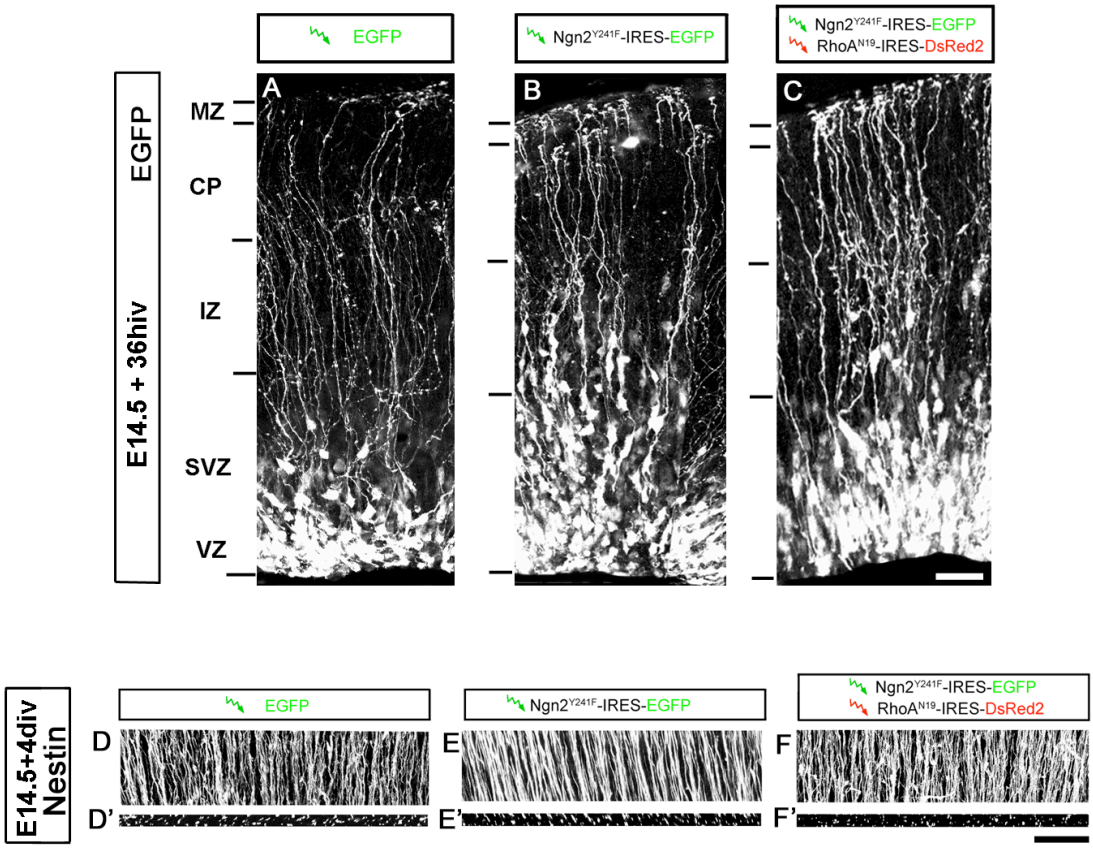

<u>Supplementary Figure 2.3.</u> Expression of Ngn2^{Y241F} and/or RhoA^{N19} does not affect the structure of the radial glial scaffold

(A-C) Cortical electroporation of E14.5 progenitors with EGFP (A) Ngn2Y241F or Ngn2Y241F and RhoAN19 expressing constructs does not alter the morphology of radial glial cells after 36 hours *in vitro*. Cells still display long their radial process (green arrows) with attachment to the basal membrane of the pia (red arrowheads).

(D-F') After 4 days *in vitro* the radial glial scaffold integrity was assessed more globally using anti-Nestin immunofluorescence followed by examination using laser-scanning confocal microscopy. Both maximum projection of 10 microns stacks (D-F) and orthogonal Z-sections (D'-F') of slices electroporated with the 3 sets of constructs indicated in panels A-C did not have any significant effect on the morphology or the number of radial glial processes.

Scale bar values: 50 microns in A-C; 25 microns in D-F'.

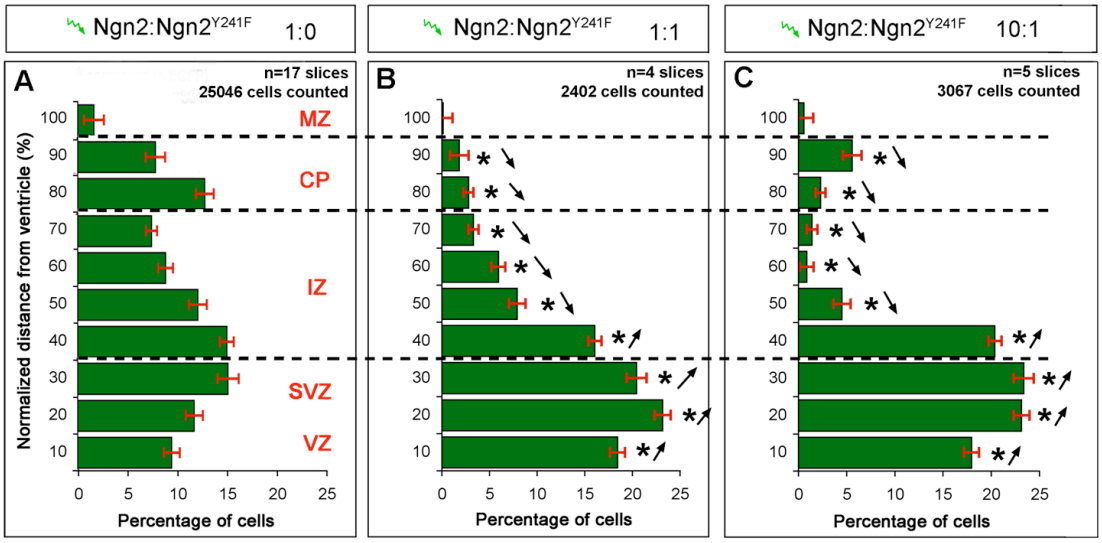

<u>Supplementary Figure 2.4.</u> Demonstration of the dominant-negative nature of Ngn2^{Y241F} over full-length Ngn2

(A-C) Histograms of the radial distribution of cells derived from progenitors co-electroporated with different ratios of Ngn2 versus Ngn2^{Y241F} (1:0 in A; 1:1 in B and 10:1 in C). Note that at a 1:1 ratio or a 10:1 ratio, cortical progenitors are still strongly inhibited in their ability to migrate radially suggesting that Ngn2^{Y241F} is playing a dominant-negative function over Ngn2.

Error bars represent standard error to the mean. Stars indicate significant ($p<0.01$- Chi square) differences of the proportion of neurons find in similar bins in B or C compared to A.

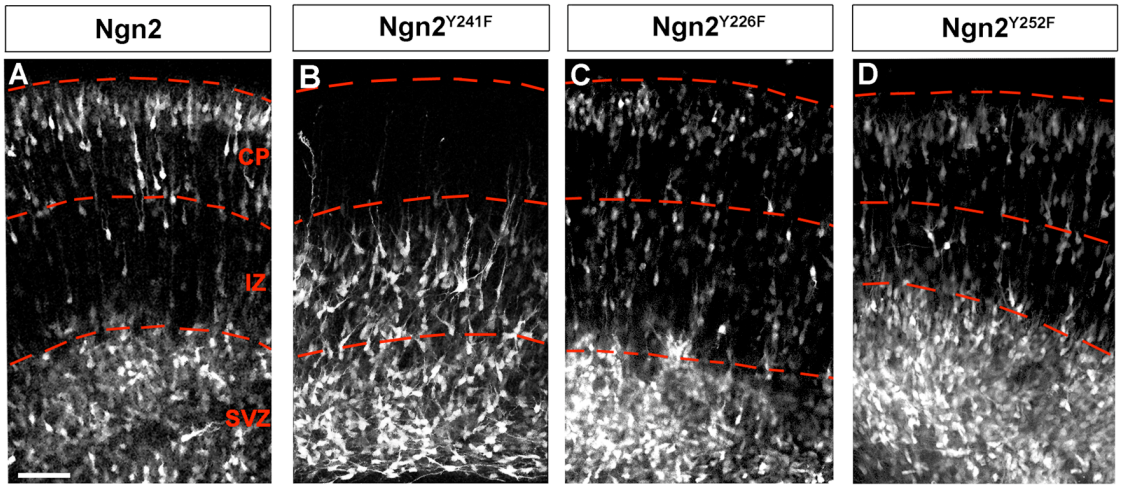

Supplementary Figure 2.5. Specificity of tyrosine 241 in inhibiting the radial migration properties of cortical progenitors

(A-C) Confocal micrograph of wild-type E14.5 slices electroporated *ex vivo* with full-length Ngn2 (A), Ngn2^{Y241F} (B), Ngn2^{Y226F} (C) and Ngn2^{Y252F} (D). Only expression of Ngn2^{Y241F} inhibits the radial migration of cortical progenitors, expression of either Ngn2^{Y226F} (C) or Ngn2^{Y252F} has no effect on the migration properties of cortical progenitors with a similar proportion of neurons reaching the cortical plate (C-D) compared to full-length Ngn2 electroporation (A).

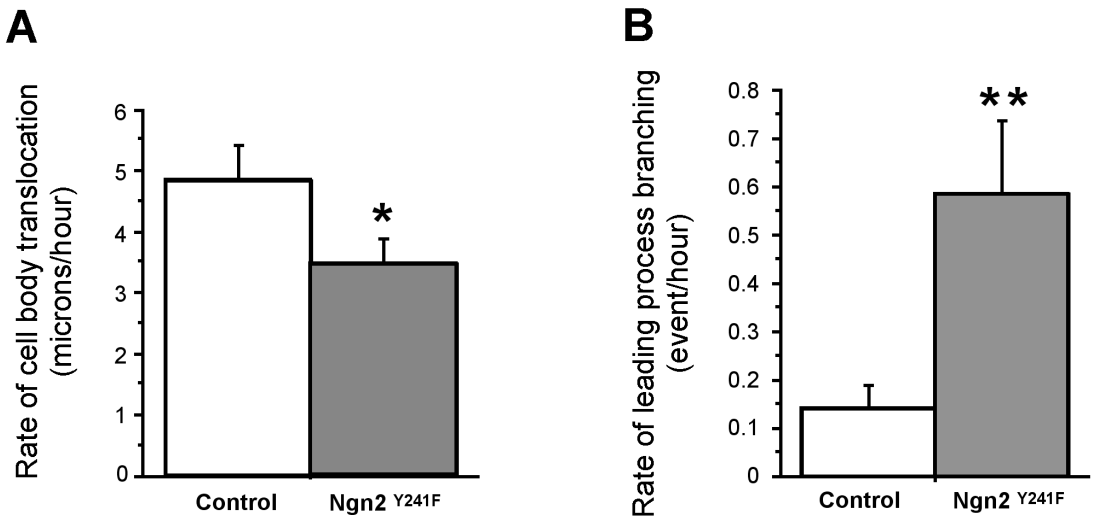

<u>Supplementary Figure 2.6.</u> Expression of Ngn2^{Y241F} decreases rate of cell body translocation and increases the rate of leading process branching of radially migrating neurons

(A-B) Quantification of the rate of cell body translocation (expressed in microns/hour, A) and the rate of leading process branching (event/hour, B) in neurons located in the intermediate zone and electroporated with control EGFP only (endogenously expressing Ngn2; white bars; n=17 cells from independent experiments) or Ngn2^{Y241F} (grey bars; n=12 cells from 3 independent experiments). * $p<0.05$ and ** $p<0.001$ according to a Mann-Whitney non-parametric test.

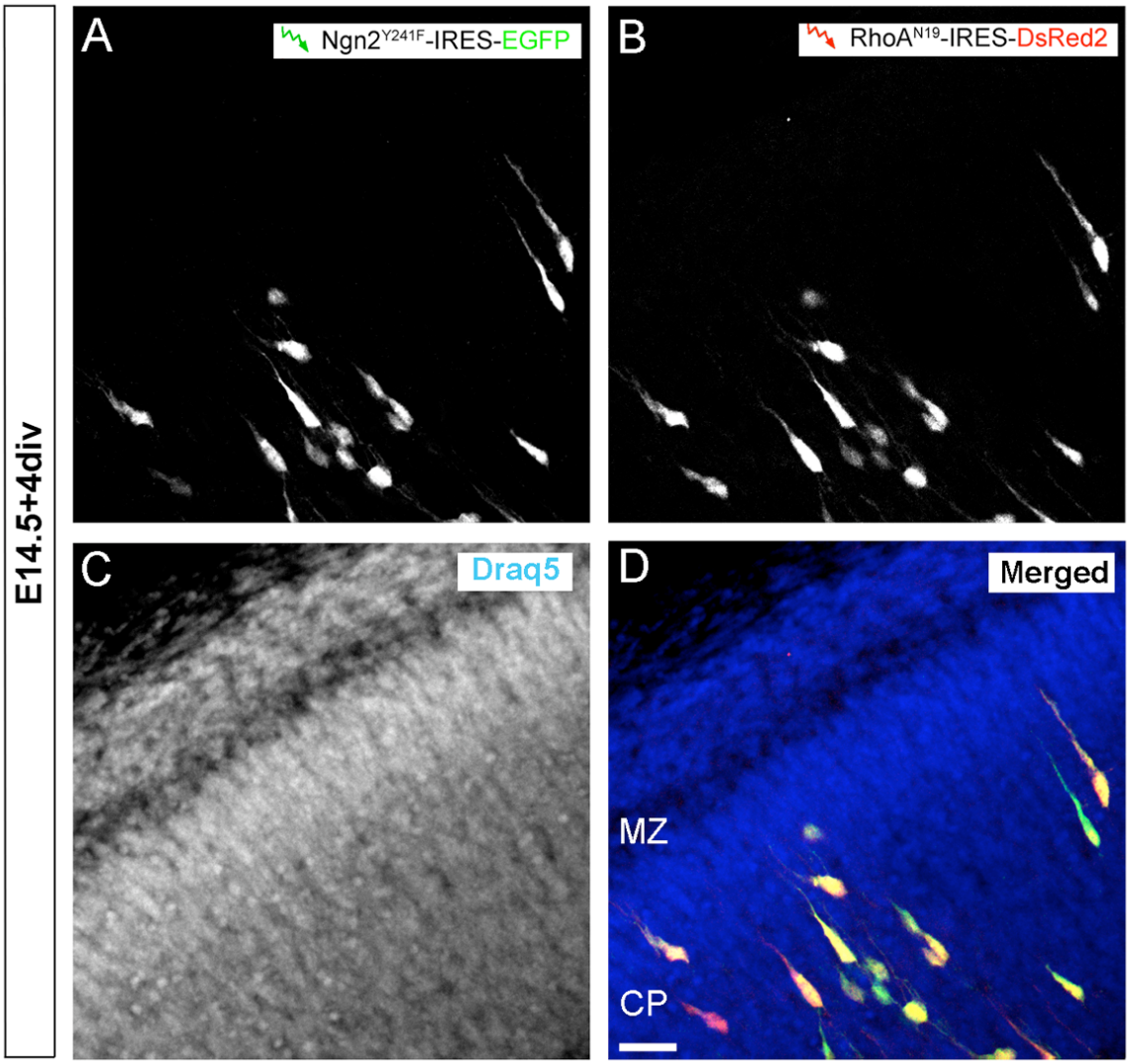

<u>Supplementary Figure 2.7.</u> High percentage of co-expression of two constructs following cortical co-electroporation

(A-D) E14.5 cortical slices co-electroporated with 1:1 ratio of Ngn2^{Y241F}-IRES-EGFP (A, green in D) and RhoA^{N19}-IRES-DsRed2 (B, red in D) are almost perfectly co-expressed in all neurons present in the cortical plate (merged in D). Slices were counterstained with nuclear staining Draq5 to reveal the cytoarchitecture (C).

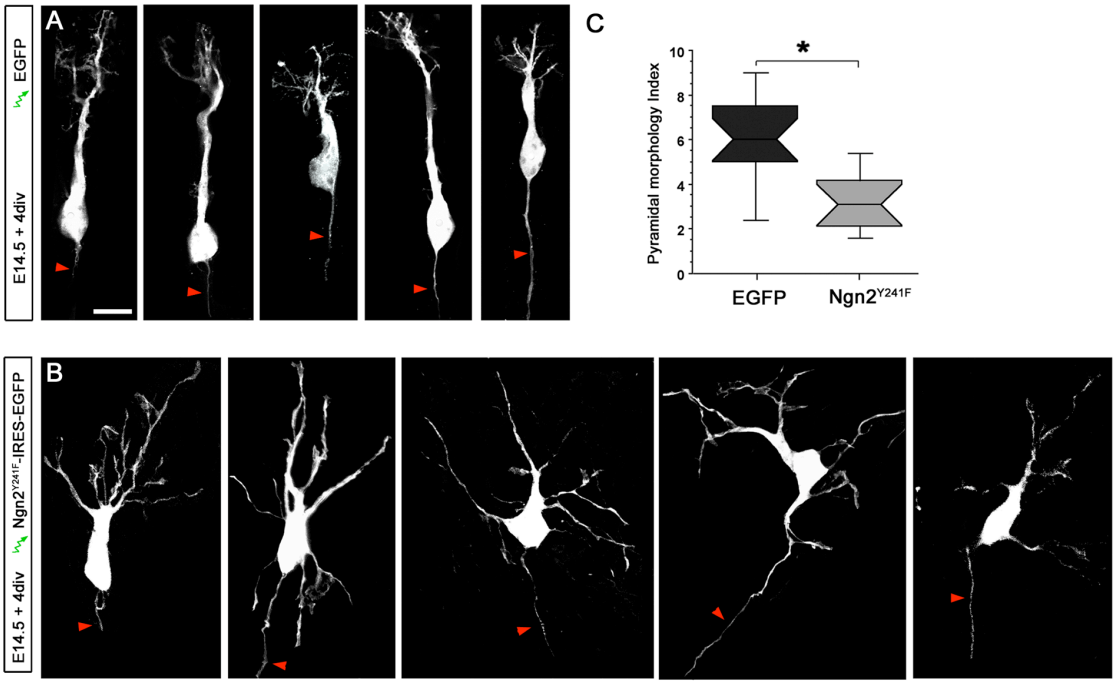

Supplementary Figure 2.8. Quantification of the dendritic morphology of electroporated neurons in the cortical plate

(A-B) Five representative dendritic morphologies of individual neurons located in the cortical plate after 4 div following progenitors electroporation at E14.5 with control EGFP (A) or Ngn2^{Y241F} (B) constructs. Note the prominent multipolar dendritic morphologies of neurons expressing the Ngn2^{Y241F} mutation. The pial surface is systematically oriented towards the top of the picture. Interestingly, the red arrowheads point to morphologically identified axons that do not seem to be affected by expression of Ngn2^{Y241F} at least with regard to their direction of outgrowth towards the ventricle.

(C) Box plot representation of the Pyramidal Morphology Index values obtained for EGFP-expressing neurons (n=17) and Ngn2^{Y241F} expressing neurons (n=12) in the cortical plate of E14.5 + 4 div. * $p<0.001$ Mann-Whitney non-parametric test. See Figure 8P for details regarding the box plot representation.

Scale bar value: 15 microns for A-B.

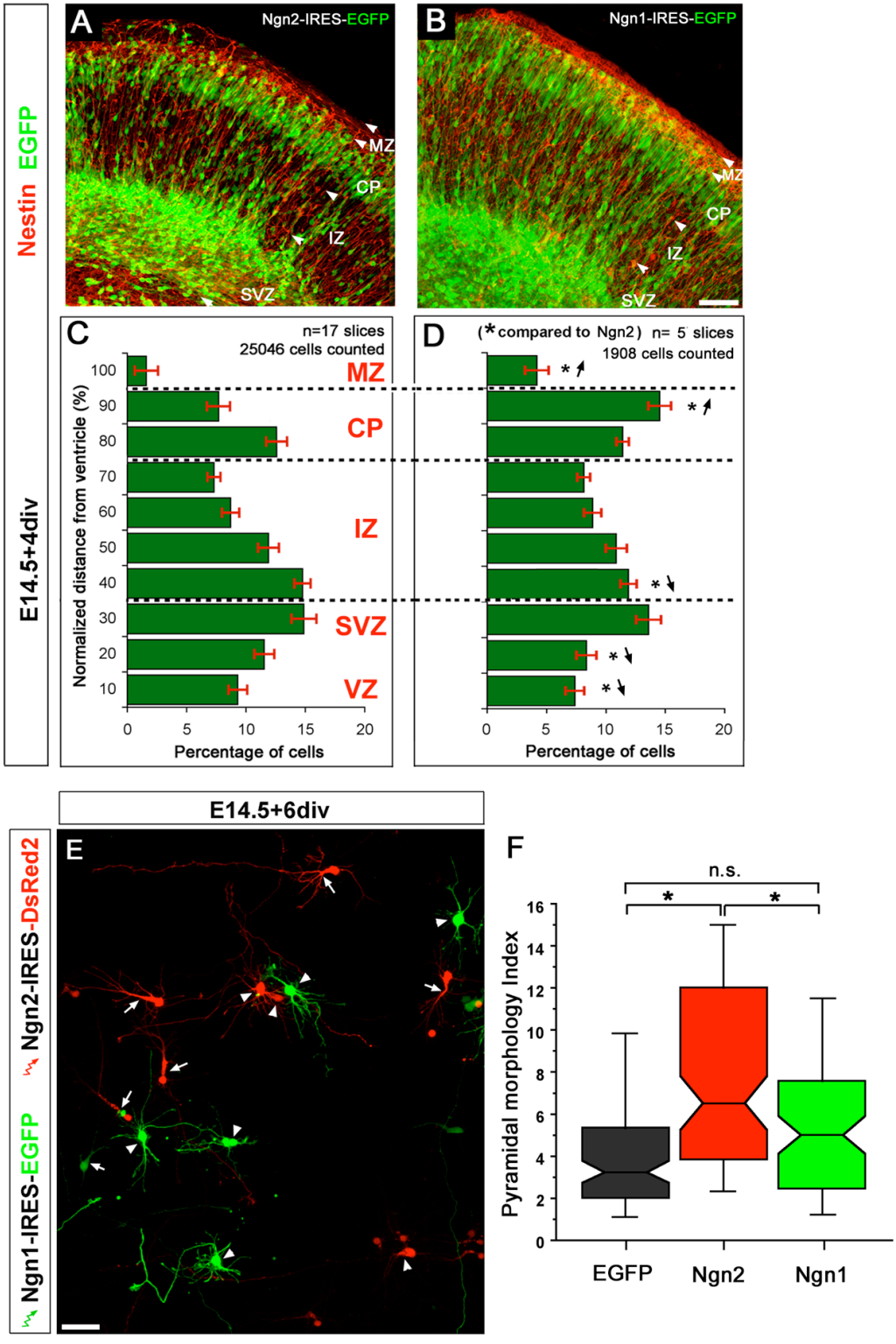
Nestin EGFP
E14.5+4div
A
Ngn2-IRES-EGFP
MZ
CP
IZ
SVZ
B
Ngn1-IRES-EGFP
MZ
CP
IZ
SVZ
C
n=17 slices
25046 cells counted
MZ
CP
IZ
SVZ
VZ
Normalized distance from ventricle (%)
100
90
80
70
60
50
40
30
20
10
0
5
10
15
20
Percentage of cells
D
(*compared to Ngn2) n= 5 slices
1908 cells counted
0
5
10
15
20
Percentage of cells
E14.5+6div
Ngn1-IRES-EGFP
Ngn2-IRES-DsRed2
E
F
n.s.
*
*
Pyramidal morphology Index
16
14
12
10
8
6
4
2
0
EGFP
Ngn2
Ngn1

Supplementary Figure 2.9. Ngn1 induces radial migration but is not promoting unipolar neuronal morphologies to the same extent than Ngn2

(A-B) Low magnification confocal micrographs illustrating the radial distribution of cell emerging from progenitors electroporated with Ngn2 (A) and Ngn1 (B).

(C-D) Histograms of the distribution of EGFP+ cells along the radial axis of the cortical wall (normalized as a percentage). Error bars represent standard error to the mean. Stars indicate significant ($p<0.01$- Chi square) differences of the proportion of neurons find in similar bins (for example comparing the 50% normalized distance bins between Ngn2 and Ngn1 over-expression). Ngn1 produces similar increase in the percentage of cells migrating to the cortical plate than Ngn2 when compared to control electroporation (EGFP only, see Figure 5). Note a slight but significant re-distribution of cells within the cortical plate and marginal zone in Ngn1 compared to Ngn2 electroporation.

(E-F) Electroporation of EGFP (not shown) Ngn1-IRES-EGFP and Ngn2-IRES-DsRed2 (E) in two distinct sets of E14.5 cortical progenitors followed by dissociation and co-culture for 6 div reveals than Ngn2 but not Ngn1 is sufficient to promote pyramidal dendritic morphologies compared to control EGFP expressing progenitors (quantified in F). See Figure 8P for details about the box plot representation.

* $p<0.001$ according to ANOVA one-way test and Fisher PLSD post-hoc test; n.s.: non significant according to the same analysis.

Scale bar values: 100 microns A-B; 30 microns E.

Supplementary Experimental Procedures

Immunofluorescent staining of cryostat sections

Ngn2 immunofluorescence was performed on freshly dissected brains were fixed in 4% paraformaldehyde/PBS for two hours, cryoprotected in 20% sucrose/PBS overnight, and cryopreserved in OCT. Ten micron thick sections were washed 3 times in TBST (25 mM Tris pH 7.5, 0.14 M NaCl, 0.1% Triton X-100), and blocked at room temperature for 1 hr in TBST supplemented with 5% goat serum (Invitrogen, Burlington ON) and 3% Bovine Serum Albumin (Sigma, St. Louis MO). Primary antibodies were co-incubated overnight at 4ºC with rabbit anti-Ngn2 (obtained from Dr Masato Nakafuku, Cincinnati Children's Hospital Research Foundaton, Cincinnati, OH, USA) diluted 1:2000 as follows: mouse anti-MAP2 (Clone HM-2; Sigma;1:500); mouse anti-NeuN (MAB377; Chemicon, Temecula CA; 1:500); mouse anti-Tuj1 (Covance, Berkeley CA; 1:1000). Sections were washed 3 times in TBST, and incubated with donkey anti-rabbit Cy3-conjugated (Jackson Immunoresearch, West Grove PA) and goat anti-mouse Alexa-488-conjugated (Molecular Probes, Eugene OR) secondary antibodies, diluted 1:500 in blocking solution for 2 hrs at room temperature. Sections were washed 3 times in TBST, incubated with TBST supplemented with 1 µg/ml DAPI (Santa Cruz Biotechnology, Santa Cruz CA) for 10 min at room temperature, washed 3 times in TBST, and coverslipped using Aqua Polymount (Polysciences Inc., Washington PA).

Sections stained for Ngn2 (n=20) were visualized using a Leica DMRXA2 microscope fitted with a Q Imaging Retiga EX camera under constant imaging conditions. Bins were generated by drawing lines at 100 μm intervals from the surface of the ventricle, extending into the cortical plate using Adobe Photoshop. Ngn2-positive cells were counted and scored for the presence or absence of NeuN immunofluorescence.

Automatic quantification of radial cell distribution in slice culture

Using a tile-scan function on a Leica TCS-SL confocal microscope (mounted on a DM-IRE2 inverted microscope stand) and equipped with a X-Y motorized Märzhäuser stage, assembly of multiple 20x fields (15 microns Z-stacks) were acquired to reconstruct the entire neocortical region electroporated along the radial and the latero-medial axis. Using ImageJ (http://rsb.info.nih.gov/ij/), the entire montage was run through a Bandpass Filter to segment and isolate cell-sized shapes. The image was then thresholded and segmented into radial regions of interest were individual cell position along the radial axis was recorder relative to the distance between the ventricle and the pial surface. Cell coordinates were recorded using ImageJ's Analyze Particles feature. These coordinates were imported into Excel along with the top (pial) and bottom (ventricle) boundaries coordinates obtained using ImageJ's Path Writer plugin. From these top and bottom boundaries, 200 boundary points were taken at

regularly spaced intervals leading to a sampling of approximately 10 microns wide. All of this processing was done using an Excel macro.

Time Lapse confocal microscopy

Using a Leica TCS-SL confocal microscope (mounted on a DM-IRE2 inverted microscope stand) and equipped with a X-Y motorized Märzhäuser stage, time-lapse confocal microscopy was performed by imaging multiple Z-stacks at different positions on a given set of electroporated slices (using X-Y motorized stage) repetitively at a frequency of 1 picture every 20 minutes. Slight drifts of the slices were corrected using an image registration tool developed in ImageJ (Turboreg and Stackreg- P. Thévenaz- Univ. Lausanne).

Automatic categorization of dendritic morphology using the Pyramidal Morphology Index (PMI)

The width of dendrites and the number of dendrites emerging from the cell body were automatically sampled using a sampling circle of fixed diameter (25 microns; see Fig. 7O) around a cell body from confocal images taken E14.5 cortical cultures maintained for 5 days *in vitro*. The java program used to record these values was adapted from William O'Connell's ImageJ plugin, *Oval Profile Plot*. Changes to this program were made with the gracious help of William O'Connell (Department of Radiology, University of California-San Diego) enabling the program to quickly record data from multiple cells into a single table. The

coordinates of the pixel values along the sampling circle were then imported into Excel (v. X- Microsoft). A macro in Excel was written to normalize 8-bit pixel values (0-255) and binarized them (>50% of max equal 1) so that contiguous positive pixels were counted as one process. The sum of adjacent positive points was used to calculate the relative width of each process. For each cell the PMI was recorded as the width of the largest process divided by the total number of processes that crossed the sampling circle.

Protein sequence analysis

Complete amino-acid sequences from human (NP_076924), mouse (NP_033848) and chick (NP_990127) Neurogenin2 (Ngn2) were aligned using Vector NTI suite 9.0.0. Putative phosphorylation sites were compared between chick, mouse and human Ngn2 using a structure- and conformation-based program ((Blom et al., 1999); NetPhos2; http://www.cbs.dtu.dk/services/NetPhos/).

Myc pull-downs and biochemistry

E14.5 cortical wholemounts electroporated with N-terminal pCIG2::cMyc-Ngn2-IRES-EGFP (Fig. 3B) were harvested at 48hiv and washed once in cold 1X PBS (containing protease and phosphatase inhibitors) and then lysed on ice for 15min in 1% NP40 buffer (containing protease and phosphatase inhibitors). The lysate was passed twice through a fine gauge needle, and cell debris was then pelleted

by centrifugation (10,000 rpm for 15min at 4°C). The supernatant was removed and used for immunoprecipitations: 250-500µg of protein lysate was mixed with 2µl of anti c-Myc antibody (final 1:250; Cell Signalling) plus 1% NP40 buffer (with protease and phosphatase inhibitors) to reach a final volume of 500 µl. Pull-downs were performed with pre-washed protein A agarose beads. Supernatants from pull-downs were denatured by boiling at 95°C for 5 minutes in the presence of SDS and proteins were separated electrophoretically on an 10% SDS-PAGE gel.

For phosphorylation experiments, cortical dissociated cells were cultured for 20 hours *in vitro* as described above. Cultured neurons were exposed to a thirty minutes 'phosphate purge' (cultured in phosphate-free, serum-free medium) and for 6 hours in the same medium containing 300mCi [γ^{32}P]-labeled ATP. After myc-pulldowns were performed, proteins were separated by electrophoresis and the blots were imaged using a Typhoon PhosphorImager (ImageQuant v1.1 Molecular Dynamics).

GST Pulldown from E15.5 cortex

Eight E15.5 embryos were electroporated *ex vivo* with pCIG2::GST-Ngn2-IRES-EGFP (N-terminal fusion; approx. 65kDa). After electroporation, the cortices were dissected from the embryos and cultured as cortical whole mounts for 48hrs *in vitro*. EGFP expressing regions of the cortices were removed and lysed in RIPA lysis buffer. 10% of the lysate was saved for analysis. Glutathione

sepharose beads were added to the remaining 90% of the lysate, and the lysate +beads were rotated at 4°C for 1hr. The beads were then pelleted by centrifugation, the supernatant was removed, and the beads were washed with 1XPBS (0.1M pH 7.4) three times. After washing with PBS, thrombin was added to the beads to cleave Ngn2 from GST. After 1hr, the supernatant containing the cleaved Ngn2 was removed and stored for analysis. Then 10mM of glutathione was added to elute GST from the glutathione sepharose beads. After 10min, the supernatant containing cleaved GST was removed and saved for analysis.

Luciferase-Renilla assay

A 1.7kB promoter sequence of *NeuroD* (also called *BETA2*; kind gift of Dr MJ Tsai- Baylor Coll. Med. (Huang et al., 2000a)) was subcloned upstream of a promoterless firefly luciferase plasmid (pGL3; Dual-Luciferase® ; Promega). Freshly plated P19 cells (ATCC) were transfected using Lipofectamine® 2000 (Invitrogen), with the appropriate combination of four constructs: (1) the *NeuroD*-Luciferase reporter, (2) a control plasmid expressing Renilla under the control of a constitutive mammalian promoter (TK-pRL; Promega), (3) an IRES-EGFP plasmid (pCIG2) expressing (or not; control empty vector) the following cDNAs: full-length mouse Ngn2, $Ngn2^{NR->AQ}$, $Ngn2^{\Delta basic}$ where the entire basic domain was deleted (amino-acid 113-124), and $Ngn2^{Y241F}$; (4) a plasmid expressing the ubiquitous bHLH protein E47 under the control of a CMV promoter (kind gift of Dr Anirvan Ghosh). Cell lysates were harvested 24 hours after transfection and the

Luciferase-Renilla normalized chemiluminescence (ratio pGL3 over TK-pRL) were assayed using a multiple fluorescence (FluoScan) plate reader as per the manufacturer's instructions (Promega).

Transactivation domain mapping

Transactivation mapping of mouse *Neurogenin2* (m*Ngn2*) was performed as above using the Dual Luciferase Assay (Promega). PCR fragments of m*Ngn2* (containing aa180-213, aa214-263, aa180-263) were subcloned into a GAL4 fusion protein plasmid (pFA, Stratagene). Human Embryonic Kidney (HEK) 293T cells were transiently co-transfected in triplicate with the respective GAL4-fusion constructs, pFRLuc (pFR-Luc, Stratagene), and Renilla plasmid (TK-pRL) using Lipofectamine® 2000. Twenty-four hours after transfection cells were lysed and assayed as mentioned above.

Chapter 3

Title: Ngn2 regulates the initial axon guidance of cortical pyramidal neurons

Randal Hand [1] and Franck Polleux[1 #]

[1] Neuroscience Center, Department of Pharmacology, School of Medicine, University of North Carolina at Chapel Hill, Chapel Hill, NC 27599, USA

This article was submitted to *Neuron*.

Keywords

Neurogenin2, cortex, pyramidal neurons, axon guidance

Summary

The formation of the mammalian central nervous system requires the establishment of complex neural circuits between a diverse array of neuronal subtypes. Here we report that the transcription factor Ngn2 is crucial for the proper formation of cortical circuits. The genetic loss of Ngn2 results in fewer callosal axons projecting towards midline as well as abnormal midline crossing. shRNA-mediated knockdown of Ngn2 revealed its cell autonomous requirement for the proper projection of axons from layer 2/3 pyramidal neurons to the midline. We found that the acute loss of Ngn2 in vivo induces superficial neurons to project axons laterally towards aberrant cortical and subcortical targets. These and previous results demonstrate that Ngn2 is required for the specification of cardinal features defining the phenotype of cortical pyramidal neurons including their migration properties, dendritic morphology and axonal projection.

Introduction

The mammalian nervous system consists of a tremendous diversity of neurons forming a complex network of neural circuits. In the cerebral cortex, the canonical microcircuitry is composed of two main subtypes of neurons: glutamatergic excitatory pyramidal neurons and GABAergic inhibitory interneurons. GABAergic neurons arise from neural progenitor cells (NPCs) located in the ventral telencephalon and subsequently migrate tangentially to the cerebral cortex (Anderson et al., 1997). Upon arriving in the cerebral cortex, GABAergic interneurons mature and display several distinct non-pyramidal dendritic morphologies and are characterized by a locally projecting axon (Ramón y Cajal, 1995). In stark contrast, glutamatergic pyramidal neurons arise from radial glial progenitors located in the dorsal telencephalon (Noctor et al., 2001). Radial glial progenitors have cell bodies located within the ventricular zone (VZ) of the cerebral cortex and have processes spanning the cortical wall thereby contacting both the apical surface located along the lateral ventricle and the basal surface located on the pia. During neurogenesis, these neural progenitors divide asymmetrically to generate another radial glial cell and a newly differentiating neuron which initiates migration to the subventricular zone (SVZ) located just superficial to the ventricular zone (Noctor et al., 2001). These neurons located in the SVZ are known as intermediate progenitor cells (IPCs) and they display a dynamic multipolar morphology characterized by the rapid

extension and retraction of neurites. It is hypothesized that these IPCs undergoing rapid morphological changes are sensing the environment in order to polarize their leading process (future apical dendrite) dorsally towards the cortical plate and their trailing process (future axon) ventrally (Barnes and Polleux, 2009). After polarization, the neuron will adhere to a radial glial cell process and migrate through the cell sparse intermediate zone (IZ) towards the pial surface. Upon reaching the top of the cortical plate (CP), just below the pial surface, pyramidal neurons detach from the radial glia cell and further mature, elaborating both their dendritic and axonal processes and begin forming neural circuits. This process of neuronal differentiation within the cerebral cortex occurs in waves starting around embryonic day 11 (E11) and ends around E18 (Angevine, 1970; Polleux et al., 1997; Takahashi et al., 1995). During each wave of neurogenesis, neurons will migrate past previously generated neurons so that the newest neurons occupy more superficial position than previously generated neurons. This pattern of neurogenesis is described as inside-first outside-last pattern and underlies the formation of six discrete layers of neurons in the neocortex (Marin and Rubenstein, 2003). Ultimately, the location of progenitors, mode of migration, neurotransmitter expression, dendritic morphology, and axonal projections are used to define subtypes cortical neurons (Nieuwenhuys, 1994).

One of the defining feature of pyramidal neurons is the types of axonal projections they form within the brain and spinal cord. Interestingly, pyramidal neurons located different cortical layers project axons to different regions both

within and outside of the cortex . The deep layers of the cortex (layers 5/6) mostly have axons projecting outside of the cortex to subcortical regions (Leone et al., 2008; Molyneaux et al., 2007). The subcortical axons must initially project laterally to exit the cortex to ultimately innervate regions outside of the cortex. These axonal projections are contrasted by the axonal projections made by neurons in superficial layers (layers 2/3) which project to other cortical areas including callosal projections via the corpus callosum (Leone et al., 2008; Molyneaux et al., 2007). These callosal axons will initially project medially towards the corpus callosum. This initial choice to project medially or laterally is one of the earliest axon guidance decision made by a pyramidal neuron. While axons of pyramidal neurons must ultimately respond to many different cues to innervate appropriate regions of the brain and spinal cord, all axons of pyramidal neurons must first differentially project along the medial-lateral axis.

Neurogenin2 (Ngn2) is a proneural basic Helix-Loop-Helix (bHLH) transcription factor that regulates several phenotypic features of pyramidal neurons. Ngn2 was first identified for its ability to promote neuronal differentiation in the brain and spinal cord (Ma et al., 1996; Sommer et al., 1996). Beyond the neurogenic function in the regulation of pan-neuronal differentiation, further studies, demonstrated that Ngn2 plays a role in specifying phenotypic features of subtypes of neuronal populations such as neurotransmitter expression (Fode et al., 2000; Schuurmans et al., 2004). In addition, we previously demonstrated that Ngn2 regulates radial migration and dendritic morphology of pyramidal neurons

(Hand et al., 2005). Since Ngn2 regulates many of the defining phenotypic features of pyramidal neurons, we tested if Ngn2 regulates the type of axon projections characterizing subset of pyramidal neurons. Using loss of function assays, we found that Ngn2 regulates the axon guidance of superficial pyramidal neurons in vivo.

Results

Temporal pattern of Ngn2 expression relative to axogenesis of callosally projecting neurons

Ngn2 is expressed within the germinal zones of the cerebral cortex during development (Hand et al., 2005). At early stages of neurogenesis (E10-E12), Ngn2 is primarily expressed in actively dividing NPCs located in the VZ (Shimojo et al., 2008) and not within in the preplate (PP) where newly differentiated neurons are located (**Supplemental Figure 3.1A-D**). Interestingly, as neurogenesis progresses, Ngn2 expression shifts from primarily being expressed in actively dividing NPCs at early time points (E10-E12) to being expressed primarily in newly differentiated neurons at later time points (>E14.5) (Shimojo et al., 2008). Our expression data confirms this shift as Ngn2 expression is found in the VZ, SVZ, and occasionally in the IZ at E16.5 (**Supplemental Figure 3.1E-H**). Additionally, at E16.5 many of the Ngn2 positive cells also express the transcription factor Tbr2 (**Supplemental Figure 3.1E-H**). Tbr2 is a transcription factor expressed in IPCs (Englund et al., 2005) and is necessary for the production of IPCs (Sessa et al., 2008). We observe frequent co-expression of Ngn2 and Tbr2 in the SVZ/IZ. Thereby, this temporal pattern of expression, suggests Ngn2 may regulate the transition from a multipolar IPC to a highly polarized migrating neuron with a unipolar leading process (future apical dendrite) and a trailing process (future axon).

To visualize if late Ngn2 expression in the SVZ/IZ matches temporally with axon initiation of callosally projecting neurons that are generated between E15.5 and E18.5 (Molyneaux et al., 2007), we used *ex vivo* electroporation followed by organotypic slice culture. This technique effectively introduces cDNA into NPCs, and within 24 hours post electroporation, neurons will begin to differentiate from the NPCs (Hand et al., 2005). To insure we labeled superficial layer neurons, we electroporated cortices at E15.5 a time point in which only superficial neurons would be labeled (Hatanaka et al., 2004)**.** To visualize the emerging axons, we optimized electroporation conditions to allow for single cell resolution using a plasmid encoding the YFP variant Venus and imaged cells 36 hours post-electroporation. At this time point, we found many newly differentiated neurons containing a long single neurite (**Supplemental Figure 3.1I**). Interestingly, these single long neurites grew medially towards the corpus callosum within the IZ, strongly suggesting that these are presumptive axons. In these neurons, the emergence of axons appears to precede the formation of a leading process and the initiation of radial migration. Therefore, the directed emergence of the axon occurs soon after differentiation of the pyramidal neurons projecting medially and correlates well with Ngn2 expression, suggesting that Ngn2 might regulate the directed emergence of axons from superficial pyramidal neurons. More importantly, these results strongly suggest that the decision to project medially to become a callosally projecting neurons is taken extremely early during neuronal

differentiation, well before the neurons reach their final position in the cortical plate.

Ngn2 is required for callosal axon projection and midline crossing

To assess the role for Ngn2 in regulating the axonal projection of pyramidal neurons, we began by assessing cortical axon projections in the Ngn2 knockin mouse. The Ngn2 knockin mouse has EGFP inserted into the Ngn2 locus creating a null allele that will faithfully report the expression of Ngn2 (Seibt et al., 2003), from this point forward the Ngn2 homozygous knockin mouse will be referred to as the Ngn2-/- mouse. We began our study by harvesting Ngn2+/- and Ngn2-/- embryos at E18.5 since the Ngn2-/- mice are perinatally lethal (Fode et al., 1998). We immunostained coronal sections from E18.5 embryos with the axonal marker L1, which labels most of the cortical axon tracts and allowed us to assess major tract formation in the embryonic brains (**Figure 3.1A-L**). Interestingly, we found a dramatic decrease in the number of callosal axons in many Ngn2-/- embryos (**Figure 3.1D-F,J-L**) compared to the Ngn2+/- embryos (**Figure 3.1A-C,F-I**). Careful examination of these embryos also revealed abnormalities at the midline. Often the Ngn2-/- embryos had an abnormal corpus callosum (**Figure 3.1D-F**) and less frequently, the Ngn2-/- embryos completely lacked a corpus callosum (**Figure 3.1 J-L**). The embryos containing malformed corpus callosums, often had axons appearing to defasciculate prior to reaching the midline (arrowheads in **Figure 3.1E,J**). To determine if the defasciculating

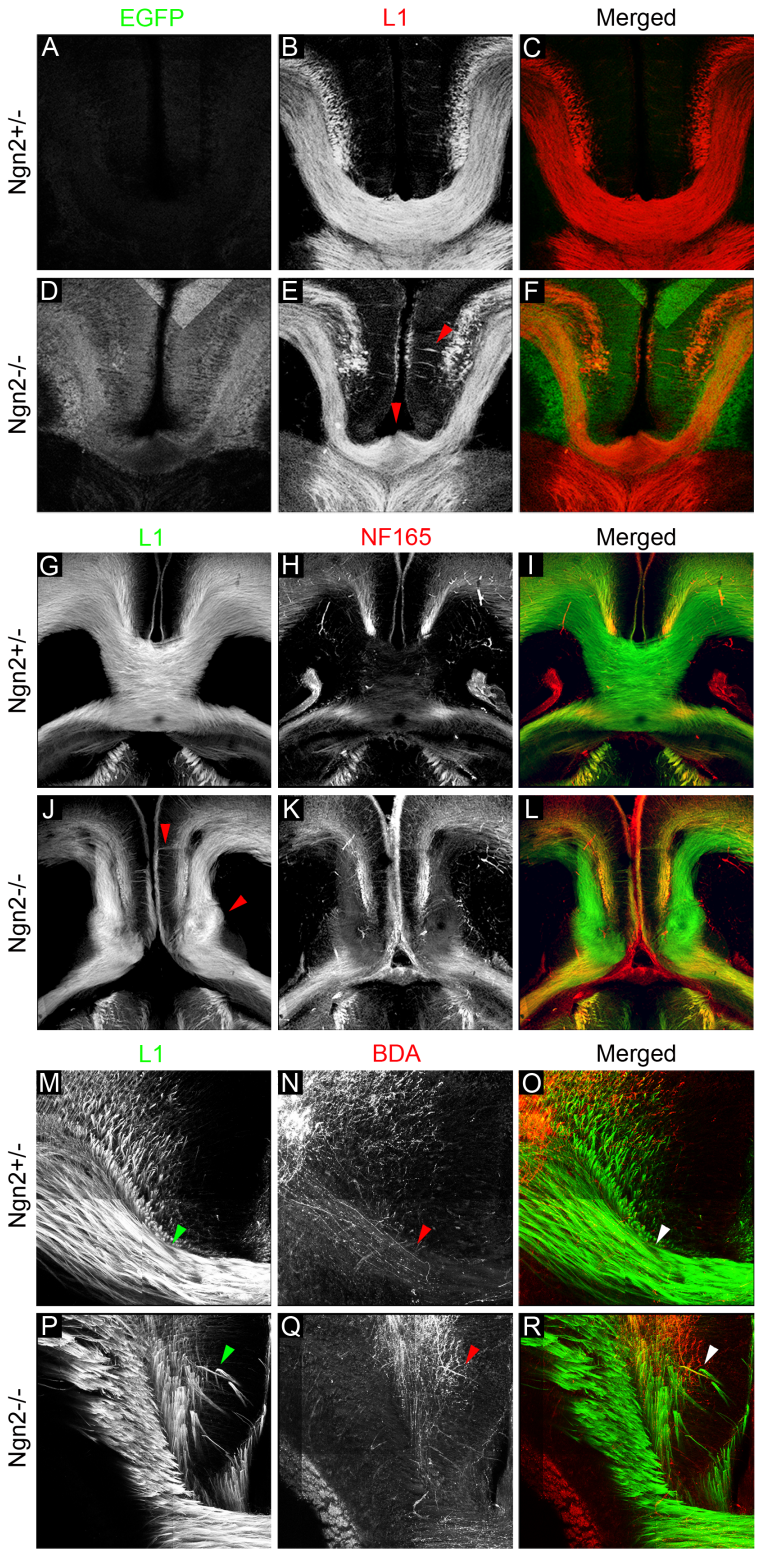

Figure 3.1: Ngn2 regulates callosal axon projection and corpus callosum formation *in vivo.*

Coronal sections of E18.5 Ngn2 +/- embryos (A-C) and Ngn2 -/- (D-F) embryos were immunostained with EGFP (A,D,) since EGFP was inserted into the Ngn2 locus to create the null allele. The sections were also immunostained with the axonal marker L1 (B,E,) to reveal many of the cortical axon tracts. Merged EGFP and L1 images (C,F) show a reduction in callosal axons in Ngn2-/- embryos compared to the heterozygous embryos. The immunostaining also revealed malformations of the corpus callosum revealed an aberrant axonal projections at the midline and an abnormal corpus callosum (red arrows, E). Horizontal sections from E18.5 Ngn2+/- embryos (G-I) and Ngn2-/- (J-L) embryos were immunostained for the axonal markers L1 (G,J) and NF165 (H,K). Merged images (I,L). The immunostaining of axonal markers shows a reduction of callosal axons shows the lack of a corpus callosum (J-L), the formation of probst bundles (red arrow, J), and a misprojecting axons at the midline (red arrow, J) in the embryos lacking Ngn2. None of these phenotypes was observed in the heterzygous embryos. Ngn2 +/- cortices (M-O) and Ngn2+/- (P-R) cortices were injected with the anterograde tracer BDA at E18.5 to determine if the axons that prematurely defasciculate orginated from cortical neurons. Coronal sections were immunostained with the axonal marker L1 to reveal callosal axons (M,P). The BDA tracings were revealed with streptavidin conjugated with Alexa546 (N,Q). Merged images (O,R). Prematurely defasciculating axons were revealed in the Ngn2 -/- embryos by both L1 staining and BDA anterograde tracings (P-R, arrows) This phenotype was not observed in Ngn2+/- embryos (M-O). BDA anterograde tracings definitively demonstrate that these axons are cortical in orgin.

axons originated from ipsilateral cortical neurons, we used Biocytin (or biotinylated dextran amine; BDA) to anterogradely trace cortical axons. Ngn2+/- and Ngn2-/- cortices were injected with BDA at E18.5 to label cortical projecting axons. The brains were sectioned and counterstained with L1 to visualize callosal axons and the BDA anterograde tracings were visualized using Alexafluor conjugated streptavidin (arrowheads in **Figure 3.1M-R**). As suspected, the BDA anterograde tracings labeled axons from cortical neurons in the Ngn2-/- embryos defasciculating before they reach the midline (arrowheads in **Figure 3.1P-Q**). This premature axon defasciculation phenotype was never found in Ngn2+/- embryos (**Figure 3.1M-O**). In total we examined 10 litters from Ngn2+/- heterozygous matings. We found no defect in any axonal tracts from the 12 Ngn2+/- embryos we examined. In the 13 Ngn2-/- embryos examined, we found 46% had a significant decrease in thickness of corpus callosum suggesting a reduced number of callosal axons, 31% had malformations and hypoplasia of the corpus callosum, and 15% had a complete agenesis of the corpus callosum. Our data demonstrates that Ngn2 regulates the number of callosal axons reaching the midline, as well as the guidance of callosal axons at the midline, and the formation of the corpus callosum.

Ngn2 regulates the initial guidance of callosal axons

The reduction of the size of the CC could be due to a reduction in the number of neurons specified to project medially. While it is clear that Ngn2

regulates callosal axon projection, it is unclear whether these effects are cell-autonomous or cell non-autonomous effects. We tested the cell autonomy of Ngn2 effects on callosal axons by documenting the emergence of callosal axons from newly differentiated neurons. We generated a bicistronic plasmid that allows simultaneously expression of a short hairpin (sh)RNA under the RNA polymerase III-specific U6 promoter and the YFP variant Venus under the RNA polymerase II-specific chicken b-actin (CAG) promoter (**Supplemental Figure 3.2A**). We generated a control plasmid (pSCV2) which expresses a nonspecific shRNA and plasmids containing shRNAs targeting Ngn2. We tested the effectiveness of the shRNA-mediated knockdown of Ngn2 in P19 cells. We found that the shRNA targeting Ngn2 effectively knocks down myc-tagged Ngn2 even when transfected at a 1:10 ratio of shRNA to myc-tagged Ngn2 (**Supplemental Figure 3.2B**). Once convinced we could effectively knockdown Ngn2 expression, we generated rescue mutant of Ngn2 ($Ngn2^{Rescue}$) in which a single noncoding point mutation was created within the region targeted by the shRNA. This noncoding point mutation reduced the ability of the shRNA to target Ngn2 (**Supplemental Figure 3.2C**) and allowed us to control for potential off-target effects of our shRNA.

The *ex utero* electroporation coupled with organotypic slice culture is ideal for rapidly assessing the many aspects of pyramidal neuron differentiation and migration, so we began by performing a developmental time course to assess if the axonal projections of cortical neurons are maintained in slice cultures *in vitro.* Embryonic cortices were electroporated at times ranging from E13.5 to E16.5

and organotypic slices cultures were prepared and culture for 5 DIV, allowing for generation, migration and axon projection of electroporated pyramidal neurons (**Supplemental Figure 3.2E-H**). We found that the axonal projections of pyramidal neurons cultured *in vitro* mimicked those found *in vivo*. At the earliest time points (E13.5 and E14.5), we found a significant proportion of axons were projecting laterally as we would expect since deep layer neurons are generated at these developmental time points (**Supplemental Figure 3.2E&F**). At later time points (E15.5-16.5), the axons of electroporated neurons almost exclusively projected medially (**Supplemental Figure 3.2 G&H**) as only superficial neurons would be generated at this later time point (Molyneaux et al., 2007). To test the cell autonomous regulation of axon projection by Ngn2, E15.5 cortices were electroporated with either control shRNA (control), shRNA targeting Ngn2 (Ngn2KD), or shRNA targeting Ngn2 plus the $Ngn2^{Rescue}$ mutant (Rescue) and cultured for 5 DIV. As expected, the majority of pyramidal neurons expressing control shRNA displayed medially projecting axons (**Figure 3.2B-D,K**). Interestingly, neurons containing the shRNA targeting Ngn2 had a significant increase in laterally projecting axons ($p<0.01$, **Figure 3.2E-G,K**). High magnification of the lateral cortex reveals the presence of neurons within the cortical plate with lateral projections (arrowheads in **Figure 3.2L**). To confirm that the presence of axons erroneously projecting laterally is a Ngn2-specific effect, we electroporated cortices with both the shRNA targeting Ngn2 and the $Ngn2^{Rescue}$ mutant. As expected, the neurons containing both the shRNA

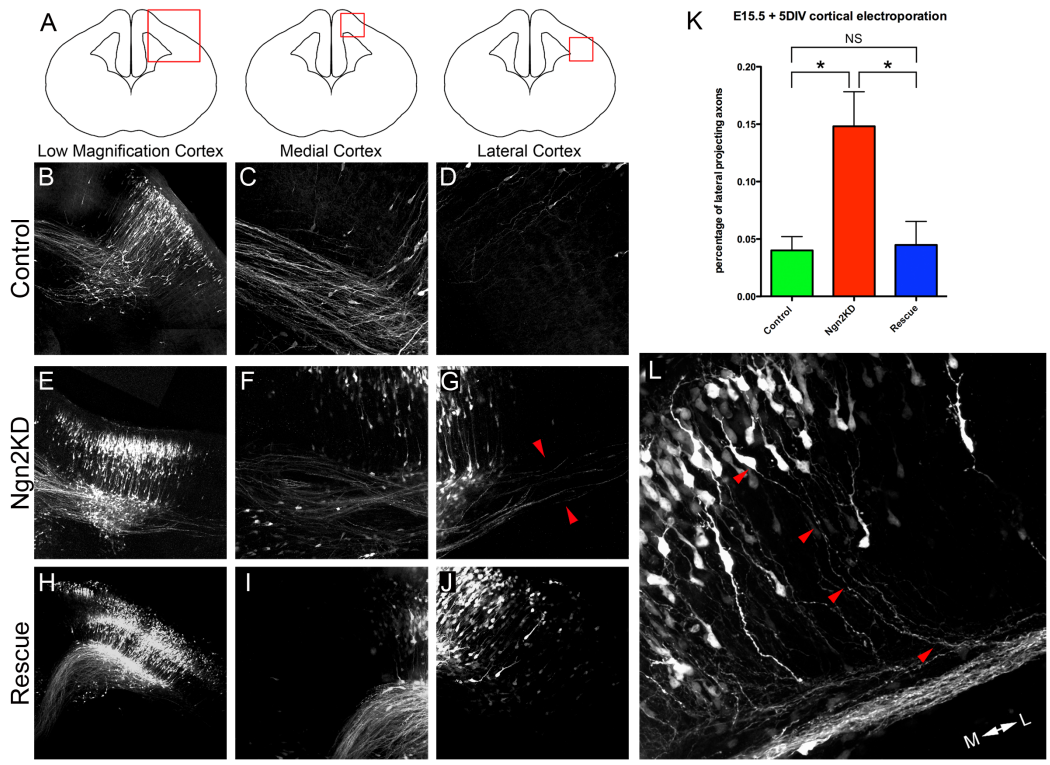

Figure 3.2: Ngn2 is required cell autonomously for proper axon guidance of upper layer cortical neurons to the midline.

(A-J) To target upper-layer cortical neurons, the dorsal telencephalon of E15.5 wild-type embryos were electroporated with plasmids encoding the fluorescent protein Venus and either a control shRNA (B-D), shRNA targeting Ngn2 (E-G), or shRNA targeting Ngn2 plus Ngn2^{Rescue} mutant that has a single non-coding point mutation reducing the ability of the shRNA to target Ngn2 (H-J). Following electroporation, organotypic slice cultures were prepared and culture for 5 DIV. Diagrams depict the areas that were imaged (A) for the expression of Venus revealing the neurons and their axons containing the shRNA. Regardless of the shRNA electroporated, all conditions contain medial (callosal) projecting axons (C,F,I). Interestingly, the neurons containing only the shRNA targeting Ngn2 had a dramatic increase in the number of lateral projecting axons (red arrows, G), many of the neurons were located within the cortical plate (L). Quantification of the axonal projections demonstrate a significant increase in the number of lateral projecting axons in neurons containing only the shRNA targeting Ngn2 (K). n.s, not significant, * $p<0.05$ according to ANOVA test.

targeting Ngn2 and the Ngn2^{Rescue} mutant had significantly fewer laterally projecting axons when compared to the neurons containing the shRNA targeting Ngn2 alone ($p<0.05$, **Figure 3.2H-J,K**) and no significant increase in laterally projecting axons compared to the control shRNA (**Figure 3.2H-J,K**). The data from the acute loss of Ngn2 suggest that Ngn2 regulates the axon guidance of callosal axons in a cell autonomous manner. This data combined with the data from the Ngn2-/- embryo demonstrates that Ngn2 is required in layer 2/3 neurons for the guidance of their axon towards the midline. Furthermore, our evidence suggest that the initial axon guidance of pyramidal neurons is an early event occurring just after neuronal differentiation well before completion of neuronal migration to their final destination in the cortical plate.

Loss of Ngn2 does not alter the laminar fate of cortical neurons

Recent studies have demonstrated that several transcription factors and transcriptional regulators regulate the molecular identity of cortical neurons and ultimately laminar identity of pyramidal neurons (Leone et al., 2008). In these cases, changes in laminar fate are altered and the axonal projections are correspondingly altered. Since, a general change in laminar fate could explain reduction of callosal axons in Ngn2-/- embryos and the increase of laterally projecting axons after shRNA mediated knockdown of Ngn2, we assessed whether there was a change in laminar fate in Ngn2-/- embryos or upon Ngn2 knockdown. We began by immunostaining Ngn2+/- embryos and Ngn2-/- at

E18.5 for deep layer molecular markers (**Supplemental Figure 3.3A-F**). Tbr1 is a transcription factor expressed primarily by layer 6 neurons (Bulfone et al., 1995), and CTIP2 is a transcription factor highly expressed in layer 5 neurons and weakly expressed in layer 6 neurons (Arlotta et al., 2005). We found no expansion in Tbr1 or CTIP2 expresssion in Ngn2-/- cortices (**Supplemental Figure 3.3D-F**) when compared to Ngn2+/- cortices (**Supplemental Figure 3.3A-C**). Although we did not see an expansion of deep layer neurons, we wished to directly test whether superficial layer neurons were generated in the absence of Ngn2. To do this, we harvested Ngn2+/- and Ngn2-/- pups at P0, the last time point possible to assess Ngn2-/- mice. Here we immunostained for CTIP2 and Cux1, a transcription factor expressed in superficial layer neurons (2-4) (Nieto et al., 2004). We found Cux1 expression in neurons just superficial to CTIP2 expressing neurons in both Ngn2+/- cortices (**Supplemental Figure 3.3G-I**) and Ngn2 -/- cortices (**Supplemental Figure 3.3J-L**). While we did not observe any change in expression of laminar markers between Ngn2+/- cortices and Ngn2-/- cortices, we did observe the presence of CTIP2-expressing neuronal heterotopias ventral to layer 5 in the Ngn2-/- cortices (arrowheads in **Supplemental Figure 3.3J&L**), and an increase of Cux1 positive neurons in layers V and VI (bracket in **Supplemental Figure 3.3K**), illustrating the migration phenotype previously reported (Hand et al., 2005; Heng et al., 2008). In addition to testing Ngn2-/- embryos for lamination defects, we also tested if there was a more subtle change in laminar fate that could be observed using shRNA

mediated knockdown of Ngn2. Here we electroporated E15.5 cortices with control shRNA or shRNA targeting Ngn2. After 5 DIV, we performed immunofluorescent staining of electroporated slices with the laminar markers CTIP2 and Cux1. As expected we found very few neurons containing the control shRNA that were CTIP2 positive (3.3%) (**Figure 3.3A-C,M**). Just as we observed with the Ngn2-/- embryos, we found that shRNA mediated knockdown of Ngn2 did not induce the expression of CTIP2 in superficial neurons containing the shRNA targeting Ngn2 (1.3%); **Figure 3.3D-F,M**). To confirm that the shRNA-mediated knockdown of Ngn2 did not alter the laminar fate of superficial neurons, we immunostained the cortices electroporated with either the control shRNA (**Figure 3.3G-I**) and the shRNA targeting Ngn2 with Cux1 (**Figure 3.3J-L**). We found that regardless of the shRNA electroporated the vast majority of neurons express the layer II-IV marker Cux1 (control shRNA 94.8% and Ngn2KD 97.5%) (**Figure 3.3N**). Based on the immunostaining of laminar markers in both Ngn2-/- embryos and in slice cultures electroporated with shRNA targeting Ngn2, we have found no altered laminar fate upon the loss of Ngn2. These results demonstrate that Ngn2 is required for the proper axonal projection of layer 2/3 neurons medially but not for the general specification of laminar fate.

Superficial pyramidal neurons lacking Ngn2 project axons to many areas postnatally

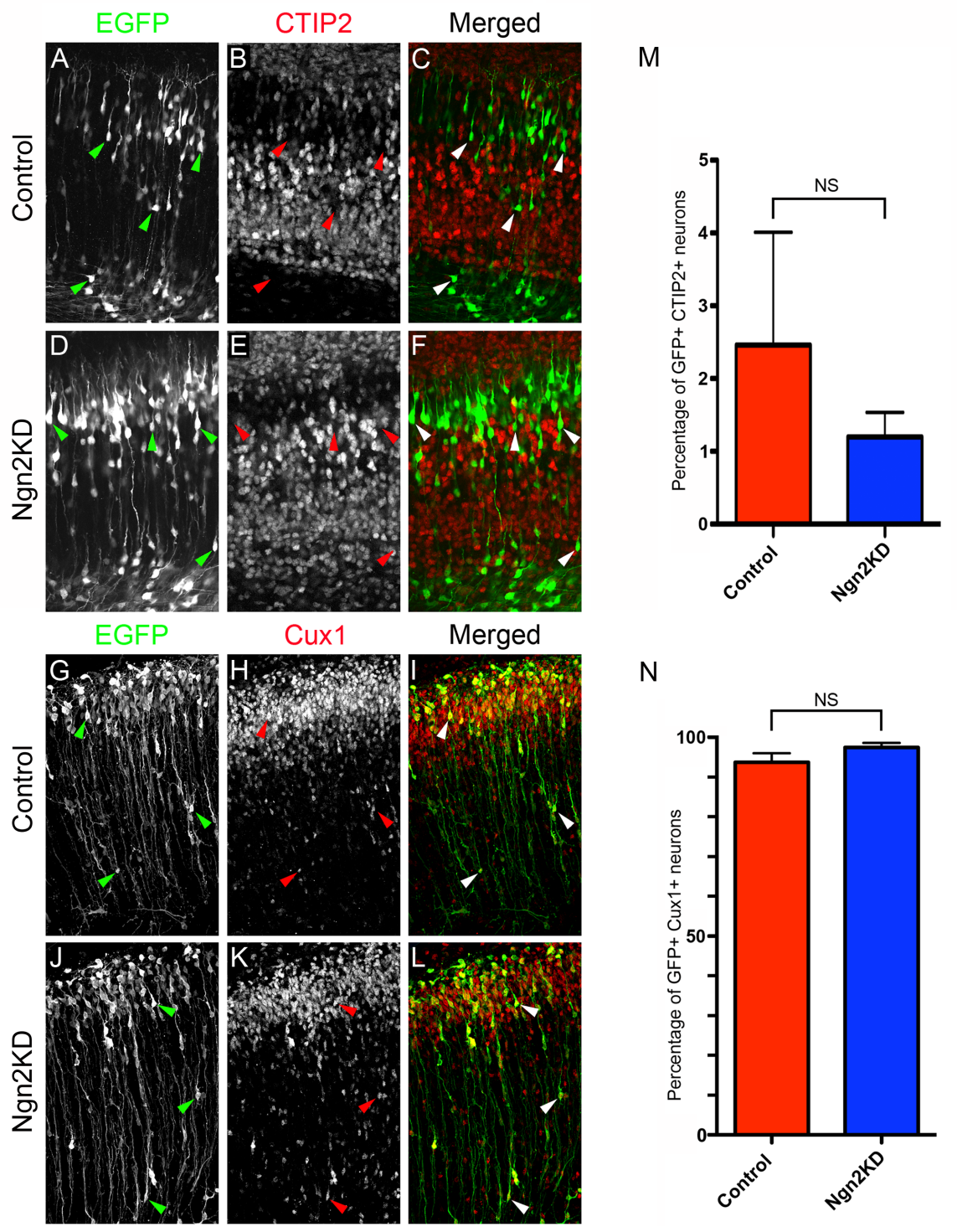

Figure 3.3: Knockdown of Ngn2 expression does not induce a change in laminar fate.

E15.5 embryonic cortices were electroporated with plasmids encoding for the YFP variant Venus and either control shRNA or shRNA targeting Ngn2. Following electroporation, organotypic slice

cultures were prepared and cultured for 5 DIV. To identify any potential change in laminar fate, slices were stained for CTIP2, a molecular marker for deep layers (5-6) and Cux1, a molecular marker for superficial layers (2-4). Electroporated cells were identified by immunostaining for EGFP (A,D,G,J). CTIP2 immunostaining (B,E) and the merged images (C,F) demonstrated that very few electroporated neurons express the deep layer marker. Quantification of this data showed no significant difference in the number of neurons that immunostained for GFP and CTIP2 (M). Cux1 immunostaining (H,K) and merged images (I,L) show that the majority of electroporated neurons express the superficial layer marker. Quantification demonstrated that there is no significant difference in the number of neurons that immunostained for GFP and Cux1 (N). Interestingly, the location of the neurons within the cortex has no effect on the expression of laminar markers (arrows). NS = no significance

Superficial neurons lacking Ngn2 have fewer callosally projecting axons (**Figure 3.1**) and acute knockdown of Ngn2 using shRNA induces superficial pyramidal neurons to project axons laterally (**Figure 3.2**). While the *ex vivo* cortical electroporation coupled with organotypic slice cultures allowed us to rapidly identify the errantly projecting axons upon Ngn2 knockdown, we were unable to decipher where these axons ultimately project postnatally. To assess where the misguided axons project, we used *in utero* electroporation of control shRNA and shRNA targeting Ngn2. The cortices of embryos were electroporated at E15.5 and the electroporated embryos were born and the mice were harvested at postnatal day 14 (P14). The P14 brains were sectioned and immunostained for GFP, Cux1, and Draq5 was used as a fluorescent nuclear stain. We imaged several regions in the brain to identify where axons innervated (**Figure 3.4A**) We found that the vast majority of axons in cortices electroporated with the control shRNA (**Figure 3.4B**) innervated the contralateral cortex (**Figure 3.4C**). Rarely did axons from neurons containing the control shRNA project to any other area such as the ipsilateral cortex (**Figure 3.4D**), internal capsule (**Figure 3.4E**), or thalamus (**Figure 3.4F**). The axons from neurons expressing shRNA targeting Ngn2 (**Figure 3.4B'**) projected to several areas. Some axons from the neurons containing the shRNA targeting Ngn2 did successfully innervated the contralateral cortex (**Figure 3.4C'**). Interestingly, the misguided axons that initially projected laterally, were found in many areas of the brain. We found an increase in axons present in the ipsilateral cortex (**Figure 3.4D'**). We also found many

axons within the internal capsule (**Figure 3.4E'**), suggesting that some of the errantly projecting axons were capable of exiting the cortex. Interestingly, we found that Ngn2-KD neurons projected axons within the thalamus (**Figure 3.4F'**), proving that these axons were capable of innervating subcortical targets. The fact that acute knockdown of Ngn2 induce axons to erroneously project to areas both within and outside of the cortex suggests that there is no default targeting of superficial neurons lacking Ngn2. This data supports the notion that Ngn2 is important in regulating the initial axon guidance choice of callosal axons to project medially towards the corpus callosum, as erroneously projecting axons appear to innervate other brain regions randomly. Interestingly, we did not observe any defects in midline crossing of axons from neurons containing the shRNA targeting Ngn2. This would suggest that the defects in midline crossing and premature defasciculation of callosal axons may be cell non-autonomous. This is plausible as Ngn2 is expressed in the cingulate cortex and at the midline (Imayoshi et al., 2008).

The long term *in utero* electroporation of shRNA targeting Ngn2 also replicated the well-documented migration phenotype attributed to Ngn2. We observed no inhibition in migration in neurons containing the control shRNA (**Supplemental Figure 3.4A**). Just as we have documented in the Ngn2-/- cortices (**Supplemental Figure 3.3J-L**) (Hand et al., 2005), we found the presence of neurons located ventral to the upper layers of the cortex containing the shRNA targeting Ngn2 (**Supplemental Figure 3.4B**). We do not believe that

the inhibition of migration induced by the loss of Ngn2 is responsible for the axon guidance phenotype, since we see more erroneously projecting axons than misplaced cells. In addition, we find neurons located in the upper layers of the cortex with laterally projecting axons (**Figure 3.2L** and **Supplemental Figure 3.4K&L**). Based on these findings, we believe that Ngn2 is necessary for the guidance of callosal axons, and that an inhibition of migration is not responsible for the laterally projecting axons originating from superficial pyramidal neurons. Just as we confirmed the impaired migration associated with a loss of Ngn2, we also replicated our previous results implicating Ngn2 in controlling the dendritic morphology and orientation. We found pyramidal neurons located in superficial layers with apical dendrites improperly oriented (**Supplemental Figure 3.4C-F**) and neurons with multiple apical dendrites (**Supplemental Figure 3.4G-J**). Overall, the *in utero* electroporation of shRNA targeting Ngn2 allowed us to identify the location of erroneously projecting axons and further demonstrate its importance in the regulation of migration, dendritic morphology, and axonal projections during cortical development.

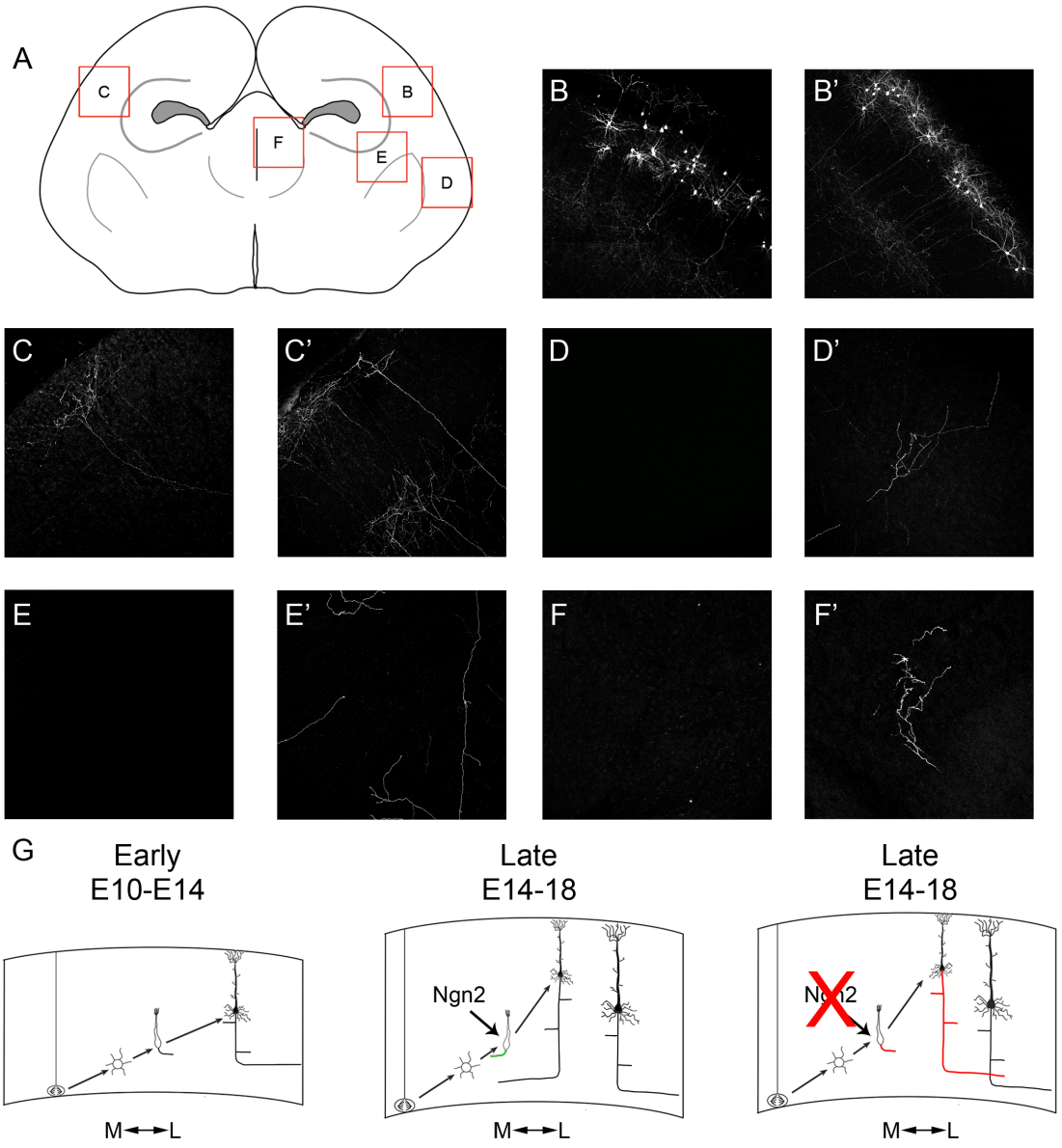

Figure 3.4: The loss of Ngn2 results in cortical axons to aberrantly project to cortical and subcortical targets *in vivo*.

In utero electroporation of plasmids encoding for the YFP variant Venus and either control shRNA or shRNA targeting Ngn2 was used to determine the final location of aberrantly projecting axons. Electroporated embryos were allowed to be born and survive to P14. Coronal sections were prepared and immunostained for GFP to enhance and reveal electroporated neurons and their axonal projections. A diagram depicting the areas imaged (A). Several areas were found to

contain axons from neurons electroporated with control shRNA (B-F) and shRNA targeting Ngn2 (B'-F'). These areas include the zone of electroporation (B,B'), the contralateral cortex (C,C'), the ipsilateral cortex (D,D'), the internal capsule (E,E') and the thalamus (F,F'). We found that several areas containing axons from neurons electroporated with the shRNA targeting Ngn2 (D',E',F') but not the control shRNA (D,E,F). We have developed a model for the regulation of cortical axon guidance by Ngn2 (G). At early stages (E10-E14) when deep layer neurons (5-6) are being generated, most of the axons initially project laterally. At later stages when superficial layer (2-4) neurons are being generated, neurons most differentially respond to cues within the cortex and project medially towards the corpus callosum . We believe Ngn2 is involved in this differential response. In the absence of Ngn2, there is a reduction in callosal axons and some of these axons project laterally towards cortical and subcortical targets.

Discussion

Here we have demonstrated a novel role for Ngn2 during cortical development. We found that the genetic loss of Ngn2 results in a reduction of callosal axons and a malformation of the corpus callosum. When Ngn2 expression is knocked down acutely using shRNA in progenitors of superficial pyramidal neurons, many of the callosal axons that initially project medially, aberrantly project laterally toward both cortical and subcortical brain regions. The change in axonal projection resulting from a loss of Ngn2 does not induce any obvious change in laminar fate at least with regard to the expression of transcriptional regulators such as CTIP2 or Cux1. Taken together our results show that Ngn2 coordinates the acquisition of many of the cardinal features of pyramidal neurons in the developing cortex including neurotransmitter expression (Fode et al., 2000), migration properties and dendritic morphology (Hand et al., 2005), and axonal projections (present study; (Seibt et al., 2003)).

During cortical development, the axons from pyramidal neurons undergo a switch in initial projection from lateral to medial as superficial neurons begin to differentiate around E14.5. Based on our evidence, we hypothesize that Ngn2 is not necessary for the ability of the axons of deep layer neurons to initially project laterally (**Figure 3.4G**). However, Ngn2 seems to be involved in regulating the switch in initial axon projection from lateral to medial as superficial neurons begin to differentiate (**Figure 3.4G**), as we observed fewer callosal axons and the

increase of laterally projecting axons with a loss of Ngn2 (**Figure 3.4G**). This suggests that the primary functions of Ngn2 differ over time. During early stages of cortical neurogenesis (such as E12.5), Ngn2 is primarily playing a proneural function due high expression in dividing progenitors (Shimojo et al., 2008), but at later time points Ngn2 has additional roles in the acquisition of the phenotypic traits associated with pyramidal neurons, including axon guidance. We believe this could be explained by the subtle change in expression pattern over time. Our data supports this as we found Ngn2 expression in the upper SVZ and the IZ, and most of these cells were also expressing Tbr2 (**Supplemental Figure 3.1E-H**), a marker for IPCs at the later time point of E16.5, when superficial layer neurons are differentiating. Since Ngn2 expression pattern changes as the cortex develops, we hypothesize Ngn2 is capable of inducing differential gene expression as the cortex develops due to the differential expression of transcriptional coactivators and differences in accessibility of transcriptional targets due to epigenetic regulation by chromatin modifying proteins. Future studies will be needed to identify which of the known the transcriptional targets of Ngn2 (Gohlke et al., 2008; Mattar et al., 2004; Seo et al., 2007) or novel transcriptional targets of Ngn2 regulate the switch in axonal projections over time, and test how Ngn2 differentially regulates these gene(s) during cortical development.

Our data suggests that the initiation of the axon is a directed process leading to the guidance of axon medially within the intermediate zone. We found this initial projection often occurred in immature neurons prior to forming a leading process and before initiating migration (**Supplemental Figure 3.1I**). This raises an interesting question of whether direct transcriptional targets of Ngn2 regulate the initial projection of the superficial pyramidal neuron or if downstream transcription factors are responsible for the observed phenotype. There are several transcription factors that are directly and indirectly downstream of Ngn2, these include transcription factors expressed in the SVZ (Tbr2 and NeuroD4) (Ochiai et al., 2009; Seo et al., 2007), in the IZ (NeuroD1) (Hand et al., 2005; Schuurmans et al., 2004), and in the cortical plate (NeuroD2 and MEF2C) (Mattar et al., 2004; Schuurmans et al., 2004). Recently, a downstream target of Ngn2, a small GTPase, Rnd2 was found to regulate radial migration of pyramidal neurons (Heng et al., 2008). Furthermore, Rnd2 was sufficient to rescue the inhibition of migration in Ngn2-/- embryos. Interestingly Rnd2 is a direct target of both Ngn2 and NeuroD1 (Heng et al., 2008), suggesting that Ngn2 is capable of directly and indirectly regulating the transcription of a gene necessary for migration. Identifying the gene(s) that are directly responsible for the directed axon initiation is of the greatest interest. Several studies have investigated genes downstream of Ngn2. Not surprisingly, receptors for several axon guidance ligands including Netrins, Slits, Semaphorins, and Ephrins are down regulated in Ngn2-/- embryos (Gohlke et al., 2008; Mattar et al., 2004; Schuurmans et al., 2004), and some of these

receptor were found to be direct targets of Ngn2, while others are presumably indirect transcriptional targets. We believe that Ngn2 is likely regulating gene expression underlying the initial projection of callosal axons medially both directly and indirectly.

We along with others, we have identified that Ngn2 is crucial for the proper formation of cortical circuitry. While Ngn2 was first identified as a proneural transcription factor, further studies have demonstrated that Ngn2 regulates many of the defining features of pyramidal neurons. Elegant genetic studies determined Ngn2, along with Ngn1, a close homolog with an overlapping expression pattern, specify the neurotransmitter fate of pyramidal neurons (Schuurmans et al., 2004). In addition, Ngn1 is largely sufficient to compensate for the proneural deficit associated with the loss of Ngn2 , and likely to compensate for some other phenotypes associated with Ngn2. This could explain the partial penetrance of our phenotypes. In addition to neurotransmitter fate, Ngn2 is necessary for the proper location of pyramidal neurons and proper dendritic morphology. The proper morphology and location are crucial to the formation of proper circuitry. Finally, the present study demonstrates that Ngn2 regulates how pyramidal neurons innervate target areas by regulating the initial axon projections of pyramidal neurons, which underlies the formation of cortical circuits. Further studies of Ngn2 regulation and of transcriptional targets of Ngn2 will lead to a better understanding of proper cortical formation and ultimately to the underlying causes of abnormal cortical development.

Experimental Procedures

Animals

In this study we used several strains of mice including Balb/c and C57Bl/6. The Ngn2 GFP knockin mice were a generous gift from Dr. Francois Guillemot. The Ngn2 knockin mice were carried on a Balb/c background. All experiments were performed in strict accordance to IACUC approved protocols.

Plasmids

For this study we created the pSCV2 construct from the pSilencer2.1 (Ambion) vector. To achieve this, we inserted has a CAG-Venus-pA cassette into the backbone of the pSilencer2.1 vector. All shRNAs are inserted downstream of the U6 promoter using BamHI and HindIII restriction sites. The sequence of control shRNA is ACTACCGTTGTTATAGGTGTTCAAGAGACACCTATAACAACGGTAGTTTTTTG GAA. The sequence of the shRNA targeting Ngn2 is GCCAACAACCGCGAGCGCAATTCAAGAGATTGCGCTCGCGGTTGTTGGCCT TTTTTGGAA. To create the rescue mutant of Ngn2 a noncoding point mutation of was generated by mutating bp 360 from cytosine to adenine using the QuickChangeII mutagenesis kit from Stratagene.

Antibodies and Immunostaining

All immunofluorescent staining was performed as previously described (Hand et al., 2005). *Primary antibodies* anti-L1 1:2500 (millipore), anti-GFP 1:2000 (Aves), anti-NF165 1:1000 (Developmental Studies Hybridoma Bank at the University of Iowa), anti-CTIP2 1:2000 (Abcam), anti-Tbr1 1:1000 (Chemicon), and anti-Cux1 1:500 (Santa Cruz Biotechnology). *Secondary antibodies* goat anti-chicken Alexa 488, goat anti-rat Alexa 546, goat anti-rat Alexa 637, goat anti-rabbit Alexa 546, goat anti-rabbit Alex 637, and goat anti-mouse Alexa 546. Streptavidin conjugated to Alexa 546 was used to detect the biotin labeled dextrose amines.

Anterograde axonal tracings

Briefly, E18.5 brains dissected and injected with 0.1 mg/ml 10,000MW BDA (Molecular Probes) in PBS with 0.1% fast green for visualization. Then the brains were incubated in aCSF at 37C oxygenated with 95/5% O_2/CO_2 for 8hrs. After 8hrs, brains were fixed overnight at 4C in 4%PFA in PBS pH7.4. The brains were then sectioned and immunostained.

Ex vivo electroporation and organotypic slice culture

All *ex vivo* electroporation and organotypic slice culture were performed essentially as described previously (Hand et al., 2005).

In utero electroporation

Briefly, E15.5 mice were deeply anesthetized using 2.5% 2,2,2 Tribromoethanol in PBS. A small 1-2cm incision was made along the midline and the uterine horns were removed from the abdominal cavity and placed on sterile gauze. The lateral ventricles of the embryos were injected with 2ug/ul of plasmid in 1XPBS, 0.1% fast green dye (for visualization). The embryos were subsequently electroporated as follows 4 pulses of 30V for 50ms with a 500ms interval. After the embryos that had been injected and electroporated, the uterine horns were placed back in the abdominal cavity and the incision was sutured. Mice were allowed to recover and embryos were harversted at post natal day 14. All surgeries strictly adhered to IACUC approved protocols.

Supplemental Figures

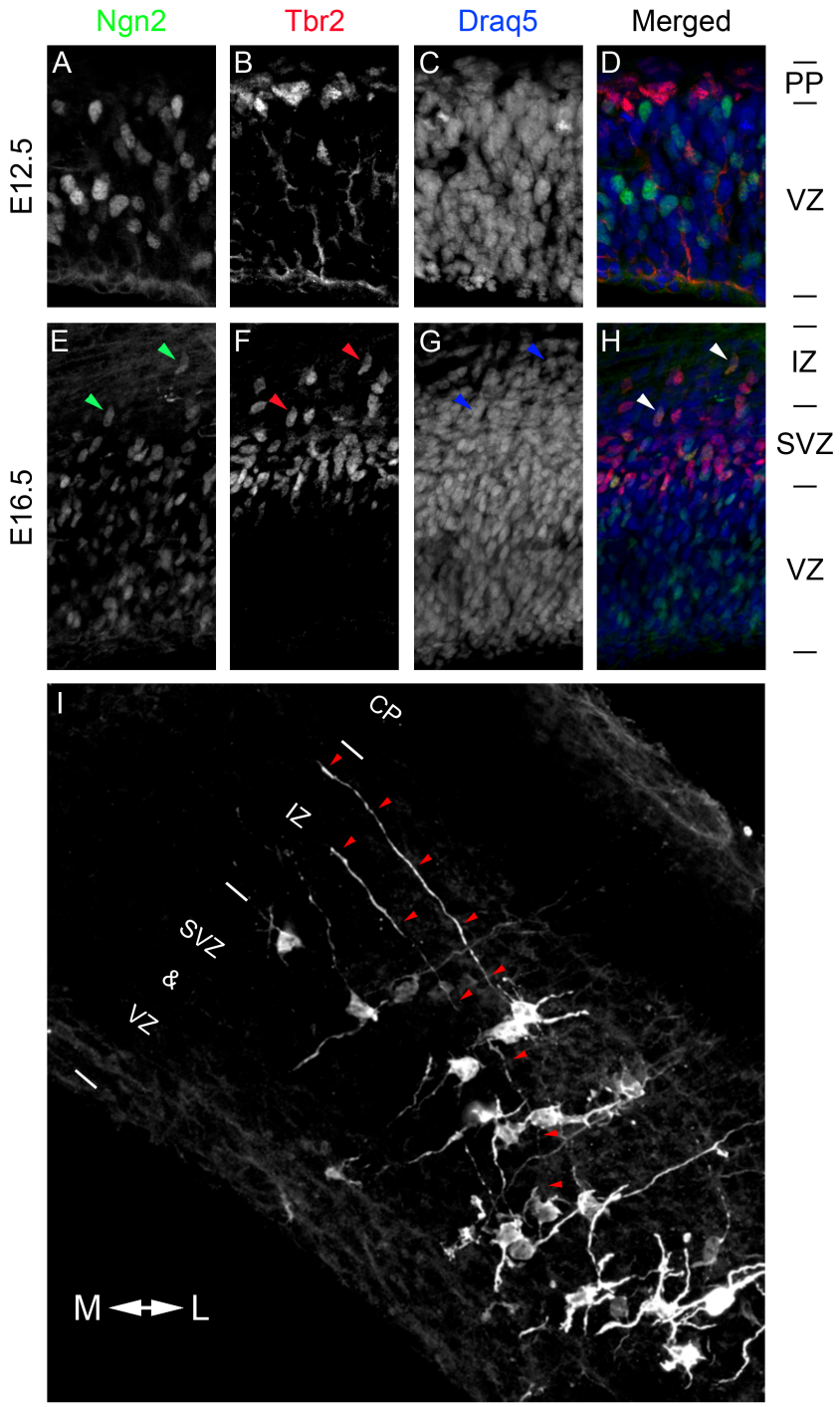

Supplemental Figure 3.1: Pattern of Ngn2 expression the developing cortex.

Coronal sections from E12.5 (A-D) and E16.5 (E-H) were immunostained for Ngn2 (A,E), Tbr2 (B,F) and Draq5 (C,G). Merged images (D,H). At E12.5 Ngn2 expression is resticted the VZ (A) and has little colocalization with Tbr2 (B,D), a marker for intermediate progenitors. In contrast at E16.5, a time in which superficial layer neurons are generated, Ngn2 is expressed widely in the VZ and SVZ, and occasionally in the IZ (E), many cells also co-stain for Ngn2 and Tbr2 (F,H), demonstrating many intermediate progenitors express Ngn2. Arrows denote cells co-expressing Ngn2 and Tbr2 located in the upper SVZ and IZ. To determine when callosal axons first emerge, E15.5 cortices were electroporation with the YFP variant Venus and cultured as organotypic slices. Electroporated neurons were immunostained for GFP 36 hours after electroporation to visualize axon initiation. At this time point, several neurons have a single long neurite growing medially (red arrows, I). Interestingly, none of these neurons have formed a leading process which is a characteristic of a radially migrating neuron. VZ = ventricular zone, SVZ = subventricular zone, IZ = intermediate zone

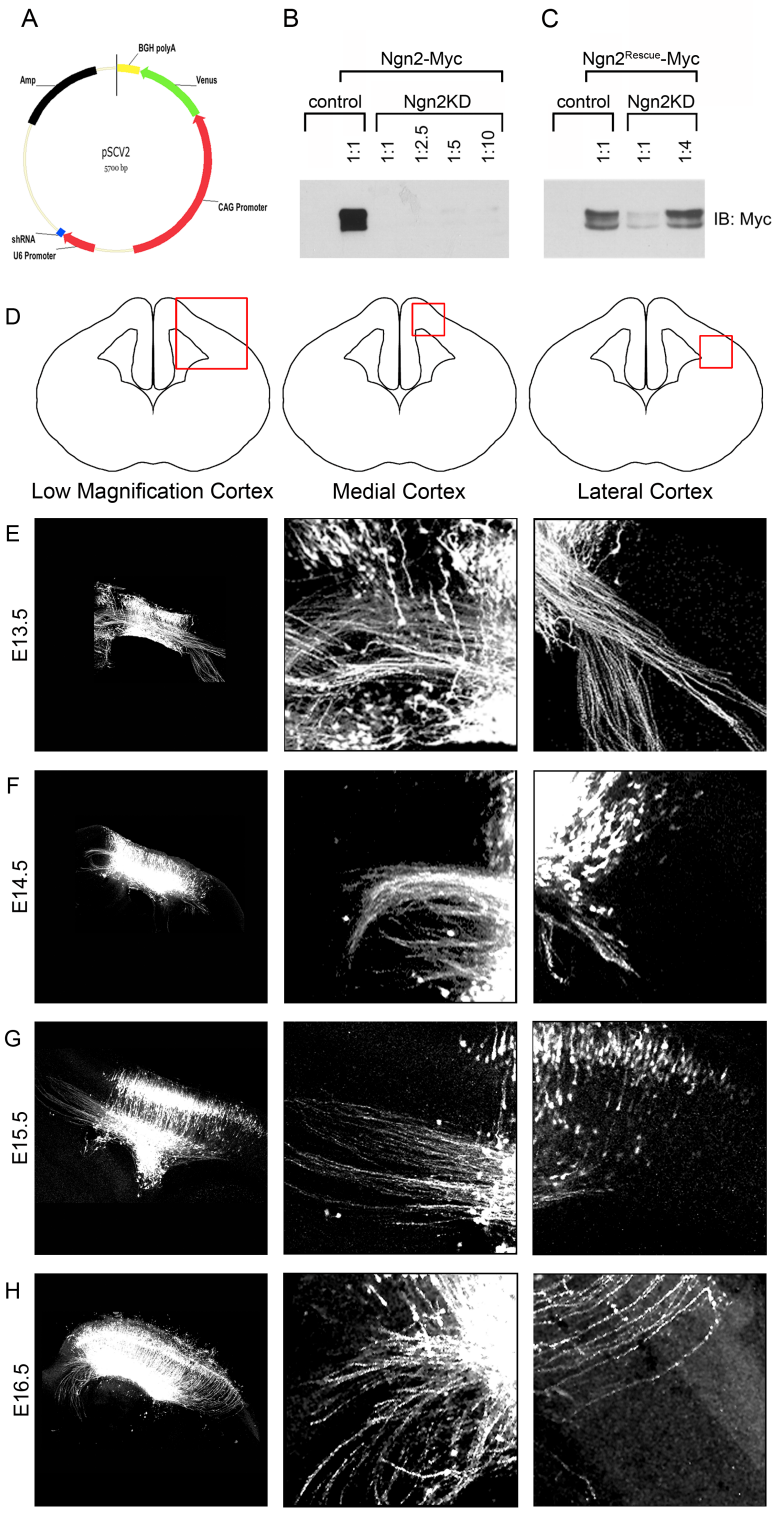

Supplemental Figure 3.2: shRNA mediated knockdown of Ngn2 and axonal projection time course using *ex vivo* electroporation coupled with organotypic slice culture.

The bicistronic pSCV2 plasmid was engineered to allow for the visualization of cells expressing the shRNA (A). This plasmid contains a nonspecific control shRNA under the control of the pol-III U6 promoter and the YFP variant Venus under control of the pol-II CAG promoter. The control vector with the nonspecific shRNA does not reduce expression of Myc tagged Ngn2 in P19 cells (B,C). Myc tagged Ngn2 expression is drastically reduced in the presence of shRNA targeting Ngn2 (Ngn2KD) (B). This shRNA effectively knocks down Ngn2 expression even at a 1:10 ratio of shRNA to Myc tagged Ngn2 plasmids. In order to rescue shRNA mediated knockdown of Ngn2, we generated a Ngn2 rescue mutant ($Ngn2^{Rescue}$) containing a single noncoding point mutation that reduces the ability of the shRNA to target Ngn2 (C). A 1:1 ratio of shRNA to myc tagged $Ngn2^{Rescue}$ allows for weak expression of Ngn2, and a 1:4 ratio of shRNA to myc tagged $Ngn2^{Rescue}$ allows for expression of Ngn2 equal to control shRNA (C). For the axonal projection time course, embryonic cortices were electroporated with a plasmid encoding for the YFP variant Venus under the control of the CAG promoter at time points varying from E13.5 to E16.5 (E-H). After 5DIV, the electroporated neurons were immunostained for GFP to assess the axonal projections of cortical neurons labeled at each time point. Diagrams depict the areas that were imaged (D), low magnification images (left) reveal the area of the cortex electroporated, high magnification of the medial cortex (middle) to visualize medial projecting axons, and high magnification of the lateral cortex (right) to visualize lateral projecting axons. At E13.5, a large portion of the electroporated neurons have laterally projecting axons (E). Starting at E14.5, the number of laterally projecting steadily decreases (F), and by E15.5 there are very few laterally projecting axons (G). Virtually no laterally projecting axons were seen at E16.5 (H).

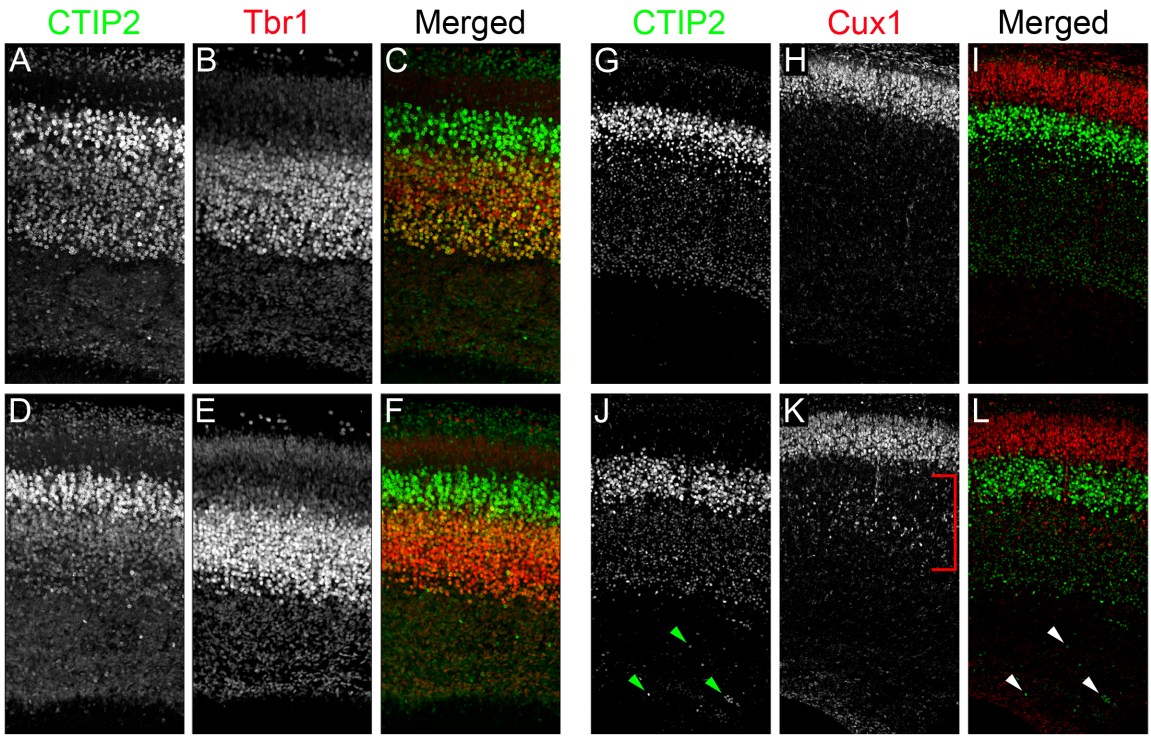

Supplemental Figure 3.3: Ngn2-/- embryos have normal cortical lamination

To assess any changes in cortical lamination upon the loss of Ngn2, we harvested Ngn2+/- embryos and Ngn2-/- embryos at E18.5 (A-F), and at the last possible time point, P0 (G-L). To assess deep layer formation we immunostained section with CTIP2, which strongly labels layer 5 and weakly labels layer 6a (A,D,G,J) and Tbr1 (B,E), which labels layer 6a. Merged images revealed (C,F) no difference in size or location of layers V and VI between Ngn2+/- (A-C) and Ngn2-/- (D-F) embryos. To compare any differences in superficial layer formation we immunostained sections with Cux1 (H,K) which labels layers 2-4. Again we observed no obvious difference in laminar formation when Ngn2+/- (G-I) and Ngn2-/- sections were stained for superficial layer markers, merged images (I,L). Immunostaining for laminar markers did reveal the presence of heterotopias attributed to the migration phenotype associated with Ngn2 (arrows, J,L) and the presence of Cux1 positive neurons in deep layers (bracket, K).

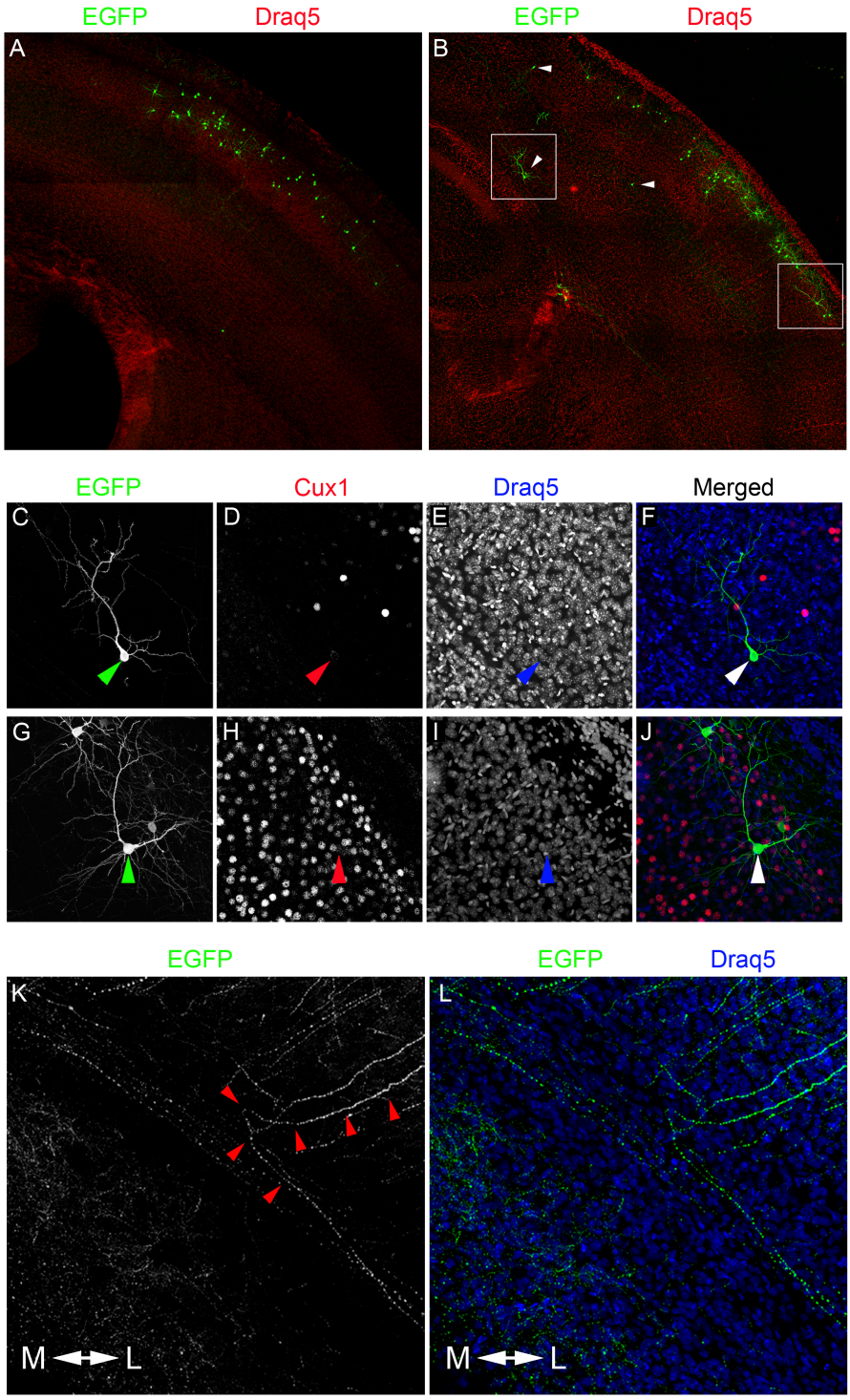

Supplemental Figure 3.4: Ngn2 knockdown by *in utero* electroporation reproduces previously described phenotypes attributed to Ngn2.

In utero electroporation of shRNA targeting Ngn2 reproduced several of the phenotypes we previously attributed to Ngn2. Low magnification of the cortex at P14 electroporated with either the control shRNA (A) or the shRNA targeting Ngn2 (B) were immunostained for EGFP and DNA was stained with Draq5. While no detectable phenotype was identified in cortices electroporated with the control shRNA (A), several phenotypes were identified in the cortices electroporated with the shRNA targeting Ngn2. Arrows denote misplaced cells due to an inhibition of migration. Boxes identify neurons with either misoriented or multiple apical dendrites (C-J). High magnification reveals the dedritic defects. The neurons were immunostained with EGFP (C,G) to reveal morphology, Cux1 (D,H) to confirm laminar identity, and Draq 5 (E,I). Merged images (F,J). *In utero* electroporation also identified lateral projecting axons emerging from neurons located in the cortical plate (K,L)

Chapter 4

Conclusions

My results have identified novel aspects of cortical development regulated by Neurogenin2. Furthermore, these results lend insight into how Neurogenin2 is regulated. While the basic proneural activity of Neurogenin2 is well understood (Bertrand et al., 2002), there are properties of Neurogenin2 that are still unresolved. In particular, Neurogenins (1 & 2) are sufficient to inhibit gliogenesis in a DNA independent manner (Sun et al., 2001). In this study, it was suggested that the Neurogenins may sequester transcriptional co-activators from the transcription factors that promote gliogenesis. These transcriptional co-activators include the histone acetyltransferases CBP/p300. The importance of CBP/p300 in regulating Neurogenin2 function has become an area of increasing interest. Our unpublished data (Hand and Polleux, manuscript in preparation) along with others (Ge et al., 2006) have demonstrated that mutating tyrosine 241 of Neurogenin2 reduces the interaction between Neurogenin2 and CBP/p300. While this interaction may not be necessary for promoting neuronal differentiation, it appears to be necessary for Neurogenin2 to regulate radial

migration and proper dendritic morphology (see Chapter 2, (Hand et al., 2005)). While it is clear there is a reduction in the interaction between Neurogenin2 and CBP/p300 upon mutating tyrosine 241, we believe this reduced interaction is not solely responsible for the effects induced by mutating tyrosine 241 of Neurogenin2. We hypothesize Neurogenin2 regulates different aspects of cortical development through differential gene expression, and Neurogenin2 could achieve this differential gene expression through interactions with different transcriptional co-activators or co-repressors. This could explain why the proneural activity is not altered upon mutating tyrosine 241. Furthermore, we see that Neurogenin2 differentially regulates axon guidance in addition to differentially regulating migration and dendritic morphology from neuronal differentiation. Here, we found Neurogenin2 regulates the initial guidance of superficial layer pyramidal neurons but not deep layer neurons (see Chapter 3). Again we believe Neurogenin2 is capable of differentially regulating gene expression, in this example, regulating genes over developmental time (E11-13 versus E14-17). This is most likely due to differential interactions of transcriptional co-regulators and changes in the state of chromatin regulated by chromatin-modifying proteins. Future studies are needed to identify novel interacting proteins of Neurogenin2 and how these interactions could regulate Neurogenin2 activity and gene targeting.

Understanding how Neurogenin2 is regulated at the molecular level will ultimately lead to a better understanding of cortical development. Here we have

demonstrated that Neurogenin2 is regulate by tyrosine phosphorylation, and that this phosphorylation is necessary for the proper migration and dendritic morphology of pyramidal neurons (see Chapter 2, (Hand et al., 2005). Since our initial observation, others have identified novel phosphorylation sites within Neurogenin2. Specifically, two other phosphorylation sites Serines 231 and 234 were found to be phosphorylated (Ma et al., 2008). These serine phosphorylation sites were found to be downstream of sonic hedgehog-mediated activation of GSK-3β and necessary for the proper specification of motor neurons within the spinal cord. Interestingly, sonic hedgehog signaling is important for the generation of the ventral telencephalon but absent in the formation of the cortex (Gaspard et al., 2008), and the knockin mouse in which serines 231 and 234 of Neurogenin2 were mutated to alanines contained no cortical phenotypes (Ma et al., 2008). These results suggest that Neurogenin2 is differentially regulated in different regions of the nervous system. In addition to phosphorylation, we have identified other post-translational modification of Neurogenin2. We have demonstrated that Neurogenin2 is ubiquitinated and acetylated (data not shown, Hand and Polleux manuscript in preparation). Interestingly, CBP/p300 have been shown to acetylate other proteins in addition to histones, including transcription factors (Sterner and Berger, 2000), making these the likely histone acetyltransferases acetylating Neurogenin2. We have found that mutating Lysine 101 of Neurogenin2, which appears to be the major site of acetylation, seems to increase the activity of Neurogenin2. Furthermore, mutating this lysine has no

effect on the ubiquitination of Neurogenin2 or the stability of Neurogenin2 (data not shown, Hand and Polleux manuscript in preparation). While the *in vivo* effects of Neurogenin2 acetylation are still unclear, future studies may address how acetylation of Neurogenin2 regulates the development of the cerebral cortex. We and others have identified post-translation modification of Neurogenin2 and phenotypes regulated by these modifications, but many unanswered questions remain. Future studies will identify the signaling pathways responsible for these modifications and how these signaling pathways regulate the development of the cerebral cortex.

Future directions

Understanding the development of the cerebral cortex at the molecular level is of tremendous importance since many cognitive disorders are due to the improper development of the cerebral cortex. Identifying the molecular and structural defects underlying cognitive disorders will lead to better diagnosis and treatments for these disorders. Our work and others has identified the importance of a transcription factor, Neurogenin2 in regulating the development of the cerebral cortex. In this dissertation, the importance of Neurogenin2 in migration, dendritic morphology, and axonal projection of pyramidal neurons were demonstrated. Unfortunately, the precise molecular mechanisms underlying the regulation of cortical development by Neurogenin2 still elude us. This is largely due to the nature of transcription factors. Transcription factors are often studied

for their ability to produce dramatic phenotypes by regulating gene expression, and their study has made significant contribution to all aspects of biology. While the importance of transcription factor is undeniable, future studies need to focus on the expression of specific genes regulated by these transcription factors. In the case of Neurogenin2, many genes downstream of Neurogenin2 and direct transcriptional targets have been identified (Mattar et al., 2004; Seo et al., 2007; Sugimori et al., 2007). Some of these genes are known to play important roles in cortical development, such as doublecortin. Doublecortin is a microtubule binding protein necessary for the proper migration of pyramidal neurons, and mutation in humans leads to mental retardation (Gleeson et al., 1998). More recently, other important genes downstream of Neurogenin2 have been identified, such as srGAP2, which regulates the migration and morphology of pyramidal neurons (Guerrier et al., 2009). These are just two of the many, possibly hundreds of genes regulated by Neurogenin2. Identifying the role of all transcriptional targets of Neurogenin2 and the precise role each gene undertakes alone and in concert with all other genes target by Neurogenin2 is essential to understanding cortical development. Once we understand the exact mechanism in which the cerebral cortex is formed, and how each precise type of cortical neuron is generated, the ability to diagnose and treat cognitive disorders will be greatly improved, through the identification of novel drug targets, the ability of treatments using gene therapies, and *in vitro* generated cell based therapies. Medical science will benefit greatly from ongoing research into the developing nervous system.

Currently, there are many disorders such as schizophrenia, biopolar disorder, depression and autism that lack any significant laboratory diagnostics, and the diagnosis of these disorders is limited to the presentation of outward symptoms. Many studies have identified genetic links to these disorders. Further research pursing genes implicated in these disorders and their effect on the developing nervous system, could lead to genetic testing and earlier detection. Genetic testing could lead to earlier treatments prior to the onset of symptoms resulting in a better prognosis for these patients. Furthermore, the identification of genes contributing to these disorders may lead to novel drug targets for these disorders.

Traditional drug treatments for some cognitive disorders use broad acting drugs that cause undesirable side effects. For example, neuroleptics are the most common treatment for schizophrenia (American Psychiatric Association., 2000). Neuroleptics are a class of drug antagonizing the D2 dopamine receptor, but they commonly antagonize the 5H2 serotonin receptor as well (Goodman et al., 2008). While antipsychotics such as clozapine (a commonly used neuroleptic) are effective, they cause many undesirable side effects including motor defects that persist months or years after treatment (Goodman et al., 2008). Currently, it is hypothesized that the underlying cause of schizophrenia involves the dopaminergic projections to the frontal cortex. Understanding how these dopaminergic circuits are formed and maintained at the molecular level could lead to better and more specific drugs that have fewer undesirable side effects. While schizophrenia is just one example, there are many disorders of the

nervous system that will benefit from better and more specific pharmaceuticals, once the molecular basis of the disorder is understood.

In addition to new and better pharmaceuticals, some disorders could be treated with novel cell based therapies using stem cells. The current research on embryonic stem cells and induced pluripotent stem cells has potential to treat congenital and degenerative disorders. Researchers have demonstrated the ability differentiate cortical neurons from human embryonic stem cells (Gaspard et al., 2008) and induce neuronal differentiation directly from fibroblast (Vierbuchen et al., 2010), suggesting that new cortical neurons could be generated from other cell types *in vitro.* While this research is still in its infancy, it could lead to cell based therapies for many disorders including epilepsy. Patients suffering from epilepsy have regions of hyper-excitability within their brain. Within the cortex, neural circuits are excited by pyramidal neurons that release glutamate as an excitatory neurotransmitter. The excitatory neurons are balanced by GABAergic inhibitory interneurons, that form local inhibitory circuits within the cortex. In the future, scientist may be able to harvest cells from a patients suffering from epilepsy, induce the differentiation of GABAergic interneurons and inject these interneurons into regions suffering from hyper-excitability restoring the proper balance between excitation and inhibition. Treating epileptic patient is only one of many potential applications for cell based therapies. Stem cell based therapies will have tremendous potential to cure and treat a wide range of diseases and disorders of the nervous system, but scientists must first

understand the precise mechanisms regulating the development of the nervous system.

The ability of medical scientist to diagnose and treat disorders involving the nervous system will be enhanced by basic research studying the development of the nervous system at the molecular level. This research will provide new insights into how our nervous system forms and functions, and this research will allow for a better understanding of the causes underlying disorders of the nervous system.

Reference

Alcamo, E.A., Chirivella, L., Dautzenberg, M., Dobreva, G., Farinas, I., Grosschedl, R., and McConnell, S.K. (2008). Satb2 regulates callosal projection neuron identity in the developing cerebral cortex. Neuron *57*, 364-377.

Allendoerfer, K.L., and Shatz, C.J. (1994). The subplate, a transient neocortical structure: its role in the development of connections between thalamus and cortex. Annu Rev Neurosci *17*, 185-218.

American Psychiatric Association. (2000). Diagnostic criteria from DSM-IV-TR (Washington, D.C., American Psychiatric Association).

Anderson, S.A., Eisenstat, D.D., Shi, L., and Rubenstein, J.L. (1997). Interneuron migration from basal forebrain to neocortex: dependence on Dlx genes. Science *278*, 474-476.

Angevine, J.B., Jr. (1970). Time of neuron origin in the diencephalon of the mouse. An autoradiographic study. J Comp Neurol *139*, 129-187.

Arlotta, P., Molyneaux, B.J., Chen, J., Inoue, J., Kominami, R., and Macklis, J.D. (2005). Neuronal subtype-specific genes that control corticospinal motor neuron development in vivo. Neuron *45*, 207-221.

Arthur, W.T., and Burridge, K. (2001). RhoA inactivation by p190RhoGAP regulates cell spreading and migration by promoting membrane protrusion and polarity. Mol Biol Cell *12*, 2711-2720.

Bai, J., Ramos, R.L., Ackman, J.B., Thomas, A.M., Lee, R.V., and LoTurco, J.J. (2003). RNAi reveals doublecortin is required for radial migration in rat neocortex. Nat Neurosci *6*, 1277-1283.

Bar, I., Lambert de Rouvroit, C., and Goffinet, A.M. (2000). The evolution of cortical development. An hypothesis based on the role of the Reelin signaling pathway. Trends Neurosci *23*, 633-638.

Barnes, A.P., and Polleux, F. (2009). Establishment of axon-dendrite polarity in developing neurons. Annu Rev Neurosci *32*, 347-381.

Berry, M., and Rogers, A.W. (1965). The migration of neuroblasts in the developing cerebral cortex. J Anat *99*, 691-709.

Bertrand, N., Castro, D.S., and Guillemot, F. (2002). Proneural genes and the specification of neural cell types. Nat Rev Neurosci *3*, 517-530.

Bielle, F., Griveau, A., Narboux-Neme, N., Vigneau, S., Sigrist, M., Arber, S., Wassef, M., and Pierani, A. (2005). Multiple origins of Cajal-Retzius cells at the borders of the developing pallium. Nat Neurosci *8*, 1002-1012.

Blom, N., Gammeltoft, S., and Brunak, S. (1999). Sequence and structure-based prediction of eukaryotic protein phosphorylation sites. J Mol Biol *294*, 1351-1362.

Britanova, O., de Juan Romero, C., Cheung, A., Kwan, K.Y., Schwark, M., Gyorgy, A., Vogel, T., Akopov, S., Mitkovski, M., Agoston, D.*, et al.* (2008). Satb2 is a postmitotic determinant for upper-layer neuron specification in the neocortex. Neuron *57*, 378-392.

Bulfone, A., Smiga, S.M., Shimamura, K., Peterson, A., Puelles, L., and Rubenstein, J.L. (1995). T-brain-1: a homolog of Brachyury whose expression defines molecularly distinct domains within the cerebral cortex. Neuron *15*, 63-78.

Chen, B., Schaevitz, L.R., and McConnell, S.K. (2005a). Fezl regulates the differentiation and axon targeting of layer 5 subcortical projection neurons in cerebral cortex. Proc Natl Acad Sci U S A *102*, 17184-17189.

Chen, J.G., Rasin, M.R., Kwan, K.Y., and Sestan, N. (2005b). Zfp312 is required for subcortical axonal projections and dendritic morphology of deep-layer pyramidal neurons of the cerebral cortex. Proc Natl Acad Sci U S A *102*, 17792-17797.

Coyle, I.P., Koh, Y.H., Lee, W.C., Slind, J., Fergestad, T., Littleton, J.T., and Ganetzky, B. (2004). Nervous wreck, an SH3 adaptor protein that interacts with Wsp, regulates synaptic growth in Drosophila. Neuron *41*, 521-534.

des Portes, V., Pinard, J.M., Billuart, P., Vinet, M.C., Koulakoff, A., Carrie, A., Gelot, A., Dupuis, E., Motte, J., Berwald-Netter, Y.*, et al.* (1998). A novel CNS gene required for neuronal migration and involved in X-linked subcortical laminar heterotopia and lissencephaly syndrome. Cell *92*, 51-61.

Englund, C., Fink, A., Lau, C., Pham, D., Daza, R.A., Bulfone, A., Kowalczyk, T., and Hevner, R.F. (2005). Pax6, Tbr2, and Tbr1 are expressed sequentially by radial glia, intermediate progenitor cells, and postmitotic neurons in developing neocortex. J Neurosci *25*, 247-251.

Fode, C., Gradwohl, G., Morin, X., Dierich, A., LeMeur, M., Goridis, C., and Guillemot, F. (1998). The bHLH protein NEUROGENIN 2 is a determination factor for epibranchial placode-derived sensory neurons. Neuron *20*, 483-494.

Fode, C., Ma, Q., Casarosa, S., Ang, S.L., Anderson, D.J., and Guillemot, F. (2000). A role for neural determination genes in specifying the dorsoventral identity of telencephalic neurons. Genes Dev *14*, 67-80.

Gaspard, N., Bouschet, T., Hourez, R., Dimidschstein, J., Naeije, G., van den Ameele, J., Espuny-Camacho, I., Herpoel, A., Passante, L., Schiffmann, S.N.*, et al.* (2008). An intrinsic mechanism of corticogenesis from embryonic stem cells. Nature *455*, 351-357.

Gaudilliere, B., Konishi, Y., de la Iglesia, N., Yao, G., and Bonni, A. (2004). A CaMKII-NeuroD signaling pathway specifies dendritic morphogenesis. Neuron *41*, 229-241.

Ge, W., He, F., Kim, K.J., Blanchi, B., Coskun, V., Nguyen, L., Wu, X., Zhao, J., Heng, J.I., Martinowich, K.*, et al.* (2006). Coupling of cell migration with neurogenesis by proneural bHLH factors. Proc Natl Acad Sci U S A *103*, 1319-1324.

Gleeson, J.G., Allen, K.M., Fox, J.W., Lamperti, E.D., Berkovic, S., Scheffer, I., Cooper, E.C., Dobyns, W.B., Minnerath, S.R., Ross, M.E.*, et al.* (1998). Doublecortin, a brain-specific gene mutated in human X-linked lissencephaly and double cortex syndrome, encodes a putative signaling protein. Cell *92*, 63-72.

Gohlke, J.M., Armant, O., Parham, F.M., Smith, M.V., Zimmer, C., Castro, D.S., Nguyen, L., Parker, J.S., Gradwohl, G., Portier, C.J.*, et al.* (2008). Characterization of the proneural gene regulatory network during mouse telencephalon development. BMC Biol *6*, 15.

Goodman, L.S., Gilman, A., and Brunton, L.L. (2008). Goodman & Gilman's manual of pharmacology and therapeutics (New York, McGraw-Hill Medical).

Guerrier, S., Coutinho-Budd, J., Sassa, T., Gresset, A., Jordan, N.V., Chen, K., Jin, W.L., Frost, A., and Polleux, F. (2009). The F-BAR domain of srGAP2

induces membrane protrusions required for neuronal migration and morphogenesis. Cell *138*, 990-1004.

Gupta, A., Tsai, L.H., and Wynshaw-Boris, A. (2002). Life is a journey: a genetic look at neocortical development. Nat Rev Genet *3*, 342-355.

Hand, R., Bortone, D., Mattar, P., Nguyen, L., Heng, J.I., Guerrier, S., Boutt, E., Peters, E., Barnes, A.P., Parras, C*., et al.* (2005). Phosphorylation of Neurogenin2 specifies the migration properties and the dendritic morphology of pyramidal neurons in the neocortex. Neuron *48*, 45-62.

Hasegawa, H., Ashigaki, S., Takamatsu, M., Suzuki-Migishima, R., Ohbayashi, N., Itoh, N., Takada, S., and Tanabe, Y. (2004). Laminar patterning in the developing neocortex by temporally coordinated fibroblast growth factor signaling. J Neurosci *24*, 8711-8719.

Hassan, B.A., Bermingham, N.A., He, Y., Sun, Y., Jan, Y.N., Zoghbi, H.Y., and Bellen, H.J. (2000). atonal regulates neurite arborization but does not act as a proneural gene in the Drosophila brain. Neuron *25*, 549-561.

Hatanaka, Y., Hisanaga, S., Heizmann, C.W., and Murakami, F. (2004). Distinct migratory behavior of early- and late-born neurons derived from the cortical ventricular zone. J Comp Neurol *479*, 1-14.

Hatanaka, Y., and Murakami, F. (2002). In vitro analysis of the origin, migratory behavior, and maturation of cortical pyramidal cells. J Comp Neurol *454*, 1-14.

Hausser, M., Spruston, N., and Stuart, G.J. (2000). Diversity and dynamics of dendritic signaling. Science *290*, 739-744.

Hayashi, K., Ohshima, T., and Mikoshiba, K. (2002). Pak1 is involved in dendrite initiation as a downstream effector of Rac1 in cortical neurons. Mol Cell Neurosci *20*, 579-594.

Heng, J.I., Nguyen, L., Castro, D.S., Zimmer, C., Wildner, H., Armant, O., Skowronska-Krawczyk, D., Bedogni, F., Matter, J.M., Hevner, R*., et al.* (2008). Neurogenin 2 controls cortical neuron migration through regulation of Rnd2. Nature *455*, 114-118.

Hevner, R.F., Shi, L., Justice, N., Hsueh, Y., Sheng, M., Smiga, S., Bulfone, A., Goffinet, A.M., Campagnoni, A.T., and Rubenstein, J.L. (2001). Tbr1 regulates differentiation of the preplate and layer 6. Neuron *29*, 353-366.

Huang, M.L., Hsu, C.H., and Chien, C.T. (2000). The proneural gene amos promotes multiple dendritic neuron formation in the Drosophila peripheral nervous system. Neuron *25*, 57-67.

Huber, A.B., Kolodkin, A.L., Ginty, D.D., and Cloutier, J.F. (2003). Signaling at the growth cone: ligand-receptor complexes and the control of axon growth and guidance. Annu Rev Neurosci *26*, 509-563.

Imayoshi, I., Shimogori, T., Ohtsuka, T., and Kageyama, R. (2008). Hes genes and neurogenin regulate non-neural versus neural fate specification in the dorsal telencephalic midline. Development *135*, 2531-2541.

Jan, Y.N., and Jan, L.Y. (2003). The control of dendrite development. Neuron *40*, 229-242.

Jarman, A.P., Grau, Y., Jan, L.Y., and Jan, Y.N. (1993). atonal is a proneural gene that directs chordotonal organ formation in the Drosophila peripheral nervous system. Cell *73*, 1307-1321.

Kageyama, R., Ohtsuka, T., Hatakeyama, J., and Ohsawa, R. (2005). Roles of bHLH genes in neural stem cell differentiation. Exp Cell Res *306*, 343-348.

Katoh, M. (2004). Identification and characterization of human FCHSD1 and FCHSD2 genes in silico. Int J Mol Med *13*, 749-754.

Kawauchi, T., Chihama, K., Nabeshima, Y., and Hoshino, M. (2003). The in vivo roles of STEF/Tiam1, Rac1 and JNK in cortical neuronal migration. EMBO J *22*, 4190-4201.

Kriegstein, A.R., and Noctor, S.C. (2004). Patterns of neuronal migration in the embryonic cortex. Trends Neurosci *27*, 392-399.

Lai, T., Jabaudon, D., Molyneaux, B.J., Azim, E., Arlotta, P., Menezes, J.R., and Macklis, J.D. (2008). SOX5 controls the sequential generation of distinct corticofugal neuron subtypes. Neuron *57*, 232-247.

Lee, S.K., Lee, B., Ruiz, E.C., and Pfaff, S.L. (2005). Olig2 and Ngn2 function in opposition to modulate gene expression in motor neuron progenitor cells. Genes Dev *19*, 282-294.

Lee, S.K., and Pfaff, S.L. (2003). Synchronization of neurogenesis and motor neuron specification by direct coupling of bHLH and homeodomain transcription factors. Neuron *38*, 731-745.

Leone, D.P., Srinivasan, K., Chen, B., Alcamo, E., and McConnell, S.K. (2008). The determination of projection neuron identity in the developing cerebral cortex. Curr Opin Neurobiol *18*, 28-35.

Ma, P.C., Rould, M.A., Weintraub, H., and Pabo, C.O. (1994). Crystal structure of MyoD bHLH domain-DNA complex: perspectives on DNA recognition and implications for transcriptional activation. Cell *77*, 451-459.

Ma, Q., Fode, C., Guillemot, F., and Anderson, D.J. (1999). Neurogenin1 and neurogenin2 control two distinct waves of neurogenesis in developing dorsal root ganglia. Genes Dev *13*, 1717-1728.

Ma, Q., Kintner, C., and Anderson, D.J. (1996). Identification of neurogenin, a vertebrate neuronal determination gene. Cell *87*, 43-52.

Ma, Y.C., Song, M.R., Park, J.P., Henry Ho, H.Y., Hu, L., Kurtev, M.V., Zieg, J., Ma, Q., Pfaff, S.L., and Greenberg, M.E. (2008). Regulation of motor neuron specification by phosphorylation of neurogenin 2. Neuron *58*, 65-77.

Marin, O., and Rubenstein, J.L. (2003). Cell migration in the forebrain. Annu Rev Neurosci *26*, 441-483.

Markram, H., Toledo-Rodriguez, M., Wang, Y., Gupta, A., Silberberg, G., and Wu, C. (2004). Interneurons of the neocortical inhibitory system. Nat Rev Neurosci *5*, 793-807.

Marmorstein, R., and Roth, S.Y. (2001). Histone acetyltransferases: function, structure, and catalysis. Curr Opin Genet Dev *11*, 155-161.

Mattar, P., Britz, O., Johannes, C., Nieto, M., Ma, L., Rebeyka, A., Klenin, N., Polleux, F., Guillemot, F., and Schuurmans, C. (2004). A screen for downstream effectors of Neurogenin2 in the embryonic neocortex. Dev Biol *273*, 373-389.

Megason, S.G., and McMahon, A.P. (2002). A mitogen gradient of dorsal midline Wnts organizes growth in the CNS. Development *129*, 2087-2098.

Miller, M. (1981). Maturation of rat visual cortex. I. A quantitative study of Golgi-impregnated pyramidal neurons. J Neurocytol *10*, 859-878.

Miller, M.W. (1986). Maturation of rat visual cortex. III. Postnatal morphogenesis and synaptogenesis of local circuit neurons. Brain Res *390*, 271-285.

Miyata, T., Kawaguchi, A., Saito, K., Kawano, M., Muto, T., and Ogawa, M. (2004). Asymmetric production of surface-dividing and non-surface-dividing cortical progenitor cells. Development *131*, 3133-3145.

Mizuguchi, R., Sugimori, M., Takebayashi, H., Kosako, H., Nagao, M., Yoshida, S., Nabeshima, Y., Shimamura, K., and Nakafuku, M. (2001). Combinatorial roles of olig2 and neurogenin2 in the coordinated induction of pan-neuronal and subtype-specific properties of motoneurons. Neuron *31*, 757-771.

Molla, R., Garcia-Verdugo, J.M., Lopez-Garcia, C., and Martin-Perez, V. (1986). Neuronal development of the chick cerebral cortex. A Golgi study. J Hirnforsch *27*, 625-637.

Molyneaux, B.J., Arlotta, P., Hirata, T., Hibi, M., and Macklis, J.D. (2005). Fezl is required for the birth and specification of corticospinal motor neurons. Neuron *47*, 817-831.

Molyneaux, B.J., Arlotta, P., Menezes, J.R., and Macklis, J.D. (2007). Neuronal subtype specification in the cerebral cortex. Nat Rev Neurosci *8*, 427-437.

Moore, K.B., Schneider, M.L., and Vetter, M.L. (2002). Posttranslational mechanisms control the timing of bHLH function and regulate retinal cell fate. Neuron *34*, 183-195.

Murciano, A., Zamora, J., Lopez-Sanchez, J., and Frade, J.M. (2002). Interkinetic nuclear movement may provide spatial clues to the regulation of neurogenesis. Mol Cell Neurosci *21*, 285-300.

Nakada, Y., Hunsaker, T.L., Henke, R.M., and Johnson, J.E. (2004). Distinct domains within Mash1 and Math1 are required for function in neuronal differentiation versus neuronal cell-type specification. Development *131*, 1319-1330.

Nieto, M., Monuki, E.S., Tang, H., Imitola, J., Haubst, N., Khoury, S.J., Cunningham, J., Gotz, M., and Walsh, C.A. (2004). Expression of Cux-1 and Cux-2 in the subventricular zone and upper layers II-IV of the cerebral cortex. J Comp Neurol *479*, 168-180.

Nieto, M., Schuurmans, C., Britz, O., and Guillemot, F. (2001). Neural bHLH genes control the neuronal versus glial fate decision in cortical progenitors. Neuron *29*, 401-413.

Nieuwenhuys, R. (1994). The neocortex. An overview of its evolutionary development, structural organization and synaptology. Anat Embryol (Berl) *190*, 307-337.

Noctor, S.C., Flint, A.C., Weissman, T.A., Dammerman, R.S., and Kriegstein, A.R. (2001). Neurons derived from radial glial cells establish radial units in neocortex. Nature *409*, 714-720.

Noctor, S.C., Martinez-Cerdeno, V., Ivic, L., and Kriegstein, A.R. (2004). Cortical neurons arise in symmetric and asymmetric division zones and migrate through specific phases. Nat Neurosci *7*, 136-144.

Ochiai, W., Nakatani, S., Takahara, T., Kainuma, M., Masaoka, M., Minobe, S., Namihira, M., Nakashima, K., Sakakibara, A., Ogawa, M*., et al.* (2009). Periventricular notch activation and asymmetric Ngn2 and Tbr2 expression in pair-generated neocortical daughter cells. Mol Cell Neurosci *40*, 225-233.

Ogawa, M., Miyata, T., Nakajima, K., Yagyu, K., Seike, M., Ikenaka, K., Yamamoto, H., and Mikoshiba, K. (1995). The reeler gene-associated antigen on Cajal-Retzius neurons is a crucial molecule for laminar organization of cortical neurons. Neuron *14*, 899-912.

Olenik, C., Aktories, K., and Meyer, D.K. (1999). Differential expression of the small GTP-binding proteins RhoA, RhoB, Cdc42u and Cdc42b in developing rat neocortex. Brain Res Mol Brain Res *70*, 9-17.

Olson, M.F., Ashworth, A., and Hall, A. (1995). An essential role for Rho, Rac, and Cdc42 GTPases in cell cycle progression through G1. Science *269*, 1270-1272.

Parras, C.M., Schuurmans, C., Scardigli, R., Kim, J., Anderson, D.J., and Guillemot, F. (2002). Divergent functions of the proneural genes Mash1 and Ngn2 in the specification of neuronal subtype identity. Genes Dev *16*, 324-338.

Peters, A., and Jones, E.G. (1984). Cerebral cortex (New York, Plenum Press).

Peters, A., and Kara, D.A. (1985a). The neuronal composition of area 17 of rat visual cortex. I. The pyramidal cells. J Comp Neurol *234*, 218-241.

Peters, A., and Kara, D.A. (1985b). The neuronal composition of area 17 of rat visual cortex. II. The nonpyramidal cells. J Comp Neurol *234*, 242-263.

Peters, A., Kara, D.A., and Harriman, K.M. (1985). The neuronal composition of area 17 of rat visual cortex. III. Numerical considerations. J Comp Neurol *238*, 263-274.

Pinto Lord, M.C., and Caviness, V.S., Jr. (1979). Determinants of cell shape and orientation: a comparative Golgi analysis of cell-axon interrelationships in

the developing neocortex of normal and reeler mice. J Comp Neurol *187*, 49-69.

Pinto-Lord, M.C., Evrard, P., and Caviness, V.S., Jr. (1982). Obstructed neuronal migration along radial glial fibers in the neocortex of the reeler mouse: a Golgi-EM analysis. Brain Res *256*, 379-393.

Polleux, F., Dehay, C., and Kennedy, H. (1997). The timetable of laminar neurogenesis contributes to the specification of cortical areas in mouse isocortex. J Comp Neurol *385*, 95-116.

Polleux, F., and Ghosh, A. (2002). The slice overlay assay: a versatile tool to study the influence of extracellular signals on neuronal development. Sci STKE *2002*, pl9.

Polleux, F., Morrow, T., and Ghosh, A. (2000). Semaphorin 3A is a chemoattractant for cortical apical dendrites. Nature *404*, 567-573.

Polleux, F., Whitford, K.L., Dijkhuizen, P.A., Vitalis, T., and Ghosh, A. (2002). Control of cortical interneuron migration by neurotrophins and PI3-kinase signaling. Development *129*, 3147-3160.

Puri, P.L., and Sartorelli, V. (2000). Regulation of muscle regulatory factors by DNA-binding, interacting proteins, and post-transcriptional modifications. J Cell Physiol *185*, 155-173.

Quan, X.J., Denayer, T., Yan, J., Jafar-Nejad, H., Philippi, A., Lichtarge, O., Vleminckx, K., and Hassan, B.A. (2004). Evolution of neural precursor selection: functional divergence of proneural proteins. Development *131*, 1679-1689.

Ramón y Cajal, S. (1995). Histology of the nervous system of man and vertebrates (New York, Oxford University Press).

Ridley, A.J., Schwartz, M.A., Burridge, K., Firtel, R.A., Ginsberg, M.H., Borisy, G., Parsons, J.T., and Horwitz, A.R. (2003). Cell migration: integrating signals from front to back. Science *302*, 1704-1709.

Ross, S.E., Greenberg, M.E., and Stiles, C.D. (2003). Basic helix-loop-helix factors in cortical development. Neuron *39*, 13-25.

Scardigli, R., Schuurmans, C., Gradwohl, G., and Guillemot, F. (2001). Crossregulation between Neurogenin2 and pathways specifying neuronal identity in the spinal cord. Neuron *31*, 203-217.

Schmechel, D.E., and Rakic, P. (1979). A Golgi study of radial glial cells in developing monkey telencephalon: morphogenesis and transformation into astrocytes. Anat Embryol (Berl) *156*, 115-152.

Schuurmans, C., Armant, O., Nieto, M., Stenman, J.M., Britz, O., Klenin, N., Brown, C., Langevin, L.M., Seibt, J., Tang, H.*, et al.* (2004). Sequential phases of cortical specification involve Neurogenin-dependent and -independent pathways. EMBO J *23*, 2892-2902.

Schuurmans, C., and Guillemot, F. (2002). Molecular mechanisms underlying cell fate specification in the developing telencephalon. Curr Opin Neurobiol *12*, 26-34.

Scott, E.K., and Luo, L. (2001). How do dendrites take their shape? Nat Neurosci *4*, 359-365.

Seibt, J., Schuurmans, C., Gradwhol, G., Dehay, C., Vanderhaeghen, P., Guillemot, F., and Polleux, F. (2003). Neurogenin2 specifies the connectivity of thalamic neurons by controlling axon responsiveness to intermediate target cues. Neuron *39*, 439-452.

Seo, S., Lim, J.W., Yellajoshyula, D., Chang, L.W., and Kroll, K.L. (2007). Neurogenin and NeuroD direct transcriptional targets and their regulatory enhancers. EMBO J *26*, 5093-5108.

Sessa, A., Mao, C.A., Hadjantonakis, A.K., Klein, W.H., and Broccoli, V. (2008). Tbr2 directs conversion of radial glia into basal precursors and guides neuronal amplification by indirect neurogenesis in the developing neocortex. Neuron *60*, 56-69.

Sharma, A., Moore, M., Marcora, E., Lee, J.E., Qiu, Y., Samaras, S., and Stein, R. (1999). The NeuroD1/BETA2 sequences essential for insulin gene transcription colocalize with those necessary for neurogenesis and p300/CREB binding protein binding. Mol Cell Biol *19*, 704-713.

Shimojo, H., Ohtsuka, T., and Kageyama, R. (2008). Oscillations in notch signaling regulate maintenance of neural progenitors. Neuron *58*, 52-64.

Shu, T., Ayala, R., Nguyen, M.D., Xie, Z., Gleeson, J.G., and Tsai, L.H. (2004). Ndel1 operates in a common pathway with LIS1 and cytoplasmic dynein to regulate cortical neuronal positioning. Neuron *44*, 263-277.

Sidman, R.L., and Rakic, P. (1973). Neuronal migration, with special reference to developing human brain: a review. Brain Res *62*, 1-35.

Skowronska-Krawczyk, D., Ballivet, M., Dynlacht, B.D., and Matter, J.M. (2004). Highly specific interactions between bHLH transcription factors and chromatin during retina development. Development *131*, 4447-4454.

Smith, C.I., Islam, T.C., Mattsson, P.T., Mohamed, A.J., Nore, B.F., and Vihinen, M. (2001). The Tec family of cytoplasmic tyrosine kinases: mammalian Btk, Bmx, Itk, Tec, Txk and homologs in other species. Bioessays *23*, 436-446.

Sommer, L., Ma, Q., and Anderson, D.J. (1996). neurogenins, a novel family of atonal-related bHLH transcription factors, are putative mammalian neuronal determination genes that reveal progenitor cell heterogeneity in the developing CNS and PNS. Mol Cell Neurosci *8*, 221-241.

Sterner, D.E., and Berger, S.L. (2000). Acetylation of histones and transcription-related factors. Microbiol Mol Biol Rev *64*, 435-459.

Sugimori, M., Nagao, M., Bertrand, N., Parras, C.M., Guillemot, F., and Nakafuku, M. (2007). Combinatorial actions of patterning and HLH transcription factors in the spatiotemporal control of neurogenesis and gliogenesis in the developing spinal cord. Development *134*, 1617-1629.

Sun, Y., Nadal-Vicens, M., Misono, S., Lin, M.Z., Zubiaga, A., Hua, X., Fan, G., and Greenberg, M.E. (2001). Neurogenin promotes neurogenesis and inhibits glial differentiation by independent mechanisms. Cell *104*, 365-376.

Tabata, H., and Nakajima, K. (2003). Multipolar migration: the third mode of radial neuronal migration in the developing cerebral cortex. J Neurosci *23*, 9996-10001.

Takahashi, T., Nowakowski, R.S., and Caviness, V.S., Jr. (1995). The cell cycle of the pseudostratified ventricular epithelium of the embryonic murine cerebral wall. J Neurosci *15*, 6046-6057.

Takiguchi-Hayashi, K., Sekiguchi, M., Ashigaki, S., Takamatsu, M., Hasegawa, H., Suzuki-Migishima, R., Yokoyama, M., Nakanishi, S., and Tanabe, Y. (2004). Generation of reelin-positive marginal zone cells from the caudomedial wall of telencephalic vesicles. J Neurosci *24*, 2286-2295.

Talikka, M., Perez, S.E., and Zimmerman, K. (2002). Distinct patterns of downstream target activation are specified by the helix-loop-helix domain of proneural basic helix-loop-helix transcription factors. Dev Biol *247*, 137-148.

Tessier-Lavigne, M., and Goodman, C.S. (1996). The molecular biology of axon guidance. Science *274*, 1123-1133.

Threadgill, R., Bobb, K., and Ghosh, A. (1997). Regulation of dendritic growth and remodeling by Rho, Rac, and Cdc42. Neuron *19*, 625-634.

Tsai, H.M., Garber, B.B., and Larramendi, L.M. (1981a). 3H-thymidine autoradiographic analysis of telencephalic histogenesis in the chick embryo: I. Neuronal birthdates of telencephalic compartments in situ. J Comp Neurol *198*, 275-292.

Tsai, H.M., Garber, B.B., and Larramendi, L.M. (1981b). 3H-thymidine autoradiographic analysis of telencephalic histogenesis in the chick embryo: II. Dynamics of neuronal migration, displacement, and aggregation. J Comp Neurol *198*, 293-306.

Van Aelst, L., and Cline, H.T. (2004). Rho GTPases and activity-dependent dendrite development. Curr Opin Neurobiol *14*, 297-304.

Vierbuchen, T., Ostermeier, A., Pang, Z.P., Kokubu, Y., Sudhof, T.C., and Wernig, M. (2010). Direct conversion of fibroblasts to functional neurons by defined factors. Nature *463*, 1035-1041.

Vojtek, A.B., Taylor, J., DeRuiter, S.L., Yu, J.Y., Figueroa, C., Kwok, R.P., and Turner, D.L. (2003). Akt regulates basic helix-loop-helix transcription factor-coactivator complex formation and activity during neuronal differentiation. Mol Cell Biol *23*, 4417-4427.

Whitford, K.L., Dijkhuizen, P., Polleux, F., and Ghosh, A. (2002). Molecular control of cortical dendrite development. Annu Rev Neurosci *25*, 127-149.

Wong, K., Ren, X.R., Huang, Y.Z., Xie, Y., Liu, G., Saito, H., Tang, H., Wen, L., Brady-Kalnay, S.M., Mei, L.*, et al.* (2001). Signal transduction in neuronal migration: roles of GTPase activating proteins and the small GTPase Cdc42 in the Slit-Robo pathway. Cell *107*, 209-221.

Yu, T.W., and Bargmann, C.I. (2001). Dynamic regulation of axon guidance. Nat Neurosci *4 Suppl*, 1169-1176.